PhD in Clinical & Experimental Medicine

UNIVERSITÀ DEGLI STUDI DEL PIEMONTE ORIENTALE
"AMEDEO AVOGADRO"

Dipartimento di Medicina Traslazionale

Corso di Dottorato di Ricerca in Medicina Clinica e Sperimentale

ciclo XXVII

Optical Coherence Tomography, from bench to bedside:

Shining the light during percutaneous vascular intervention

SSD MED 11

Coordinatore

Prof.ssa Marisa Gariglio

Tutor

Prof. Paolo Nicola Marino

Dottorando

Gioel Gabrio Secco

INDEX

1. INTRODUCTION

In the past decades angiography has been the keystone tool to assess coronary anatomy, leading to the development of largely applied revascularisation techniques such as coronary bypass surgery and percutaneous transluminal angioplasty.

Despite the widespread dissemination and high reproducibility, angiography alone can only provide a limited analysis of lumen profile without the possibility to disclose vessel wall characteristics and composition of coronary lesions. In fact, coronary angiography depicts arteries as planar silhouette of the contrast-filled lumen and disease assessment is based on the comparison of the stenostic segment with the adjacent "normal appearing" artery, which is often an incorrect assumption due to the diffuse nature of atherosclerosis as shown by pathological studies. Moreover, angiography interpretation is flawed by large inter- and intra-observer variability and usually underestimates the severity of the disease and vessel dimension (1). Three-dimensional angiography may provide more accurate assessment of the luminogram but it still does not allow visualisation of the arterial wall and plaque composition.

Intracoronary imaging techniques have been developed to overcome these limitations.

Intravascular ultrasound (IVUS) was the first intracoronary imaging modality introduced in interventional cardiology in the early '90ies (2), followed more than a decade after by optical coherence tomography (OCT) a light based technology. OCT is similar to IVUS providing information about intravascular anatomy that far exceeds the level of detail obtained from conventional angiography. The use of near-infrared light rather than ultrasound reflectance allows OCT to have higher spatial resolution (with up to 10 to 15 μm of spatial resolution compared with the

100- to 200 µm resolution of IVUS) but lower penetration power (1 to 3 mm into vessel wall compared with the 4 to 10 mm of IVUS). Moreover, near-infrared light is scattered by red blood cells, and therefore OCT use for guidance of intervention was limited by the need of prolonged crystalloid infusion during imaging. In so forth, OCT has been initially employed as a research tool to investigate plaque morphology and stent strut endothelisation.

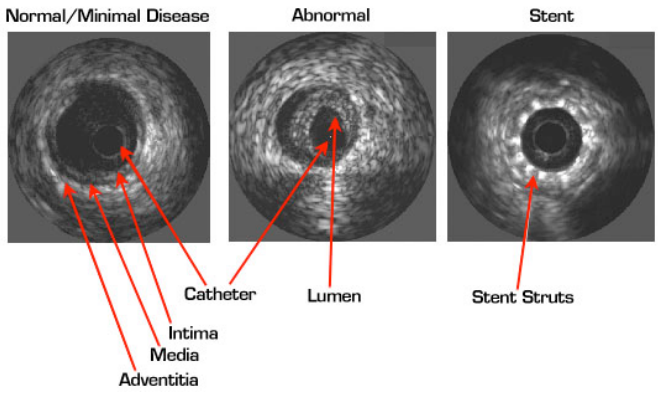

The Frequency domain OCT system (FD-OCT) has the advantage of a more rapid image acquisition due to the fast-scanning laser systems able to minimise the contrast use and to increase imaging speed while delivering an improved image quality than with the earlier time domain systems (TD-OCT). Thus this allows multiple acquisitions of the entire segment of interest with an amount of contrast only slightly greater than contrast required for the control angiogram (3).

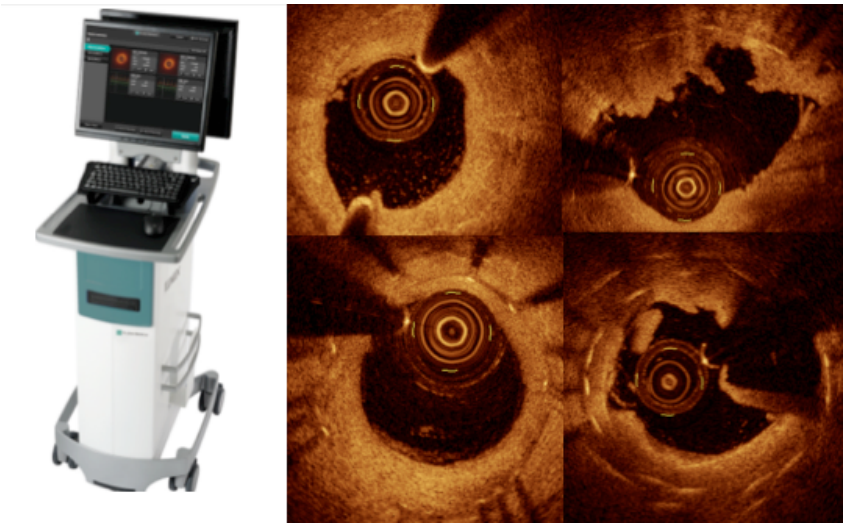

Despite these features, the use of OCT as an additional imaging technique is still debated in daily clinical practice.

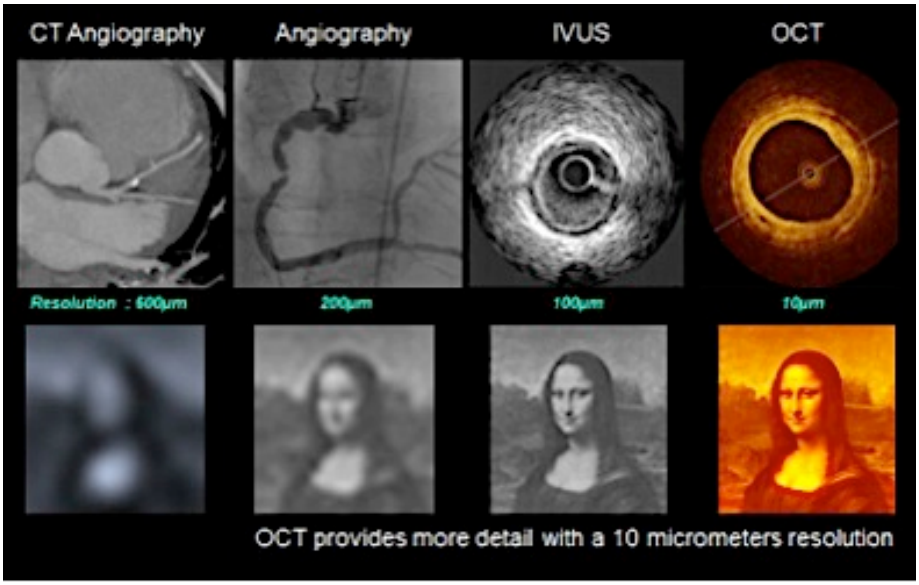

The aim of this thesis was to evaluate the role of OCT in contemporary vascular intervention enlarging its use not only during coronary revascularization but even in new field such as during peripheral vascular intervention, renal nerve denervation and carotid artery stenting.

2. EXPERIMENTAL RESULTS

2.1 OPTICAL COHERENCE TOMOGRAPHY DURING CORONARY INTERVENTION.

2.1.1 Study 1

Title: Optical Coherence Tomography for Guidance of Treatment of In-stent Restenosis with Cutting Balloons.

Background

The treatment of ISR remains a challenge with poor immediate results and higher restenosis rate than in de novo lesions. IVUS studies (4-5) have shown that, despite the use of larger balloons, higher pressure and new stents, the final minimal lumen cross sectional area (MLCSA) achieved was smaller than the minimal stent cross section area (MSCSA) after initial stent deployment. We hypothesized that this was due to the inability to apply direct pressure to the previously deployed stent due to the cushion-like protection of the neointima, precluding adequate stent expansion.

Aim

We tested an alternative treatment strategy based on the use of cutting balloons (CB) sized with Optical Coherence Tomography (OCT) to achieve effective cutting as close as possible to the struts, allowing subsequent better extrusion of the neointima outside the stent and direct transmission of the expanding force of the balloon to the stent struts.

Materials and Methods

We assessed 14 consecutive ISR lesions involving the right coronary artery (n.2), left circumflex (n.6), left anterior descending (n.4), first diagonal branch (n.1) and a saphenous vein graft to RCA (n.1). All the stents initially implanted in the restenotic segment were DES (Table 1).

Angiographic and Optical coherence tomography images acquisition

ISR lesions were classified according to Mehran et al (14) in:

- Class I: (Focal ISR): lesion < 10 mm in length and positioned at the unscaffolded segment, the body of the stent, the proximal or distal margin (not both) or a combination of these sites;
- Class II: (Diffuse intrastent ISR): lesion > 10mm in length and confined to the stent, without extending outside the margins;
- Class III: (Diffuse proliferative ISR): lesion < 10 mm in length extending beyond the margins;
- Class IV: ISR with total occlusion".

Subsequently OCT acquisition was performed with a frequency domain analysis system (C7, LightLab Imaging Inc., Westford, Massachusetts, USA). A motorized pullback at 2 cm/s was activated during injection of iodixanol 320 (Visipaque, GE Health Care, Cork, Ireland) via 6 or 7 Fr guiding catheter at a flow rate sufficient to have full substitution of blood with contrast with no streaming (non-occlusive technique). The position of the imaging probe at the time of the start of pull-back was documented angiographically. Frames were analyzed every 0.5 mm. Anatomical landmarks such as side branches, calcifications, or stent edges were used for longitudinal orientation.

Optical coherence tomography data analysis:

Qualitative and quantitative analysis of OCT images was performed offline using proprietary software (C7LightLab Imaging). MLCSA and MSCSA were measured

before and after each CB inflation and after stent deployment and high pressure post-expansion. Neointimal area was calculated by subtracting the luminal area from the stent area. The minimal distance between neointimal fissures created by the microatherotome blades and stent struts was calculated after each cutting balloon inflation. The first CB was selected by the operator according to the visual estimation of the angiographic reference diameter. In 3 patients a smaller conventional balloon had to be used for initial predilatation because of the impossibility to perform OCT in a total occluded vessel. In 2 patients a smaller conventional balloon had to be used for initial predilatation because the CB did not cross directly. In a tortuous RCA the CB could be used only in a proximal but not in the distal segment of ISR. The CB diameter was then upsized based on the OCT assessment of the stent diameter aiming at achieving a CB/ stent ratio of 1.1-1.2/1.0. New DES were implanted in all patients except two lesions with small diameter and multiple previously implanted stents in which the operator felt that a sufficient result was achieved with CB dilatation only (Figures 1 and 2). No dissections requiring new stent implantation were observed after the final OCT acquisition.

Clinical follow up

In-hospital, 30 days, and cumulative 6 months MACE were defined as death, myocardial infarction and repeat revascularization (CABG or PTCA). Twelve-lead electrocardiograms were recorded before, immediately after the procedure and at hospital discharge.

Figure 1: Lesion treated with only cutting balloon expansion. A: Angiogram and OCT pre-treatment: a thick, nearly concentric layer of hyperplasia is revealed by the OCT examination inside a double crown of struts due to the deployment of a 3.0 EES stent inside a 3.5 bare metal stent. B: Angiogram and OCT after 3.0×10 mm CB (16 ATM): the lumen is improved, but there is a filling defect inside the stent due to residual hyperplasia; the corresponding OCT image indicates that a deep cut approaching the struts is present only in one direction (4 o'clock); based on the stent diameter a larger CB is selected. C: Angiogram and OCT after 3.5×10 mm CB (16 ATM): the good angiographic result is explained by the second deep cut (struts in contact with the lumen at 4 o'clock and 9 o'clock) with MLCSA increased from 4.4 mm2 to 5.4 mm2.

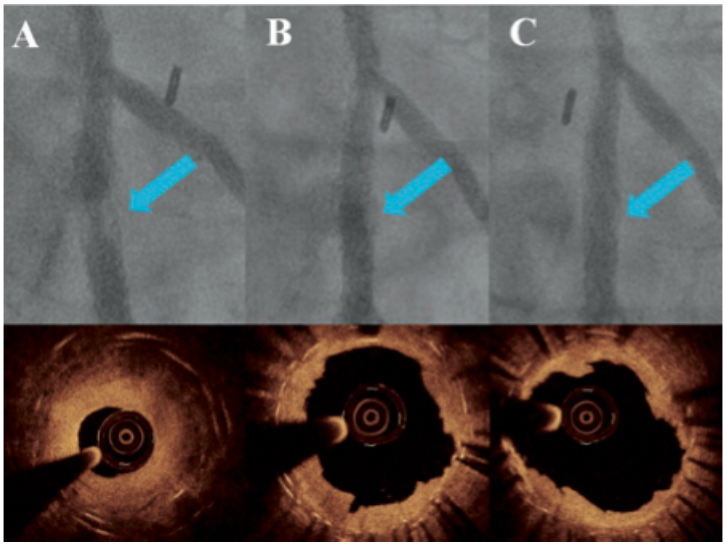

Figure 2: OCT 3-D reconstruction of a plaque treated by cutting balloon expansion. A: Angiogram, OCT and OCT 3-D reconstruction pre-treatment: a thick layer of intimal thickening justifies the severe stenosis. Please note that the OCT image has been obtained after predilation with a 2.0 mm balloon while the angiogram is before treatment. B: Angiogram, OCT and OCT 3-D reconstruction after CB 3.0×10 mm (16 ATM): An acceptable and regular lumen has been created by the dilatation with some struts visible in the corresponding 3D reconstruction.

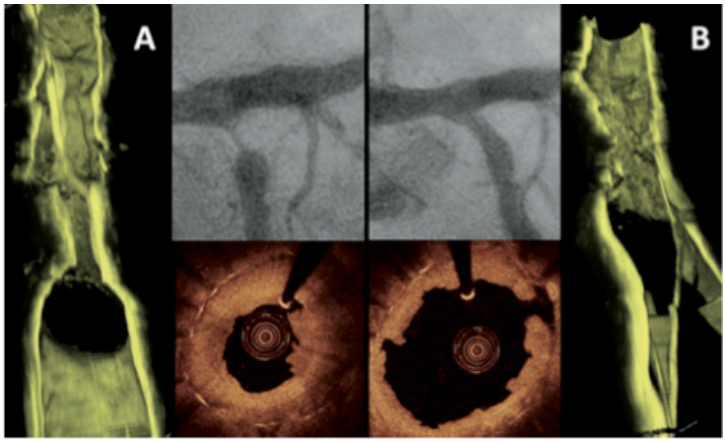

Results

Angiographic analysis (tab. 1)

Of the ISR lesions treated 6 were focal, 3 had diffuse ISR, 2 had diffuse proliferative ISR and 3 had a total occlusive restenosis.

Table 1: Months after stent implantation, type of stent used and angiographic findings.

Vessel	Months	Type of stent	Length (mm)	Diam (mm)	P ATM	Visual angiographic stenosis	Mehran classification
LCX	15	ZES	24	3.0	33	90%	I
LCX	49	PES	18	3.0	18	50%	I
RCA	3	EES	23	3.0	26	60%	I
DG1	59	PES	24	2.5	24	75%	II
LADd	5	EES	24	2.5	24	90%	I
LCX	8	SES	23	2.75	30	95%	III
LCXd	8	SES	23	2.25	24	75%	II
LCX	17	EES	8	3.0	12	80%	III
LADd	10	SES	18	3.0	20	100%	IV
RCA	14	SES	23	3.5	24	100%	IV
LCX	9	PES	18	3.5	20	100%	IV
LAD	7	PES	24	3.0	16	60%	I
LAD	60	SES	23	3	14	70%	I
SVG to RCA	5	EES	24	2.75	16	60%	II

ZES: zotarolimus-eluting stent (Endeavor, Medtronic, Minneapolis, MN, USA); PES: paclitaxel-eluting stent (Taxus Express, Boston Scientific, Natick, MS, USA); EES: everolimus-eluting stent (Promus, Boston Scientific, Natick, MS, USA; Xience, Abbott, Abbott Park, Illinois, USA); SES: sirolimus-eluting stent (Cypher, Cordis, Johnson & Johnson, Warren, NJ, USA

Optical coherence tomography analysis (tab. 2)

The mean MCSA of the lumen and stent pre treatment was respectively 2.22 + 0.73 mm^2 and 7.01 + 1.30 mm^2. The mean MCSA lumen after first and second cutting balloon inflation, were respectively 5.19 + 1.12 mm^2 and 6.08 + 1.01 mm^2 .The mean final MCSA lumen was 6.68 + 1.14 mm^2. In the patients with

a two step strategy using a first CB guided by angiography and a second CB guided by OCT, the increase in CB diameter was 0.5 mm, achieving an increase in MLCSA area from 4.9 + 0.42 to 6.35 + 0.92 mm2 with a reduction from 41% to 27% of neointimal hyperplasia (Figure 3 and 4).

Table 2: OCT data analysis.

VESSEL	MLCSA mm²	MSCSA mm²	NEOIN-TIMAL AREA mm²	CB1 mm	P ATM	MLCSA mm²	MSCSA mm²	NEOIN-TIMAL AREA mm²	CB2 mm	P ATM	MLCSA mm²	MSCSA mm²	NEOIN-TIMAL AREA mm²	STENT USED	DIAM mm	P ATM	MLCSA mm²	MSCSA mm²	NEOIN-TIMAL AREA mm²
LCX	1.15	6.82	5.67	3.0	16	4.4	8.46	4.06	3.5	16	5.4	8.66	3.26				5.4	8.66	3.26
LCX	2.78	7.63	4.85	3.0	16	6.17	9.4	3.23									6.17	9.4	3.23
RCA	2.77	7.25	4.48	3.0	16									ZES	2.75	18	5.98	9.49	3.51
DG1	1.61	5.47	3.86	2.5	18	3.49	5.85	2.36						EES	2.75	18	4.67	6.02	1.35
LAD	3.27	6.29	3.02	3.0	14	6.18	7.36	1.18						EES	3.0	16	6.49	7.48	0.99
LCX	3.6	8.48	4.88	2.5	18				3.0	16	4.98	8.54	3.56	EES	3.0	24	7.46	8.66	1.2
LCX	2.85	5.61	2.76	2.5	18	4.73	6.24	1.51	3.0	12	5.72	6.78	1.06	EES	2.75	18	6.09	7.01	0.92
LCX	1.75	6.48	4.73	3.0	10	3.88	7.99	4.11						EES	3.0	10	5.84	8.23	2.39
LAD	1.54*	7.13	5.59	2.5	16	5.39	8.03	2.64	3.0	16	7.21	8.65	1.44	PES	3.0	14	8.09	9.39	1.3
RCA	1.65*	10.23	8.58	3.0	16	5.08	10.39	5.31	3.5	16	7.09	10.98	3.89	EES	3.5	24	8.87	11.2	2.33
LCX	1.87*	8.32	6.45	3.5	16	6.72	8.98	2.26						EES	3.5	24	7.26	9.42	2.16
LAD	2.04	5.87	3.83	3.0	12	5.19	8.03	2.84						EES	3.0	12	6.83	8.55	1.72
LAD	2.53	6.27	3.74	3.5	12	6.96	9.1	2.14						EES	3.5	12	7.95	9.66	1.71
SVG to RCA	1.77	6.35	4.58	3.0	18	4.13	7.46	3.33						ZES	3.5	18	6.52	7.76	1.24
mean	2.22	7.01	4.78			5.19	8.10	2.91			6.08	8.72	2.64				6.68	8.63	1.95
SD ±	0.73	1.30	1.48			1.12	1.29	1.17			1.01	1.49	1.29				1.14	1.29	0.88

Please note that the OCT was employed to guide a clinically oriented strategy, avoiding unnecessary passes and contrast overload when the angiographic result was grossly inadequate or there was no possibility to further increase in CB diameter. This can explain the frequent occurrence of missing values in the various procedural steps. * After a pre-dilatation with a 2.0 conventional low profile balloon

Clinical Follow Up

No in-hospital, no 30 days and no 6 months MACE (death, myocardial infarction and repeat revascularization CABG or PTCA) were reported.

Figure 3: Increase in MLCSA and MCSA of the stent in four patients treated with a two-step strategy: first CB guided by angiography and second CB guided by OCT (Please note that the increase in CB diameter was 0.5 mm, achieving an increase in MLCSA from 4.9±0.42 to 6.35±0.92 mm2)

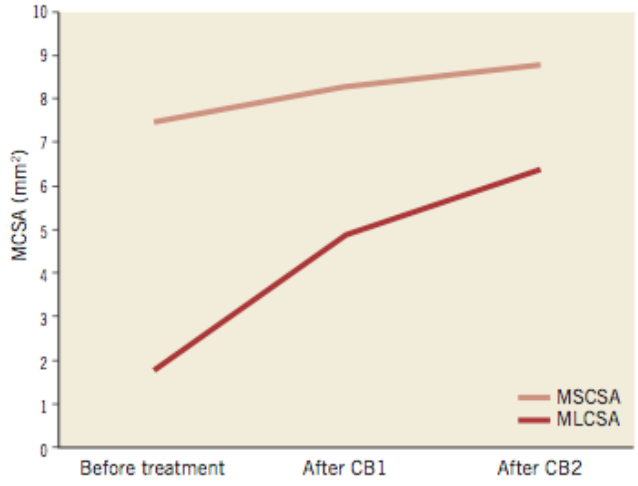

Figure 4: Mean reduction in neointimal plaque area in 11 patients with FD-OCT examinations available both after CB expansion and stent deployment. (Two patients were excluded because they were treated only with CB and one patient was excluded because no OCT examination was performed after CB expansion). The neointimal area after stent implantation was considered the tissue located between the two stents layers.

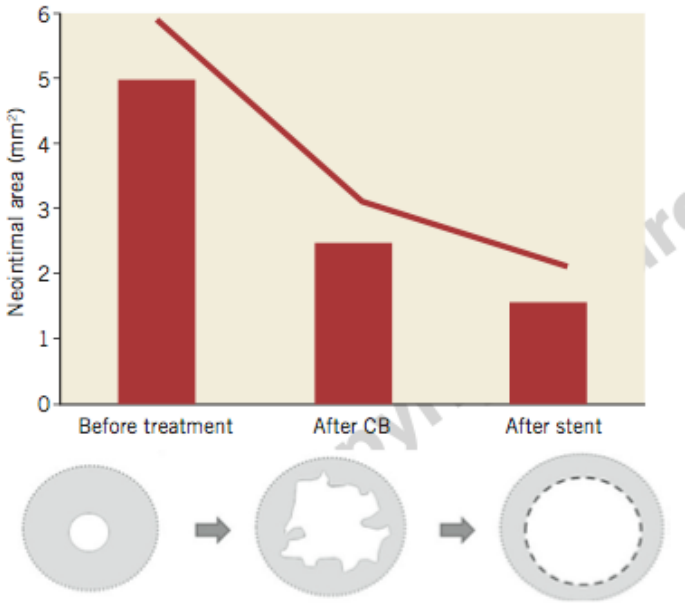

Discussion

Cutting balloons are used for treatment of ISR mainly because of the practical advantage that they do not move during inflation due to the stabilising effect of the blades, preventing damage outside the stenting segment (watermelon seeding effect).

The lack of clinical benefit observed in the early studies of CB vs conventional PTCA in de novo lesions or after treatment of ISR have created scepticism on the potential mechanical advantage offered by a focal concentration of force on the intimal plaque. Hoop stress is a circumferential stress in the vessel wall that balances the intra-arterial pressure and prevents vessel expansion (6). In a pressurised vessel where r is the inner radius and R is the outer radius, the hoop stress can be estimated by the Laplace law : $\sigma = P(R + r) / (R - r)$, where P is the pressure on the vessel wall (17). During PTCA, balloons are often inflated with pressure up to 20 ATM (2025 kPA), 150 times higher than the normal arterial wall's pressure (approximately 100 mmHg =13 kPa = 0.13 ATM). The mechanical properties of the arterial wall are critically dependent on the thickness of the wall and the characteristics of the intimal plaque. Consequently, the balloon pressure necessary to achieve circumferential overstretch and a satisfactory lumen expansion is intrinsically dependent of the tissue property and wall thickness. Thick neointimal hyperplasia and the stent itself contribute to increase the hoop stress to the point that even high pressure non-compliant balloons might be insufficient to overcome the hoop stress and induct a persistent plastic deformation of the vessel wall (7).

CBs have been designed to relieve the vessel hoop stress by creating controlled small incisions in the vessel wall. CBs present several advantages for the treatment of ISR, allowing a larger luminal gain at lower pressure compared to PCTA alone and preventing the late elastic recoil due to the incisions created by the blades.

When CBs were compared with conventional balloons for treatment of ISR the advantages observed in registries (8) were not confirmed in appropriately sized randomised trials (9). These trials were performed in the BMS era and without systematic IVUS guidance, not allowing the distinction between ISR due to stent underexpansion, unlikely to respond better to CB, and ISR due to excessive neointimal proliferation, as in all cases in this case series where IVUS was already used in most cases before and after stenting. IVUS is seldomly used to check the adequacy of the effect of CB because of its inability to detect the cuts in most of the cases. Suzuki et al., studying animal and in vitro models of ISR, demonstrated that IVUS tends to overestimate lumen area and underestimate the signal-poor in-stent hyperplasia (10). The OCT measurements were closer to the histological measurements because of the better delineation of the neointima-lumen interface. Balloon angioplasty was the initial strategy for treatment of ISR and proved to be user friendly and associated with good initial results, low incidence of in-hospital complications but relatively high late repeat ISR . In an IVUS study investigating treatment of ISR, Mehran et al (11) demonstrated that when treating ISR with PCTA, luminal gain is achieved by a combination of additional stent expansion and neointimal tissue compression through the stent resulting in a displacement through the stent strut and compression of neointimal tissue. Although satisfactory initial clinical and angiographic results were obtained with balloon angioplasty, a significant early lumen loss was also observed shortly after ISR treatment due to recoil and re-intrusion of neointimal tissue in the lumen (12). This early phenomeon possibly influences the long-term outcome after POBA for ISR, affected by a high re-restenosis rate. CBs, compared with conventional angioplasty balloons, present the significant advantage that the incisions of the microblades reduce the recoil of neointimal tissue into the lumen and allow greater stent expansion by reducing the hoop stress in the neointimal tissue. This explanation is

based on a previous study that demonstrated a greater capacity of CB over PCTA to extrude fibrous plaque and residual neointimal tissue out of the stent struts. OCT has been shown to be a greatly valuable tool to identify pattern and severity of restenosis (13) and to study its mechanisms. Furthermore, due to its high resolution, OCT is able to provide detailed characteristics of restenotic lesions such as the presence of neovascular formation in the neointimal tissue and identify the changes induced by the thin cuts of the CB blades. In fact, using OCT we were able to guide the selection of the CB based on the distance between neointimal fissures created by the micro blades and stent struts in order to eventually upgrade the CB diameter when the result was unsatisfactory. We believe that this allows greater expansion of the DES implanted in most cases as final step of treatment and has the potential of an even greater advantage if drug eluting balloons are used. This can lead to a greater MLCSA in order to achieve the largest final lumen, providing a "safety margin" for possible reactive hyperplasia ("bigger-is-better"). In fact, in all of the 14 ISR lesions we were able to achieve a satisfactory final MLCSA, always greater than 5.0 mm2, considered to be a valuable predictor for the long-term stent patency (14).

Limitations

The major limitation of this pilot study is the small size of the study population, justified by the rarity of restenoses after DES and, especially, DES restenoses with significant intimal hyperplasia. However, while DES are implanted in more than 90% of our practice and second generation DES are likely to reduce even more the phenomenon, other countries still use a majority of BMS or do not have second generation DES available.

Another limitation of our study is the lack of angiographic follow up, however, initial clinical follow up data are encouraging.

The OCT was employed to guide a clinically oriented strategy, avoiding unnecessary passes and contrast overload when the angiographic result was grossly inadequate or there was no possibility to further increase in CB diameter. This can explain the frequent occurrence of missing values in the various procedural steps.

2.1.2 Study 2

Title: Long-term tissue coverage of a biodegradable polylactide polymer-coated biolimus-eluting stent: Comparative sequential assessment with optical coherence tomography until complete resorption of the polymer.

Background

Biolimus-eluting stents (BESs) with a biodegradable polymer in abluminal coating achieve more complete coverage at 9 months compared with sirolimus-eluting stents (SESs) with a durable polymer, as assessed by optical coherence tomography (OCT). Whether this advantage persists or augments after complete resorption of the polymer (n.12 months) is unknown.

Aim

The aim of this study was to assess whether this difference persists after complete resorption of the BES polymer.

Materials and Methods

Study population and design

The design and main results from the LEADERS trial have been published elsewhere (15). It was an international randomized multicenter noninferiority trial comparing the BES BioMatrix Flex stent (Biosensors International, Morges, Switzerland) with the SES Cypher SELECT stent (Cordis, Miami Lakes, FL), following an all-comers approach with minimal exclusion criteria: patients with symptomatic coronary heart disease or silent ischemia were eligible if they had at least one coronary lesion of 50% diameter stenosis in vessels with 2.25- to 3.50-mm reference diameters, amenable for percutaneous treatment. The primary end point was a composite of cardiac death, myocardial infarction, and clinically

indicated target vessel revascularization at 9 months of follow-up. Patients were randomly allocated on a 1:1 basis to receive either BES or SES using random computer-generated sequences, stratified according to center. In a factorial design, they were additionally randomized on a 1:3 basis to angiographic and clinical follow-up at 9 months or clinical follow-up alone. Patients allocated to angiographic follow-up in 2 of the study sites (Royal Brompton Hospital, London, UK, and Erasmus MC, Rotterdam, the Netherlands) were also included in the OCT substudy. Serum creatinine 200 mol/L and left ventricular ejection fraction < 30% were the exclusion criteria for the OCT substudy. The primary end point for the OCT substudy was the proportion of uncovered struts at 9 and 24 months. The study complied with the Declaration of Helsinki, was approved by all institutional ethics committees, and was registered at clinical-trials.gov (NCT00389220). All patients provided written informed consent for participation.

Intervention and study stents

Direct stenting was allowed, and full lesion coverage was pursued by implanting one or several stents, as required. Only 1 type of DES was used per patient. The BioMatrix Flex stent (Biosensors International) consists of a stainless-steel platform (Juno; Biosensors International) coated by an abluminal 11-μm layer of polylactide polymer. The polymer contains Biolimus-A9 (Biosensors International, Morges, Switzerland) at a concentration of 15.6 μg/mm of stent length. Polylactide is linearly degraded by surface hydrolysis to lactide during a period of 6 to 12 months, resulting in simultaneous release of the drug. The Cypher SELECT stent (Cordis) consists of a stainless-steel platform coated by a durable blend of poly(ethylene-vinyl-acetate) and poly(butyl-methacrylate) containing sirolimus at a concentration of 8.3 to 10.4 μg/mm, depending on the stent nominal diameter. The drug elution period is estimated to be 90 days. After the intervention, the patients

received at least 75 mg of acetylsalicylic acid indefinitely and dual-antiplatelet therapy with 75 mg of clopidogrel for 12 months.

OCT study and analysis

Optical coherence tomography pullbacks were obtained at 9 and 24 months of follow-up with M3 or C7 systems (Lightlab Imaging, Westford, MA), depending on availability, using a nonocclusive technique10 (Table I).

		M3	C7
Domain		Time	Fourier
Catheter*		ImageWire	Dragonfly
Rotation speed (Hz)		20	100
Pullback speed (mm/s)		3	20
Patients with SES	9 mo	11	0
	24 mo	3	8
Patients with BES	9 mo	10	0
	24 mo	3	7

*All systems and catheters were obtained from Lightlab Imaging.

OCT pullbacks were analyzed offline in a core laboratory (Cardialysis BV, Rotterdam, the Netherlands) by independent staff blinded to allocation and to clinical or procedural characteristics of the patients using proprietary software (Lightlab Imaging). Cross sections at 1-mm intervals within the stented segment were analyzed. Lumen and stent areas were drawn in each cross section, and incomplete stent apposition (ISA) or neointimal hyperplasia (NIH) areas were calculated, as appropriate (16). Apposition was assessed per strut by placing a marker at the adluminal leading edge, in the midpoint of the strut's long axis, and by measuring the distance between this marker and the lumen contour, following a straight line directed to the center of gravity of the vessel (17). Struts were considered malapposed if the distance was 170 μm (for SES) or 140 μm (for BES), the thresholds resulting from rounding up the sum of the strut-polymer thickness of

each stent (SES 153 μm, BES 120 μm) plus the axial resolution of OCT (14 μm). Struts located at the ostium of side branches, with no vessel wall behind, were labeled as nonapposed side-branch struts and excluded from the analysis of apposition.

Struts were classified as uncovered if any part of the strut was visibly exposed to the lumen, or as covered if a layer of tissue was visible over all the reflecting surfaces. In covered struts, thickness of coverage was measured from the strut marker to the adluminal edge of the tissue, following a straight line connecting the strut marker with the center of gravity of the vessel.

The clustering and spatial distribution of uncovered struts were summarized in "spread-out vessel graphics"13 (Figure 1).

Figure 1: Examples of spatial distributions of uncovered struts in spread-out-vessel graphs. Examples of 1 BES (upper panel) and 1 SES (lower panel) studied with OCT at 9 and 24 months. The x-axis represents the distance from the distal edge of the stent to the strut; the y-axis represents the angle where the strut is located in the circular cross section with respect to the center of gravity of the vessel. The result is a graph representing the spatial distribution of the noncovered struts (red spots) along the stent, as if it had been cut along the reference angle (0°) and spread out on a flat surface.

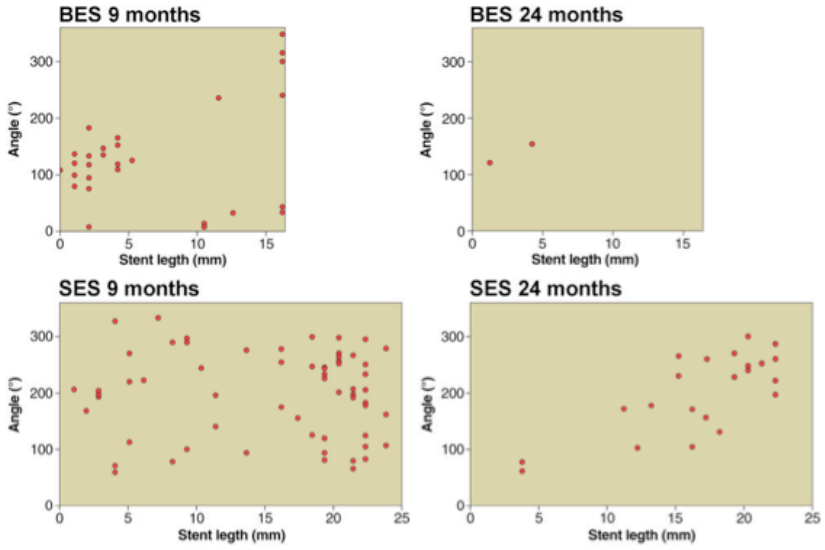

Statistical analysis

Prespecified primary outcome was the difference in percentage of uncovered struts at 24 months. Assuming an average number of 1.5 lesions per patient and 180 struts per lesion, an intracluster correlation coefficient of 0.04 for binary coverage of struts within lesions, and a design factor of 1.3, we estimated that the inclusion of 22 patients (with 33 lesions and 5,940 struts) per group would yield a greater than 90% power to detect a difference in uncovered struts of 4% at 9 months between BESs and SESs at a 2-sided type I error of 0.05. Secondary outcomes comprised other variables assessing coverage, ISA, and the geometric mean thickness of coverage. To estimate the differences between BES and SES, we used a Bayesian hierarchical random-effects model based on Markov chain Monte Carlo simulations with minimally informative priors. The model included random effects at the level of lesions and patients, fully accounting for the correlation of lesion characteristics within patients and their variation between patients. We used the Wilcoxon test for continuous variables and the Pearson $\chi 2$ or Fisher exact test as appropriate for dichotomous variables to compare baseline characteristics as well as areas and volumetric parameters per stent. Statistical analyses were performed using WinBUGS version 1.4.3 (Imperial College and Medical Research Council, London, UK) and Stata release 11 (StataCorp, College Station, TX).

Results

Eighty-eight patients (43 BES, 45 SES) were allocated to angiographic follow-up in the OCT study centers. Optical coherence tomography studies from 46 patients were finally analyzed at 9 months. All 46 patients were contacted at 24 months, but 25 refused to participate in a second invasive follow-up (20 BES, 26 SES). Sequential OCT follow-up was analyzed in 10 patients, 11 lesions, and 12 stents in

the BES group (2,455 struts at 9 months, 2,131 struts at 24 months) and in 10 patients, 11 lesions, and 18 stents in the SES group (3,421 struts at 9 months, 4,170 struts at 24 months). All 9-month studies were performed with a time-domain M3 system, whereas 15 studies at 24 months (71%) were performed with a Fourier-domain C7 system (Table I).

The baseline characteristics of the patients and lesions were comparable between both groups (Tables II and III). Table IV shows the mean areas and volumes per stent. At 9 months, corrected ISA volume was higher in SES than in BES ($P \leq .047$), decreasing in both groups at 24 months and making the difference no longer significant ($P \leq .171$).

Figure 2 shows the evolution of coverage between 9 and 24 months in representative cross sections, matched using fiduciary landmarks.

Figure 2: A, Representative examples of matched cross sections at 9 and 24 months in BESs showing the pattern of coverage. B, Representative examples of matched cross sections at 9 and 24 months in SESs showing the pattern of coverage.

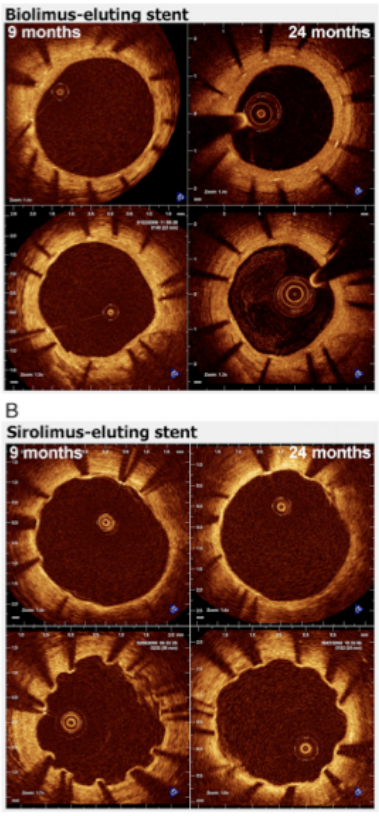

A total of 121 of 2,455 and 69 of 2,131 struts were uncovered in the BES group at 9 and 24 months, respectively; 286 of 3,421 and 109 of 4,170 struts were uncovered in the SES group at 9 and 24 months, respectively. At 9 months, the overall proportion of uncovered struts tended to be higher in SES than in BES, although it did not reach conventional levels of statistical significance (Table V). At 24 months, the proportion of uncovered struts decreased to similar levels in both groups (weighted percentage 2%) (Table V, Figure 3). The spread-out-vessel charts present the results for individual patients, showing the spatial distribution and temporal evolution of uncovered struts in 30 stents (Figure 4). There was little evidence for the differences in thickness of coverage or in the variables estimating apposition between the treatment groups at 9 or 24 months (Table V, Figure 6).

Table II: Patients Characteristics

	BES (n = 10)	SES (n = 11)	P
Age (y), mean (SD)	61.3 (6.6)	60.3 (10.8)	.78
Male	7 (70)	7 (64)	1.00
Diabetes mellitus	2 (20)	2 (18)	1.00
Hypertension	3 (30)	6 (55)	.39
Hypercholesterolemia	5 (50)	9 (82)	.18
Smoking	3 (30)	7 (64)	.20
Previous MI	4 (40)	5 (45)	1.00
Previous PCI	2 (20)	3 (27)	1.00
Previous CABG	1 (10)	1 (9)	1.00
Clinical presentation			
Stable angina	6 (60)	6 (55)	1.00
Acute coronary syndrome	4 (40)	5 (45)	1.00
Unstable angina	0 (0)	2 (18)	
NSTEMI	1 (10)	2 (18)	
STEMI	3 (30)	1 (9)	
Angiographic characteristics			
No. of lesions per patient, mean (SD)	1.8 (0.9)	1.2 (0.4)	.09
Multivessel disease	4 (40)	0 (0)	.035
Long lesions (>20 mm)	3 (30)	6 (55)	.39
Small-vessel disease (RVD < 2.75mm)	6 (60)	8 (73)	.66

Results are expressed as n (%) unless otherwise indicated. *MI* indicates myocardial infarction; *PCI*, percutaneous coronary intervention; *CABG*, coronary artery bypass graft; *NSTEMI*, non–ST elevation myocardial infarction; *STEMI*, ST elevation myocardial infarction; *RVD*, reference vessel diameter.

Table III: Angiographic and procedural characteristics of the lesions

	BES (n = 11)	SES (n = 11)	P
Coronary artery of the target lesion			.51
LAD	6 (55)	3 (27)	
LCX	1 (9)	1 (9)	
RCA	4 (36)	7 (64)	
De novo lesions	10 (91)	11 (100)	
Bifurcation	2 (18)	2 (18)	1.00
Total occlusion	5 (45)	4 (36)	1.00
Severe calcification	1 (9)	2 (18)	1.00
QCA (in-stent)			
Lesion length (mm), mean (SD)	18.4 (14.6)	30.0 (29.0)	.53
RVD (mm), mean (SD)			
Pre-stenting	2.8 (0.5)	2.7 (0.6)	.81
Post-stenting	2.5 (0.5)	2.7 (0.6)	.45
9 mo	2.5 (0.4)	2.8 (0.6)	.19
MLD (mm), mean (SD)			
Pre-stenting	0.7 (0.8)	0.7 (0.6)	.94
Post-stenting	2.3 (0.4)	2.3 (0.5)	.87
9 mo	2.1 (0.8)	2.1 (0.6)	.68
Late lumen loss (mm)	1.4 (0.8)	1.3 (0.4)	.65
Procedural characteristics, mean (SD)			
No. of study stents per lesion	1.5 (0.7)	2.0 (1.2)	.33
Maximal stent diameter per lesion	3.1 (0.3)	3.1 (0.5)	.87
Total stent length per lesion	28.6 (21.2)	45.5 (34.7)	.18
Direct stenting	5 (45)	4 (36)	1.00

Results are expressed as n (%) unless otherwise indicated. *LAD* indicates left anterior descending; *LCX*, left circumflex; *RCA*, right coronary artery; *QCA*, quantitative coronary angiography; *RVD*, reference vessel diameter; *MLD*, minimal lumen diameter.

Table IV: Areas and volumetric analysis per stent (excluding overlap segments) at 24-month follow-up

	9 mo			24 mo		
21 patients, 22 lesions, 30 stents	**BES: 10 patients, 11 lesions, 12 stents**	**SES: 11 patients, 11 lesions, 18 stents**	***P***	**BES: 10 patients, 11 lesions, 12 stents**	**SES: 11 patients, 11 lesions, 18 stents**	***P***
Stented length (mm)	23.43 (13.87)	35.84 (24.78)	.193	23.05 (13.13)	35.82 (26.20)	.401
MLA (mm^2)	4.86 (2.40)	4.58 (2.46)	.748	4.89 (1.73)	4.96 (2.30)	.898
Lumen volume (mm^3)	144.69 (69.37)	252.92 (189.96)	.438	145.91 (77.34)	260.44 (176.21)	.300
Minimum stent area (mm^2)	5.38 (2.11)	5.03 (2.18)	.606	5.87 (1.52)	5.68 (2.42)	.949
Stent volume (mm^3)	158.79 (73.43)	263.02 (197.75)	.562	170.13 (87.40)	287.54 (196.02)	.365
ISA volume (mm^3)	0.24 (0.45)	4.28 (10.09)	**.040**	0.13 (0.44)	1.48 (2.11)	.151
Corrected by stent volume (%)	0.15 (0.24)	1.76 (3.52)	**.047**	0.11 (0.35)	0.78 (1.34)	.171
NIH volume (mm^3)	14.33 (18.57)	14.50 (18.17)	1.000	24.35 (18.86)	28.58 (29.12)	.949
Percent NIH volume obstruction (%)	9.02 (10.02)	5.76 (5.03)	.606	14.53 (9.57)	9.43 (5.37)	.171

MLA, Minimal lumen area.
P-values ≤ 0.05 in bold.

Table V: Analysis of apposition and coverage per strut at 9 and 24 months

21 patients, 22 lesions, 30 stents			BES: 10 patients, 11 lesions, 12 stents; weighted % (95% CrI)	SES: 11 patients, 11 lesions, 18 stents; weighted % (95% CrI)	Comparison	
					Difference (95% CrI)	P
9 mo	Struts	6226	2640	3586		
	Coverage	Uncovered struts*	2.8 (0.9-7.3)	5.7 (2.0-14.3)	−2.9 (−11.6 to 2.9)	.31
		Lesions with				
		≥10% uncovered struts	18.6 (2.2-60.3)	29.8 (5.2-71.7)	−9.6 (−57.2 to 37.8)	.66
		≥5% uncovered struts	42.9 (9.8-82.9)	58.0 (17.7-90.6)	−14.0 (−65.3 to 43.2)	.63
		Any uncovered struts	91.6 (59.5-99.4)	100.0 (92.6-100.0)	−7.9 (−40.0 to 0.2)	.054
		Thickness of coverage (μm)†	56.7 (32.5-101.9)	41.6 (23.4-70.2)	14 (−21 to 64)	.41
	Apposition	ISA struts	0.5 (0.2-1.5)	1.4 (0.5-3.5)	−0.8 (−3.0 to 0.4)	.18
		Lesions with				
		≥10% ISA struts	0.0 (0.0-1.3)	3.2 (0.1-27.2)	−3.1 (−27.2 to −0.0)	.035
		≥5% ISA struts	0.0 (0.0-1.3)	3.2 (0.1-27.2)	−3.1 (−27.2 to −0.0)	.035
		Any ISA struts	73.2 (29.9-96.1)	91.6 (56.2-99.3)	−16.2 (−61.8 to 22.5)	.34
24 mo	Struts	6490	2337	4153		
	Coverage	Uncovered struts*	1.5 (0.5-4.2)	1.8 (0.6-4.5)	−0.2 (−3.2 to 2.6)	.84
		Lesions with				
		≥10% uncovered struts	2.9 (0.1-25.4)	0.0 (0.0 to −)‡	2.9 (0.0-25.4)	.012
		≥5% uncovered struts	31.2 (5.5-74.3)	8.2 (0.6-41.4)	20.2 (−18.1 to 66.7)	.27
		Any uncovered struts	73.1 (30.1-96.0)	97.2 (74.7-100.0)	−21.9 (−65.7 to 6.0)	.12
		Thickness of coverage (μm)†	86.4 (60.2-121.4)	62.2 (44.5-87.7)	24 (−15 to 62)	.17
	Apposition	ISA struts	0.1 (0.0 to −)‡	0.4 (0.1-1.4)	−0.3 (−1.3 to 0.1)	.15
		Lesions with				
		≥10% ISA struts	0.0 (0.0-0.7)	0.0 (0.0-0.7)	−0.0 (−0.7 to 0.6)	.49
		≥5% ISA struts	0.0 (0.0-1.1)	2.7 (0.0-25.0)	−2.6 (−24.9 to −0.0)	.042
		Any ISA struts	18.6 (2.3-60.3)	71.3 (27.0-95.1)	−48.7 (−85.1 to 5.2)	.08

Weighted percentages and differences are derived from medians and 25th and 97th percentiles of the corresponding posterior distributions in WinBugs. *CrI* indicates credibility interval.
* Prespecified primary outcome of OCT substudy.
† Averages are geometric means and differences in geometric means derived from posterior distributions in WinBugs (Imperial College and Medical Research Council, London, UK).
‡ Note that the upper limit of the 95% CrI could not be estimated.

Figure 3: trend graph showing the weighted percentage of covered struts at 9 and 24 months for both types of stent.

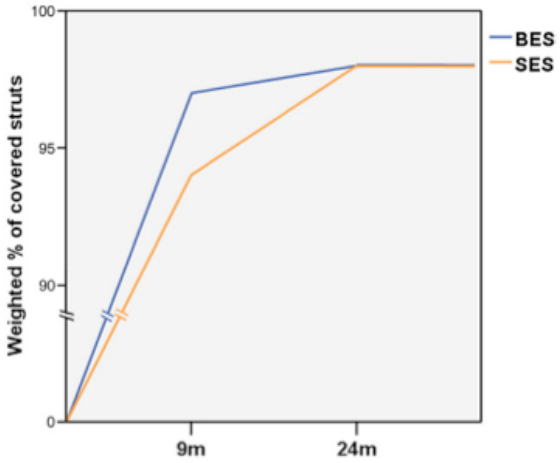

Figure 4: Spread-out-vessel charts showing the spatial distribution of uncovered struts at 9 and 24 months in the matched stents.

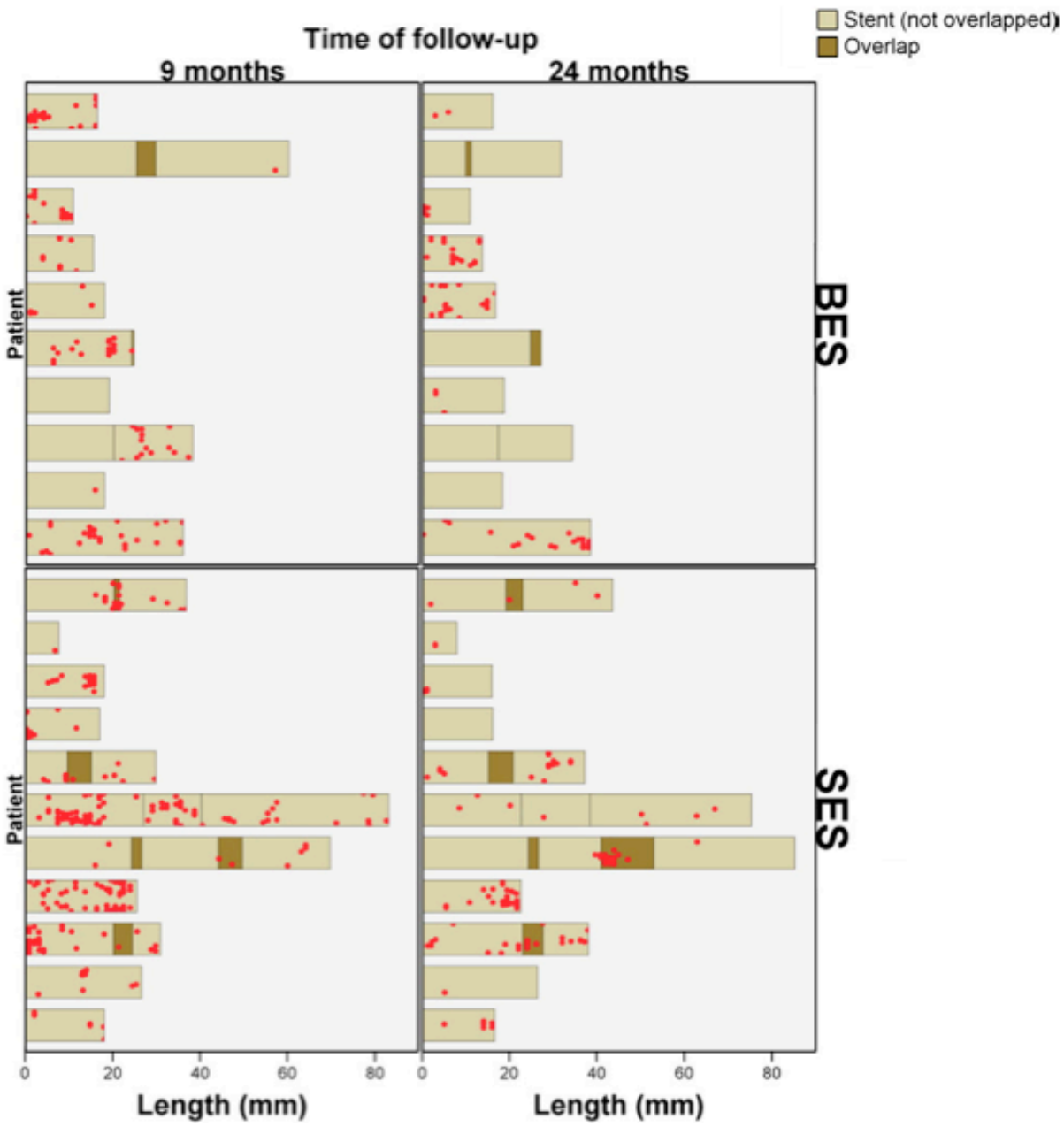

Discussion

In this sequential OCT study nested in a randomized comparison of 2 different DESs, we found that the advantage of a BES with a biodegradable polymer in abluminal coating over an SES with a durable polymer in terms of strut coverage at 9 months was followed by improvement of the SES coverage between 9 and 24 months, resulting in similar coverage in BES and SES at 24 months. Both types of stent converged at a maximum plateau around 98% strut coverage. Taken together, our results suggest that BES, indeed, is associated with faster healing compared with SES, achieving a percentage of coverage close to the maximum plateau (97%) at 9 months, whereas SES is catching up subsequently. To our knowledge, this is the first clinical in vivo study using sequential OCT to compare the coverage of 2 different types of DES. Previous sequential studies had reported SES coverage at 6 to 12 months16 and at 24 to 48 months17 using OCT, or at 4-11-21 months using angioscopy18; the latter was compared with a control bare metal stent.

"Very late healing" phenomenon

The improvement in coverage observed in SES between 9 and 24 months challenges the currently accepted evidence about the healing process after stenting and compels us to reconsider the initial interpretation of the 9-month results. Experimental studies suggested that the reendothelialization process ensuing a vessel injury, for example, stenting, was limited in time (18-20). Endothelial denudation of carotid arteries is followed by reendothelialization that stops after 2 weeks (in the rabbit) or after 6 weeks (in the rat), although endothelial continuity has not been restored (21, 22). This experimental evidence seemed consistent with the results of sequential angioscopic studies in SES, showing no improvement in the minimum coverage between 6 and 24 months, with an increase in the maximum and only slight improvement in the predominant score at 4-11-21 months, eventually suggesting an arrested healing process undergoing phenomena

of intima maturation or plaque progression. Our results question this static time-limited model of neointimal healing, suggesting a more dynamic process, still evolving between 9 and 24 months. Previous noncomparative studies using OCT suggested also this possibility: improvement of SES coverage has been reported at 3-24-48 months (23, 24) or between 6 and 12 months (25). Because of its high resolution (10-20 μm) and ability for detailed analysis, OCT could detect subtle changes in neointimal coverage, which are unnoticed for angioscopy or other imaging techniques. The evolution of neointimal volumes, increasing similarly in both stent groups between 9 and 24 months (Table IV), might indicate an actively repairing neointima but can also be the consequence of intima maturation or plaque progression. The ISA reduction between 9 and 24 months is more specific as an indicator of very late healing. Higher incidence of ISA in the SES group had been reported at 9 months and interpreted in terms of late-acquired ISA. This interpretation now becomes unlikely because the most pronounced reduction in ISA between 9 and 24 months is observed in SES. This is in disagreement with previous sequential studies reporting an increase in ISA areas and ISA struts between 24 and 48 months in SES (26). This discrepancy deserves further clarification in the future.

Different healing rates in different types of stent

The design of our study does not permit to elucidate the mechanism for the different healing rates observed between the devices. Although inflammation was the driving hypothesis for this study and was advocated to explain the differences reported at 9 months, it cannot satisfactorily explain the very late healing. Why does the initial advantage in coverage not persist after the proinflammatory polymer has completely disappeared in one of the devices? The role played by polymer-induced inflammation in the neointimal healing after stenting should be revisited: its deleterious effect might be not as sustained in time as currently

assumed, with the exception of infrequent delayed hypersensitivity reactions (27, 28). The kinetics of release differ from the coverage rates observed: the elution periods for SES and BES are 90 days and 6 to 9 months, respectively. The different inhibitory potency, lipophilicity, concentration, or pleiotropic effects of biolimus and sirolimus have played a role: the effective neointimal inhibition could be more intense in SES than in BES. Likewise, the design and geometry of the stent platforms could have promoted faster healing in the BES, especially the strut thickness. Both platforms are made of stainless steel, hence requiring thick struts (>100 μm) to provide enough radial strength for vessel scaffolding; but BES struts are slightly thinner (120 μm) than SES struts (140 and 154 μm if we add the polymer thickness), which is associated with faster healing. The selective abluminal coating of BES appears to be a more plausible explanation: the abluminal release of the drug might modulate the proliferation of smooth muscle cells in the media that minimally interferes with the reendothelialization of the adluminal side, thus promoting a faster reendothelialization.

Clinical implications

Very late healing could be key to understanding why clinical studies have failed to demonstrate higher rates of stent thrombosis in SES (29), although angioscopy or OCT have reported suboptimal coverage between 3 and 48 months. As suggested by our results and also by other studies, longer follow-up intervals would be required to assess the final neointimal coverage achieved.

To our knowledge, this is the first sequential OCT study suggesting that different types of stent can promote different healing rates. This may be relevant for tailoring the duration of dual-antiplatelet therapy after stenting.

Limitations

The refusal of some patients to undergo the 24-month OCT follow-up is the main limitation of this study. It might have induced some selection bias because the patients with more favorable outcome might have been more prone to refuse a second invasive follow-up. The lack of statistical significance at 9 months in this second analysis is also explained by the substantial loss of statistical precision resulting from the restricted sample size and not contradictory with the previously published results (30). The high percentage of refusals turned this study underpowered to detect the difference of the same magnitude.

2.1.3 Study 3

Title: Time-related changes in neointimal tissue coverage following a new generation SES implantation: an optical coherence tomography observational study.

Background

Drug eluting stent (DES) have become the treatment of choice for patients with symptomatic coronary artery disease undergoing PCI. Although this technology has reduced rates of restenosis and late lumen loss compared with bare metal setnt (BMS) it has been associated with delayed healing that might result in a small but statistically significant increase in Late and Very Late Stent Thrombosis.

Aim

The aim of our observational study was to evaluate using Optical Coherence Tomography (OCT) the time-related changes in vascular response following implantation of a new generation biodegradable polymer Sirolimus-eluting stent with an amorphous silicon carbide coating allowing higher biocompatibility and faster re-endothelisation (Orsiro DES, Biotronik AG, Bulach, Switzerland).

Materials and Methods

Study design and population

This prospective monocentric observational Registry enrolled only patients with acute STEMI and a multi-vessel disease (MVD), thus eligible for a two-step procedure. The PCI of the culprit lesion was performed with at least one Orsiro stent. The second procedure was then deferred accordingly to the severity of the non-culprit lesion and the presence of symptoms and signs of residual ischemia to

30 days, 90 days and 180 days. During the second procedure, the stent deployed at the infarct-related site was analysed by OCT.

The Orsiro Sirolimus Eluting Stent

The Orsiro DES (Biotronik Ag, Bulach, Switzerland) is a cobalt-chromium 60 micron and 80 micron stent struts (the lowest for the stent with a diameter ranging from 2.25 to 3.0 while 80 micron thickeness is for the 3.5 and 4.0 diameter stents), coated with a poly-L-lactide (PLLA) polymer that delivers sirolimus drug over 12–14 weeks and degrades over one to two years. It presents a unique thin-layer, amorphous silicon carbide coating (PROBIO) that reduces interaction between the metal stent and the surrounding tissue and blood by acting as a diffusion barrier aiming to improve the biocompatibility of the material by reducing thrombogenicity and encouraging re-endothelialisation.

Interventional Procedure

The PCI was routinely performed with the standard techniques via femoral or radial approach using 6 or 7 French guiding catheters. Patients not preloaded with oral aspirin and/or clopidogrel received a loading dose of intravenous aspirin (500mg) and clopidogrel (600mg) or prasugrel (60mg) or ticagrelor (180mg) as standard practice in our Catheterization Laboratory. Intravenous heparin (70 UI/Kg body weight) was administered before the procedure with subsequent boluses aiming at achieving an activating clotting time (ACT) between 250 and 300sec. In case of Bivalirudin administration a 0.75 mg/kg bolus dose followed by a 1.75 mg/kg per hour intravenous infusion terminated immediately after the end of the procedure was administered. Manual thrombectomy was performed in all cases and the use of GP IIb/IIIa inhibitors was left to operator's discretion. All lesions were finally treated with the study device implantation. The deferred PCI of the non culprit lesion was routinely performed with the aforementioned standard

techniques and the Orsiro stent previously deployed at the infarct-related artery (IRA) was analyzed with the Frequency Domain OCT (FD-OCT).

OCT acquisition

Frequency Domain OCT (FD-OCT) acquisitions were performed using the Ilumien system (St Jude, Minneapolis, MN, USA) with a motorized automatic pullback at 20mm/s during contrast injec¬tion at a flow rate sufficient to have full substitution of blood with contrast with no streaming according with international guidelines (3). The OCT catheter was inserted distal to the treated segment and the pullback continued until either the guiding catheter was reached or the maximal pull-back length (54 mm) was completed. Two sequential pull-backs were combined to enable assessment of the entire stented segment when required. OCT was used only during the deferred PCI, none of the stent analysed were implanted under OCT guidance.

OCT analysis

The OCT measurements were performed off-line using the LightLab Imaging workstation (LightLab St Jude, Minneapolis, MN, USA) by two blinded operators unaware of the timing of the stent implanted. Divergent opinions were resolved by consensus. Coverage and apposition of the stent struts were analyzed with strut- and cross section-level. The analysis of contiguous cross-sections was performed at 1 mm intervals within the entire stented segment and on 5mm proximal and distal to the stent in order to identify edge dissections defined as a disruption of the vessel luminal surface at the stent edge with visible flap. Struts were considered suitable for analysis only in the presence of a bright signal-intense structure with perpendicular shadow. Number of struts was determined in each cross section analysed. Thickness of the tissue coverage on the luminal side of each strut was measured at the middle of the long axis of the strut. The inner and outer strut's contours were delineated for each strut and its distance to the lumen contour was

calculated automatically to determine strut level intimal thickness. Measured tissue thickness > 0 μm was defined as coverage. Coverage and apposition of the stent struts were analysed with strut- and cross section-level (31, 32). Struts were classified as malapposed if protruding into the lumen at a distance greater than the sum of the strut and polymer thickness (71 μm and 91 μm for the 2.25, 2.5 and 3.0 stent diameter and 3.5, 4.0 stent diameter respectively) plus the minimal axial OCT resolution (20 μm).

Each stent strut was classified as:

1) Apposed and covered: strut well apposed to the vessel wall with tissue coverage:

2) Apposed and uncovered: strut apposed to the vessel wall without tissue coverage;

3) Malapposed and covered: strut malapposed to the vessel wall with tissue coverage;

4) Malapposed and uncovered: strut malapposed to the vessel wall without tissue coverage.

Non-analyzable frames were defined as frames in which in which more than 45° of the lumen border was not visualized for the presence of side branches or for inadequate blood clearance during imaging acquisition. In these cases, the next following or preceding frame of appropriate image quality was used for the analysis.

Clinical follow up

In-hospital, 30 days, and cumulative 12 months MACE were defined as death, myocardial infarction and repeat revascularization (CABG or PTCA). Twelve-lead electrocardiograms were recorded before, immediately after each procedure and at hospital discharge.

Statistical analysis

Continuous variables were expressed as mean ± standard deviation, while categorical variables were presented as numbers with percentage. Continuous variables were compared using paired student's t-test. Categorical variables were compared using chi-square test. A P value ≥ 0.05 was considered statistically significant.

Results

From January 2012 to December 2012 a total of 260 patients underwent to primary PCI in our Institution. 16 of the 95 patients with MVD underwent to OCT evaluation of the study device implanted in the culprit lesion during the second-step staged procedure and were enrolled in the present Registry. Patients and lesion characteristics are shown in table 1.

Table 1: Baseline Clinical and Procedural Characteristics

Clinical Characteristics		**Procedural Characteristics**	
Age	66 ± 12,5	TRA	100%
BMI	27 ± 2	GP IIb/IIIa	100%
Diabetes	42%	IABP	12%
Dyslipidaemia	73%	Thrombus aspiration	100%
Familiarity	47%	stent / pt	2.1
Hypertension	63%	D	2.85 ± 0.76
Smoke	73%	L	21.41 ± 6.21
IRC	10%	Direct	32%
Previous STEMI	5%	Overlapping	86%
Previous PCI	10%	Post-dilatation (ATM)	20.5 ± 3.5
Previous CABG	0%	LMT	6%
Previous TIA	5%	LAD	36%
Killip 3	15%	LCX	16%
Killip 4	5%	RCA	42%

OCT strut level analysis

OCT strut level findings are shown in table 2. A total of 3060 struts were analyzed. Of these, 1065 struts (Group-I), 874 struts (Group-II) and 1130 struts (Group-III) were analyzed at 30 days, 90 days and 180 days respectively. Stent lengths and diameters were similar in the three groups. The percentage of uncovered stent struts was 19.6% at 30 days, 1.3% at 90 days and 1.8% at 180 days ($p \leq 0.001$ Goup-I vs Group-II and vs Group-III; p=ns Group-II vs Group-III). The percentage of malapposed struts was 5.1% at 30 days, 6.2% at 90 days and 4.8% at 180 days (p=ns for all group). Of the malapposed struts 53.7% were covered at 30 days, while 81.5 % and 88.9 % were covered at 90 and 180 days respectively ($p \leq 0.01$ Group-I vs Group-II and vs Group-III; p=ns Group-II vs Group-III).

Table 2: OCT findings for strut level analysis

Variable	Overall	30 days	90 days	180 days	p
Strut analysed	3060	1065	874	1130	
Overall number covered struts	2822 (92.2%)	849 (80.4%) *	863 (98.7%)	1110 (98.2%)	<0.001 *
Apposed	2898 (94.7%)	966 (91.5%) *	825 (94.4%)	1107 (97.9%)	<0.001 *
Apposed and covered (% between apposed)	2739 (94.51%)	819 (84.8%) *	820 (99.4%)	1100 (99.4%)	<0.001 *
Malapposed	162 (5.3%)	54 (5.1%)	54 (6.1%)	54 (4.8%)	NS
Malapposed and covered (% between apposed)	83 (51.2%)	29 (53.7%)	44 (81.5%)	13 (24.1%)	0.01

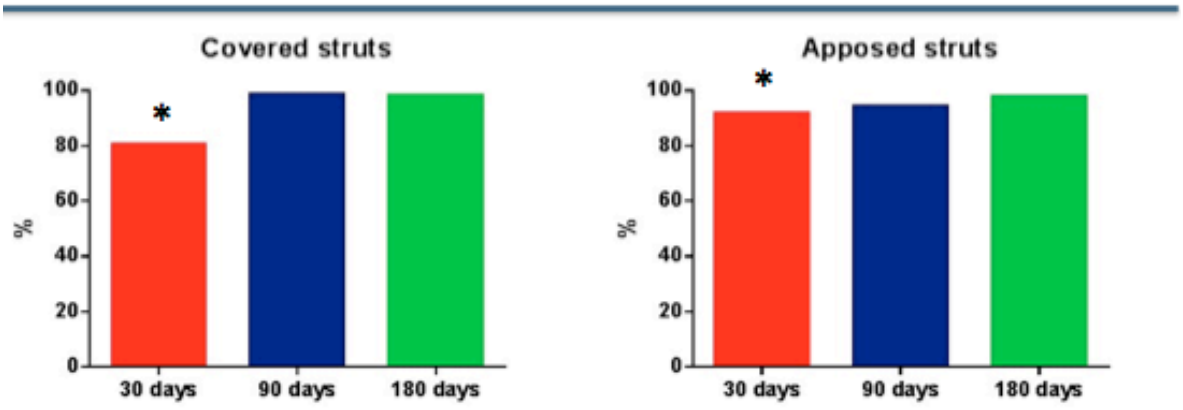

OCT cross-section level analysis

OCT cross-section findings are shown in table 3. The percentage of cross section with ≥ 1 uncovered struts were 51.3% at 30 days, 6.5% at 90 days and 5.7% at 180 days (p≤0.001 Group-I vs Group-II and vs Group-III; p=ns Group-II vs Group-III). The percentage of cross section containing thrombus was 6.2% at 30 days. No thrombus was detected at both 90 and 180 days analysis. Neointimal thickness covering stent struts increased from 0.25 ± 0.21 mm2 at 30 days to 0.81 ± 0.68 mm2 and to 0.94 ± 0.85 at 90 days and 180 days respectively (p≤0.001 Group-I vs Group-II and vs Group-III; p=ns Group II vs Group III).

Table 3: OCT findings for cross-section level analysis

Variable	Overall	30 days	90 days	180 days	p
Cross sections analysed	327	113	92	122	
Cross section with ≥ 1 uncovered strut	78 (22.9)	58 (51.3%) *	6 (6.5%)	7 (5.7%)	<0.001 *
Cross section with ≥ 1 malapposed strut	55 (16.8)	19 (16.8%) *	18 (19.5%)	18 (14.7%)	NS
Thrombus	7 (2.1)	7 (6.2%) *	0	0	NA
NIH, mm2	0.66 ± 0.72	0.25 ± 0.21 *	0.81 ± 0.68	0.84 ± 0.85	< 0.001 *

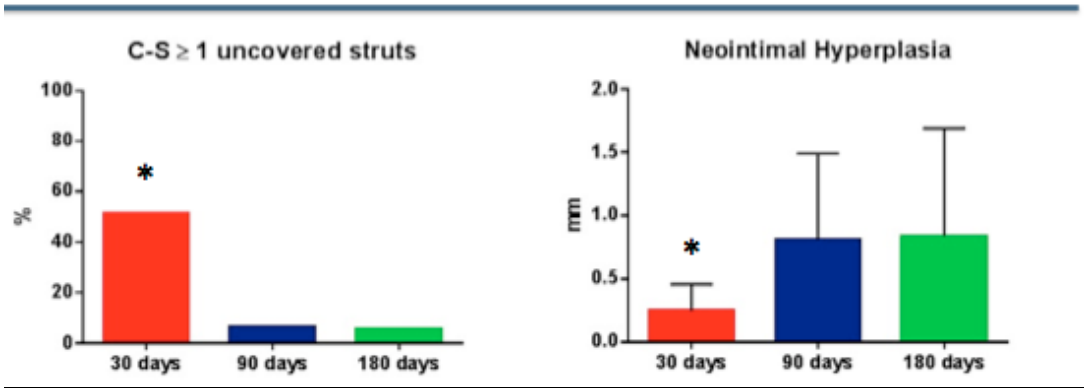

Clinical Follow Up

No in-hospital, no 30 days and no 12 months MACE (death, myocardial infarction and repeat revascularization CABG or PTCA) were reported.

Discussion

The main finding of this pilot study is that a very high percentage of stent struts (98.7%) presented a fast patter of thin layer coverage at 90 days that remain steady at 180 days follow-up. Interestingly, the homogeneous pattern of tissue coverage was found to be present even in malapposed struts that accounted for about 5% of all analysed struts. Our study population was strictly represented by a STEMI group were the trend of vessel undersizement might explain the relatively high percentage of malapposed struts found at OCT follow up. The low percentage of cross-sections containing thrombus might be related both to the ability of the PROBIO system in reducing thrombogenicity and to the high frequency of thrombectomy and GP IIb/IIIa inhibitors administration used in the current study. The almost complete homogeneous tissue coverage around stent struts found already at 90 days was somehow unexpected in a stent that elutes sirolimus, the mainly appointed drug in the pathogenesis of long-term incomplete strut coverage causing late and very late stent thrombosis.

In fact, delayed healing and poor endothelialisation were common findings in pathologic specimens of vessels treated with SES (26, 27, 33) and pathology studies demonstrated that the best predictor of late stent thrombosis was the ratio of uncovered/total stent struts (25). This complication especially affects the first generation DES, in which the mechanism for incomplete neointimal coverage seems to go beyond the antiproliferative potency of the drug and also involve a type IVb hypersensivity reaction (34). Hypersensivity is likely triggered by the polymer rather than by other components of the devices and several randomized

trials, all comers registry and metanalysis have shown a different pattern of struts endothelialisation between durable and biodegradable eluting stents (35). In a recently published metanalysis comparing durable versus biodegradable polymer DES and including more than 20.000 patients, our group found a significant reduction of late lumen loss and late stent thrombosis in biodegradable polymer DES but without significant benefits on harder end-points such as mortality, myocardial infarction or revascularization rates. Additionally, in the same study, a prespecified meta-regression highlighted the influence of stent strut thickness on target lesion revascularization and late stent thrombosis. It must be noted that the study device presents one of the lower strut thickness of the commercially available DES. The long term safety and efficacy of the study device has been tested in a randomized trail comparing Orsiro (Biotronik AG, Bulach, Switzerland) vs Xience (Abbot, Abbott Park, Illinois, USA). The results showed a non-inferiority of the Orsiro stent in term of late lumen loss, target lesion failure and cardiac death both at 9 months and 2 years follow up. However, EES-CoCr stents presents an almost unique evidence of improved safety profile. In fact, in a recently published metanalysis of 11 randomized trials, Palmerini et al. found a significant reduction of EES compared with other DES in the relative risk of early, late and very late stent thrombosis (36). Moreover, in another study, the same group also found that CoCr-EES presents the lowest rate of stent thrombosis within 2 years of implantation even when compared with BMS (37). Despite these findings, the international guidelines still sees the 12 months - dual antiplatelet therapy as the gold standard in DES treated patients irrespective of the type of polymer or drug eluted. One of the key finding potentially able to shorten the 12-month long antiplatelet therapy might be the in-vivo detection of the ratio of uncovered/total stent struts, probably the best predictor of late stent thrombosis. However, unlike conventional stents that develop circumferential coverage with an average

thickness of 500 μm or more, which are well-visualized with IVUS and angiography (1-mm late loss), DES delay and prevent the hyperplastic response so that the average late lumen loss for sirolimus or paclitaxel-eluting stents can be lower than 100 μm. Therefore, the amount of intimal thickening will not be detectable with IVUS because of its limited axial resolution and the presence of artifacts around struts. Angioscopy has been successfully used to compare neointimal coverage pattern and incidence of stent thrombosis, but its use is limited in daily clinical practice (38). The use of intravascular optical coherence tomography (OCT), an imaging technique that employs near-infrared light and provides cross-sectional images with an axial resolution of 10 μm, has provided new opportunities to perform a more refined analysis of vessel response to endovascular devices. OCT offers a unique combination of minimally invasive surface scanning technology and in-vivo images of biological samples at a resolution 10–30 times higher than conventional intravascular ultrasound (IVUS). In fact several experimental and clinical studies demonstrated the high correlation between OCT and histological measurements of neointimal coverage of stent struts, highlighting the superiority of OCT over IVUS for in-vivo detection of stent tissue coverage at follow-up. The introduction of user friendly second generation OCT probes based on frequency domain analysis, due to its fast-scanning laser system, allows multiple acquisition of the entire segment of interest without the need of prolonged crystalloid infusion but only with a small amount of contrast slightly greater than the one required for control angiogram. Using OCT we were able to evaluate the time related changes in strut tissue coverage and thrombus formation among in our study population treated with a “third” generation sirolimus eluting stent.

Limitations

The major limitation of this pilot study is the small size of the study population, justified by the rarity of STEMI patients with multivessel disease were the non-culprit lesion can be treated in an elective PCI deferred to a long term period raging from 30 to 180 days. Moreover, the OCT was employed only during the second step procedure and none of the study device was implanted under OCT guidance.

2.1.4 Study 4

Title: ABSORB biodegradable stents versus second-generation metal stents: a comparison study of 100 complex lesions treated under OCT guidance.

Background

Thick polymer-based bioresorbable vascular scaffold (BVS) have different mechanical properties than thin second generation drug eluting stent (DES). Data on acute performance of BVS are limited to simple coronary lesions treated in trials with strict inclusion criteria.

Aim

The aim of this study was to compare the acute performance of BVS versus second generation DES in the treatment of complex coronary artery lesions using Optical Coherence Tomography (OCT) to assess appropriate stent deployment.

Materials and Methods

Study population.

The study population comprised of consecutive patients undergoing PCI of complex coronary lesions with stent optimization under OCT guidance, which is our routine for complex lesion stenting (39). From September 2012 till May 2013 patients treated with BVS at the Royal Brompton Hospital (London, United Kingdom) and Columbus Hospital (Milan, Italy) were prospectively enrolled. Out of 148 patients with complex lesions treated with second generation DES at the Royal Brompton Hospital between January 2009 and May 2013 and optimised using post-deployment OCT examination (DES-group) we selected an equal number of lesions with matched angiographic characteristics to those in the BVS-group. The 1:1 selection without replacement has been performed accordingly to

the following stepwise selection criteria: lesion length, vessel reference diameter, ostial position, bifurcation involvement, severe or moderate calcifications, chronic total occlusion.

All patients signed an informed consent for stent deployment and OCT guidance. The devices used in the DES-group were the Everolimus eluting Xience Pro and Prime (Abbott Vascular,Santa Clara,CA), Promus Element and Premiere stent (Boston Scientific,Natick,Massachusetts) and the Zotarolimus eluting Resolute Integrity stent (Medtronic Vascular,Santa Rosa,CA). BVS were not used in patients presenting with acute ST-segment elevation myocardial infarction, coronary bifurcations with a default two stent strategy, target lesion in a vessel with a reference diameter <2.5mm and, because of impossibility to perform serial OCT examinations, e-GFR<30ml/min, or aorto-ostial lesions. The main inclusion criteria in the BVS group used to define the lesion complexity were length>24mm, moderate to heavy calcification, ostial (different from aorto-ostial), bifurcation involvement and chronic total occlusion (CTO).

QCA analysis and lesion characterisation

QCA was performed using a computer-based QCA system (CAAS QCA -2D system, Pie Medical Imaging BV, the Netherlands) with the dye-filled catheter used for calibration (40). For each lesion the following QCA parameters were measured: Minimum Lumen Diameter (MLD), Reference Vessel Diameter (RVD), percentage Area Stenosis (%AS) and Lesion obstruction Length (LL). The largest balloon diameter and maximal inflation pressure during lesion predilatation were recorded and used to calculate the balloon/artery ratio (mean inflated balloon diameter/mean reference vessel diameter). In addition, we assessed the presence of angiographic calcification.

Treatment procedures

In both groups, lesions were treated with pre-dilatation using conventional semi-compliant or NC balloons. The use of additional devices, cutting balloons or rotablator, was left at the operator's discretion. Unlike for DES, deployment of BVS was performed using slow balloon inflation (i.e. 2 atm per 10s) without exceeding the rated pressure indicated in the product instructions for use. Post-dilatation with short NC balloons was systematically performed both for BVS and DES, using OPN NC balloons (SIS Medical AG, Winterthur Switzerland) when pressures higher than 30 Atm were required (41). Attention was paid to avoid reaching a maximal balloon diameter beyond the recommended rupture point of the BVS, by strictly following the NC balloon compliance chart. In case of lesions involving a bifurcation, final optimization with sequential dilatation was preferentially adopted for BVS. Conversely, for DES final kissing balloon was the default strategy. OCT assessment was performed in most cases before stent deployment and repeated when stent expansion was considered optimal angiographically. In the event of suboptimal deployment as assessed with OCT, further post dilatation was performed or additional BVS/DES were implanted, after which a final OCT acquisition was performed and used for the study analysis.

OCT acquisition.

Frequency domain-OCT was performed using the C7 system or the Ilumien Optis system (St Jude, Minneapolis, MN, USA). For both systems, DragonFly or DragonFly-2 imaging catheters were used. Automatic pullbacks were performed at 20mm/s during contrast injection at a rate of 3-5ml/s using a power injector. The OCT catheter was inserted distal to the treated segment and the pullback continued until either the guiding catheter was reached or the maximal pull-back length (5.5 cm with C7 and 7.4 cm with Ilumien Optis) was completed. Two sequential pull-backs were combined to enable assessment of the entire stented segment when required.

OCT off line analysis.

The OCT measurements were repeated off-line using the LightLab Imaging workstation (St Jude, Minneapolis,MN,USA). The analysis of contiguous cross-sections was performed at 1mm intervals within the entire stented segment and on 5mm proximal and distal to the stent in order to measure the proximal and distal Reference Vessel Area (RVA) and to identify dissections. RVA was calculated as the mean of the two largest luminal areas in the 5mm proximal and distal to the DES/BVS edge (3). In case of absence of a meaningful proximal or distal segment due to the ostial location of the lesion or the presence of a large side branch at the stent edge, only a proximal or distal reference cross-section was used to calculate RVA (42). Stent edge dissection was defined as a disruption of the vessel luminal surface at the stent edge with visible flap. Stent fracture was suspected in the presence of isolated struts lying unapposed in the lumen with no connection or overridden by the contiguous stent struts. For each cross section analysed, the area, mean, maximal and minimal diameter of the stent were automatically contoured and measured by the analysis system, with manual correction as appropriate (43).

For analysis of BVS, which are transparent to the near infrared light of the OCT catheter, ISA was defined as presence of struts separated from the underlying vessel wall (44). For metallic DES, inducing a posterior drop-out, struts were considered malapposed when the axial distance between the strut's surface to the luminal surface was greater than the strut thickness. Tissue prolapse was defined as the presence of tissue protruding between stent struts extending into the lumen as a circular arc connecting adjacent struts.

The following quantitative parameters were calculated for each stent (3):

- Percentage of ISA: calculated as a ratio of the total number of struts observed at 1 mm intervals.

- Percentage of stents with ISA at the proximal and distal edges defined as the last 5mm of stent before the stent end.
- ISA area, mm2 (only for BVS) measured as illustrated in Figure 1 .
- Tissue prolapse area (mm2); calculated as the difference between the stent area and the lumen area as illustrated in Figure 1.
- Percentage of RAS calculated as (1-[min lumen area/RVA])x100 as illustrated in Figure 2.
- Eccentricity index: ratio between the minimal and the maximal diameter. For each stent both the mean and minimal eccentricity index were computed (illustrated in Figure 2).
- Symmetry index: defined as (maximum stent diameter–minimum stent diameter)/(maximum stent diameter).

Figure 1: Qualitative and quantitative assessment of OCT characteristics

A) Example of incomplete strut apposition. There are 4 malapposed struts between 10 and 12 o'clock in A1, with one more malapposed strut probably concealed by the wire shadow (asterix). In BVS the possibility to identify the abluminal border of the struts allow the evaluation of ISA area as indicated in green in panel A2. B) Tissue prolapse. In the presence of tissue prolapse, defined as tissue protruding between the struts, prolapse area was measured as the difference between the stent and lumen area (highlighted in green in Panel B2). C) Example of edge dissection (arrow) distally to the BVS. Because of the large lumen size and small circumferential extension of dissection no treatment was performed. D) BVS strut fracture. This cross section at the level of the LAD-D1 carina, shows a scaffold pattern irregularity with an overhanging strut (arrow) in the centre of the vessel without obvious connection to the expected/adjacent strut pattern. In this patient before this final OCT acquisition the BVS was rewired in order to dilate the ostium of D1 with a 2.5 mm semicompliant balloon.

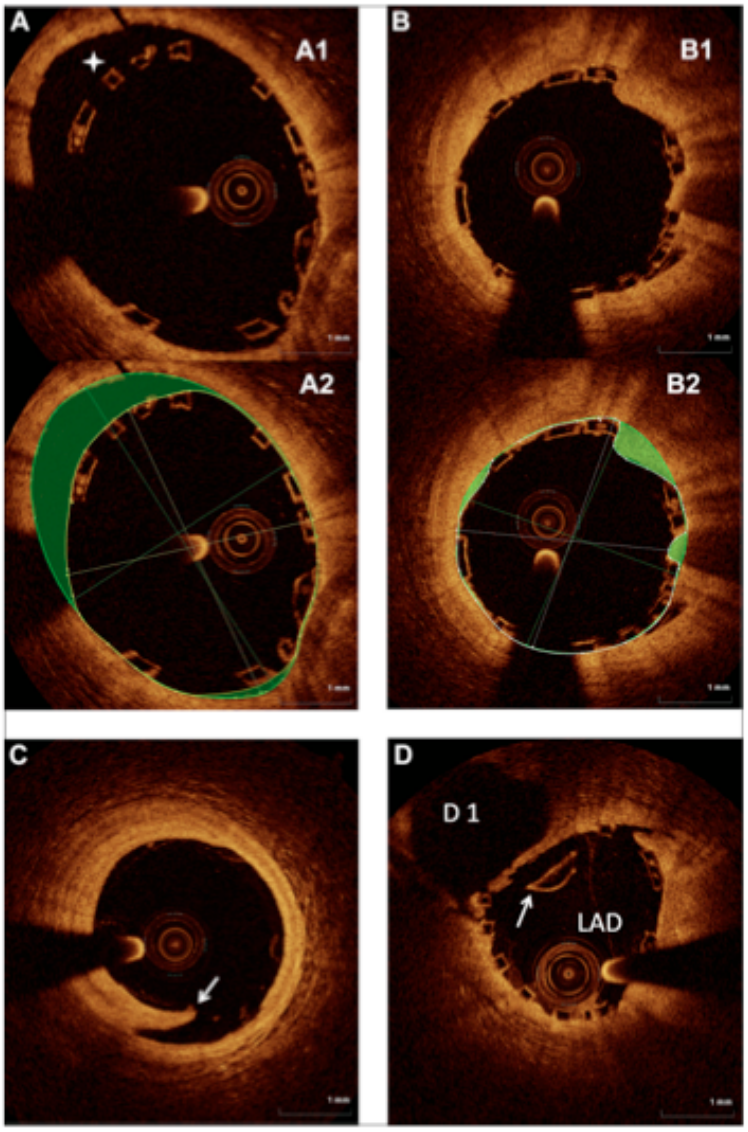

Figure 2: Residual Area Stenosis and Eccentricity Index

The proximal and distal vessel reference area (Panel A and D) were used to calculate the reference vessel area (RVA). The ratio between minimal lumen area (MLA) and RVA was used to compute the residual area stenosis (Panel C). In Panel B is reported an example of evaluation of the minimum eccentricity index.

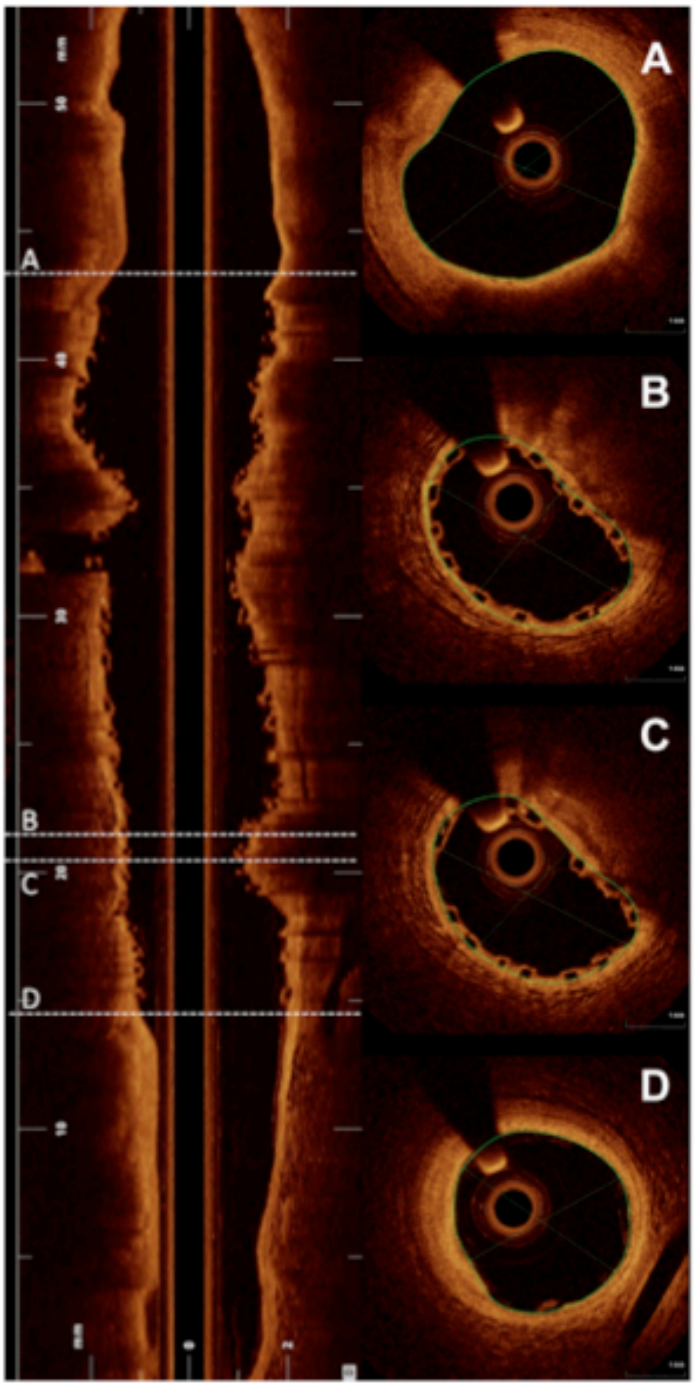

A: Proximal Reference Vessel Area (PRVA) = 10.8 mm²

B: Cross section with the Minimum Eccentricity Index =

(Minimum diameter/Maximum diameter) =

(2.34 mm/3.66 mm) = **0.64**

C: Minimal Lumen Area (MLA) = 6.9 mm²

Residual Area Stenosis =

(1- MLA/RVA*) X 100 =

(1-6.9mm²/ 8.9 mm²) X 100 = **22.5 %**

D: Distal Reference Vessel Area (DRVA) = 7.1 mm²

Reference Vessel Area (RVA) =

(PRVA + DRVA)/ 2 =

(10.8 mm² + 7.1 mm²) / 2 = **8.9 mm²**

Follow-Up

Clinical follow up was obtained approximately at 1 month after the procedure and every 6 months afterward by direct clinical examination.

Statistical analysis

Descriptive statistics (means and standard deviations for continuous variables with normal distribution, frequency and relative frequency for categorical variables) were computed according to treatment type (BVS vs DES). Comparison between groups for continuous variables was performed by unpaired T-test (in case of parametric distribution) or Mann-Whitney U-test (in case of non-parametric distribution), as appropriate. Univariate associations between treatment type and coronary lesion features were examined using two-way contingency tables. Significance of associations were assessed using the Chi-squared test or the Fisher exact test, as appropriate. For all the statistical tests used, a p level of <0.05 was required to reject the null hypothesis. The statistical analysis was performed using the SPSS statistical software package v 16.0 (IBM Corporation, Somers, NY).

Results

Population

Fifty lesions treated with 63 BVS in 35 patients were matched with 50 lesions treated with 61 second generation DES in 38 patients. Baseline patients' clinical characteristics are shown in Table 1. There were no significant differences in the two groups with a minority of patients (4.1%) presenting with unstable angina as an indication for the PCI procedure.

Table 1: Patients characteristics (n=73)

Table 1. Patient Characteristics (N = 73)

	BVS (n = 35)	DES (n = 38)	p Value
Age, yrs	59.7 (11.2)	65.2 (10.7)	0.64
Male sex	27 (77.1)	31 (81.6)	0.77
Hypertension	26 (74.3)	23 (60.5)	0.22
Hypercholesterolemia	24 (71.4)	23 (60.5)	0.45
Diabetes	12 (34.3)	11 (28.9)	0.80
Current smokers	17 (48.6)	14 (36.8)	0.35
Previous PCI	14 (40.0)	8 (21.1)	0.13
Previous myocardial infarction	7 (20.0)	4 (10.5)	0.33
Previous CABG	1 (2.9)	3 (7.9)	0.61
Clinical indication			0.61
Stable angina	34 (97.1)	36 (94.7)	
Unstable angina	1 (2.9)	2 (5.3)	
No. of diseased vessels			0.72
1	14 (40.0)	17 (44.7)	
2	14 (40.0)	16 (42.1)	
3	7 (20.0)	5 (13.2)	

Values are n (%).
BVS = bioresorbable vascular scaffold(s); CABG = coronary artery bypass graft; DES = drug-eluting stent(s); PCI = percutaneous coronary intervention.

Angiographic and QCA baseline lesion characteristics are summarized in Table 2. The left anterior descending (LAD) was the target vessel in a large proportion of cases in both groups (BVS n=34, 68%, DES n=25, 50%; p=0.11). As expected, based on the inclusion criteria, all lesions met the American College of Cardiology/American Heart Association classification criteria for B2 or C lesions. There were no significant differences in presence of calcification, ostial involvement and bifurcation involvement. Reference vessel diameter, minimal lumen diameter and lesion length, as assessed with QCA were also similar (lesion length: BVS 24.7±14.2mm, DES 25.1 ± 10.6mm; p=0.86). Two CTO were successfully treated in the BVS-group and 4 in the DES-group.

Table 2: Angiographic and QCA lesions characteristics (n=100)

Table 2. Angiographic and QCA Lesion Characteristics (N = 100)

	BVS (n = 50)	DES (n = 50)	p Value
Target vessel			0.11
LAD	34 (68.0)	25 (50.0)	
LCX	4 (8.0)	11 (22.0)	
RCA	11 (22.0)	14 (28.0)	
Venous graft	1 (2.0)	0 (0.0)	
AHA/ACC lesion classification			0.38
B2	18 (36.0)	13 (26.0)	
C	32 (64.0)	37 (74.0)	
Moderate to heavy calcification*	31 (62.0)	37 (74.0)	0.28
Chronic total occlusion	2 (4.0)	4 (8.0)	0.67
Ostial involvement	7 (14.0)	5 (10.0)	0.76
Bifurcation involvement	17 (34.0)	23 (46.0)	0.30
Side branch RVD (with QCA), mm	2.3 (0.3)	2.4 (0.4)	0.53
Medina classification†			0.88
1,1,1	5 (29.4)	6 (26.1)	
1,1,0	9 (59.2)	13 (56.5)	
1,0,0	3 (17.6)	4 (17.4)	
In-stent restenotic lesion	6 (12.0)	3 (6.0)	0.48
QCA main branch analysis			
RVD, mm	2.7 (0.4)	2.7 (0.3)	0.86
MLD, mm	0.8 (0.4)	0.7 (0.3)	0.16
AS, %	83.7 (15.2)	86.9 (11.6)	0.25
Lesion length, mm	24.7 (14.2)	25.1 (10.6)	0.86

Values are n (%). *Angiographic assessment of the degree of calcification. †Only Medina combinations represented in the study population are reported.

AS = area stenosis; LAD = left anterior descending artery; LCX = left circumflex artery; MLD = minimal lumen diameter; QCA = quantitative coronary angiography; RCA = right coronary artery; RVD = reference vessel diameter; other abbreviations as in Table 1.

Procedural characteristics

Sixty-three BVS and 61 DES were implanted with a similar number of stent per lesion in the two groups (BVS 1.3±0.6, DES 1.2±0.5; p=0.28).

Xience Prime was the most frequently used DES (n=35, 57.4%), while Promus Element or Premiere and Resolute Integrity were used in 16 (26.2%) and 10

(16.4%) of cases, respectively. The mean stent length was 28.0mm [20.5-28.0] in the BVS-group and 28.0 [20.0-38.0] in the DES-group (p=0.42). As shown in Table 3, a higher balloon diameter/mean reference vessel diameter ratio was used for predilatation in the BVS group (BVS 1.1±0.1, DES 0.9±0.1; p<0.01) with significantly higher pressure inflation for both pre and post-dilatation. NC balloons were more frequently used for lesion preparation in the BVS group. Sequential dilatation was the only technique used for bifurcation optimization in BVS group while kissing balloon was consistently used in the DES group.

Table 3: Procedural characteristics (n=100)

Table 3. Procedural Characteristics (N = 100)

	BVS (n = 50)	DES (n = 50)	p Value
Maximal diameter balloon pre-dilation, mm	3.0 (2.5–3.1)	2.5 (2.5–3.0)	<0.01
Maximal pre-dilation balloon inflation, atm	18.7 (3.5)	15.1 (3.8)	<0.01
Balloon/artery ratio	1.1 (0.1)	0.9 (0.1)	<0.01
NC balloon pre-dilation	50 (100.0)	37 (87.0)	<0.01
Cutting balloon predilation	6 (12.0)	3 (6.0)	0.48
Rotablator	2 (4.0)	2 (4.0)	NA
Stent diameter, mm	3.0 (3.0–3.5)	3.0 (3.0–3.5)	0.94
Stent length, mm	28.0 (20.5–28.0)	28.0 (20.0–38.0)	0.42
No. of stents per lesion, 1/2/3	37/9/4	40/9/1	0.28
Maximal post-dilation balloon diameter, mm	3.5 (3.0–3.5)	3.5 (3.0–3.5)	0.60
Maximal post-dilation balloon inflation, atm	21.3 (4.9)	17.1 (3.7)	<0.01
Kissing balloon, MV/SB	0 (0.0)	4 (8.0)	0.11
Sequential dilation, MV/SB	8 (16)	0 (0.0)	<0.01

Values are median (interquartile range) or n (%).

NA = not assessed; NC = noncompliant; MV = main vessel, SB = side branch; other abbreviations as in Table 1.

Optical coherence tomography findings

OCT findings are summarized in Table 4. A total of 2,953 cross-sections and 24,352 struts were analyzed. Mean and minimal lumen area were similar in the two groups. The incidence of RAS>20% was not statistically significant different in the BVS (BVS: n=25, 39.7%, DES: n=26, 42.6%; p=0.85) and there was no difference in the mean RAS (BVS 20.2±7.5, DES 21.7%±9.9; p=0.32). There was a higher incidence of ISA at the proximal edge in the BVS group (BVS n=25, 39.7%, DES n=14, 23.0%;p=0.04) but no difference in the overall percentage of ISA (BVS 1.7%±2.1, DES 1.9%±2.4; p=0.62) and number of stents with ISA (BVS n=33, 52.4%, DES n=39, 63.9%; p=0.19) (see Figure 3).

Figure 3: Histograms show a similar mean and minimal in stent lumen area (A), percentage of residual area stenosis and stent with residual area stenosis > 20% (B), overall percentage of malapposed struts (C). A higher incidence of proximal strut malapposition at the proximal edge was observed in BVS (D).

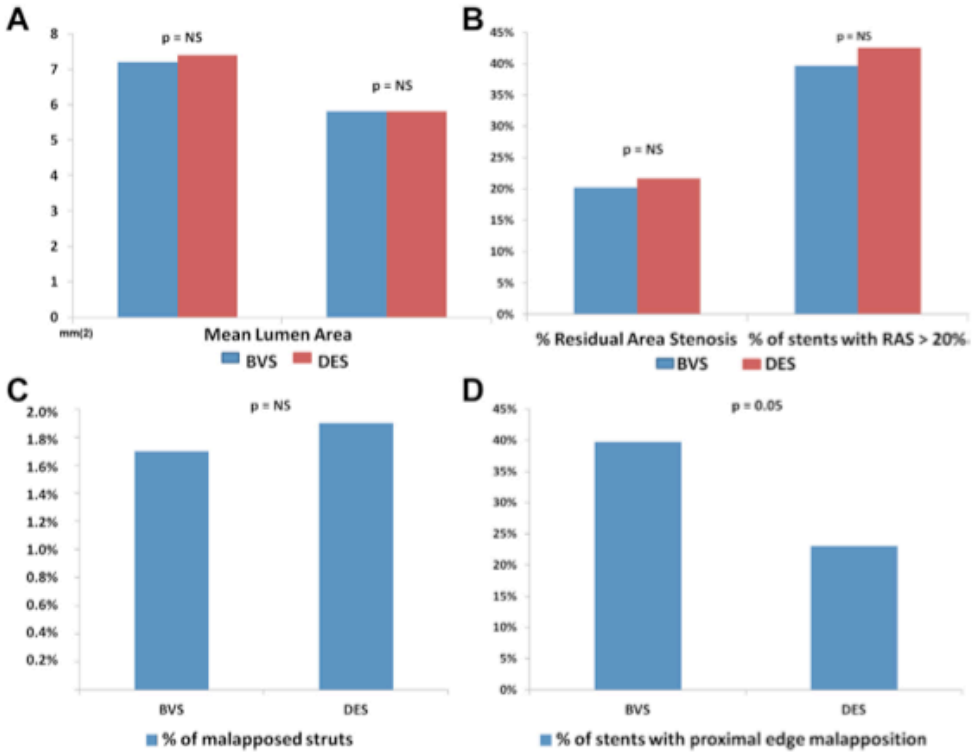

The mean and minimum eccentricity index and the symmetry index were similar in the two groups.

In the BVS group, there was a trend toward a higher prolapse area (BVS 1.5±2.4mm2, DES 0.8±1.2mm2; p=0.08) but this did not significantly impact on the final lumen area, which was similar in both groups. OCT analysis showed 12 edge dissections (BVS n=5, 7.9%, DES n=7, 11.5%; p=0.55) which were not apparent on the angiogram. None of these required further stent implantation. In the DES group, strut fractures were not observed while in two patients in the BVS group two stent fractures developed. In both cases the lesions were localized in the LAD across the origin of a diagonal branch and the scaffolds were recrossed in order optimize the result with sequential dilatation .

Table 4: Optical Coherence Tomography findings (n=124)

Table 4. Optical Coherence Tomography Findings (N = 124)

	BVS (n = 63)	DES (n = 61)	p Value
Mean stent area, mm^2	7.3 (2.3)	7.5 (1.6)	0.51
Minimal stent area, mm^2	5.9 (1.9)	5.8 (1.5)	0.67
Mean lumen area, mm^2	7.2 (2.2)	7.4 (1.6)	0.40
Minimal lumen area, mm^2*	5.8 (1.9)	5.8 (1.5)	0.97
Median stent diameter, mm	2.9 (0.5)	3.1 (0.3)	0.33
Minimal stent diameter, mm	2.7 (0.4)	2.8 (0.5)	0.46
Maximal stent diameter, mm	3.2 (0.5)	3.3 (0.4)	0.52
Percentage RAS	20.2 (7.5)	21.7 (9.9)	0.32
Stent with RAS >20%	25 (39.7)	26 (42.6)	0.85
Median eccentricity index	0.85 (0.08)	0.86 (0.04)	0.45
Minimum eccentricity index	0.73 (0.09)	0.72 (0.12)	0.73
Symmetry index	0.33 (0.08)	0.38 (0.37)	0.35
ISA analysis			
Percentage of malapposed struts	1.7 (2.1)	1.9 (2.4)	0.62
Stent with at least 1 ISA	33 (52.4)	39 (63.9)	0.19
Stent with ISA at the proximal edge	25 (39.7)	14 (23.0)	0.04
Stent with ISA at the distal edge	5 (7.9)	7 (11.5)	0.56
ISA area, mm^2 (for BVS only)	1.0 (1.2)	NA	NA
Maximal ISA length, mm†	0.4 (0.2)	0.3 (0.2)	0.09
Prolapse area, mm^2	1.5 (2.4)	0.8 (1.2)	0.08
Fracture	2 (3.2)	0 (0.0)	0.49
Edge dissection	5 (7.9)	7 (11.5)	0.55

Values are n (%). *Minimal lumen area within the scaffold. †Only for stent with ISA.
RAS = residual area stenosis; ISA = incomplete strut apposition; NA = not assessed; other abbreviations as in Table 1.

Clinical follow up

Clinical follow-up data were available for all BVS patients and for 31 (89.5%) patients in the DES group. The mean duration of follow up was significantly different in the two groups (BVS: 8.5±2.8 months; DES 17.3±8.7 months; $p<0.01$). One patient treated with two BVS in the proximal, mid and distal LAD presented two months later with ACS due to a critical lesion in a diagonal branch not treated with stenting during the index PCI, though the three previously implanted BVS were patent. One insulin-dependent diabetic patient with a proximal LAD BVS required coronary artery by-pass after 9 months because of diffuse distal disease progression (no in-stent restenosis). In the DES group 2 patients (5.3%) underwent PCI due to in-stent restenosis at 14 and 24 months respectively after the baseline PCI.

Discussion

This is the first OCT study to compare acute stent performance between BVS and second generation DES in complex coronary artery lesions.

The OCT indices used in our study are widely accepted as criteria for determining optimal stent deployment (45). These have been derived from IVUS criteria used for the evaluation of metallic stents and shown to correlate with 1-year clinical outcomes (stent thrombosis and restenosis) after implantation of BMS and first generation DES. In particular, a RAS of >20% and an absolute minimal cross-sectional area <5.5 or 6.0 mm2 were previously correlated with acute/subacute stent thrombosis and restenosis (46). In our study, both the BVS and second generation DES mean RAS and absolute MLA were close to these cut-off levels. The thresholds defined in these early IVUS evaluations of DES were derived from analysis of trials including short type A-B1 lesions. Results on more complex lesions are limited and expected to be worse because of the higher plaque burden and resistance. In a previous study from our group calcified lesions with OCT were

analyzed and a higher RAS and a greater ISA than in simple lesions was observed (47). The use of OCT rather than IVUS may explain part of the difference. By virtue of its higher resolution, OCT can define more precisely the lumen area contours and quantify plaque prolapse, which is frequently concealed by strut artefacts when using IVUS. Moreover, OCT has been shown to measure lower absolute areas than IVUS, both in vitro and in vivo (48). The areas observed in the complex lesions of our BVS group were very similar to those reported in an OCT sub-study of the ABSORB trial cohort B in which relatively simple lesions were treated. Also the type of metallic stents used may play a role. The thick stainless steel struts of first generation DES may create a rough cobblestone surface at higher risk of thrombosis but have less recoil than the thin struts of second generation stents constructed using alloys such as cobalt or platinum chromium (49).

The lack of difference between BVS and second generation DES in mean and minimal values of relative and absolute stent area, is the true novel finding of the current study. This could be expected based on in vitro studies conducted by the industry for registration and on small comparative studies with IVUS between BVS and Xience V stents. The observations made using OCT in the current study support the application of BVS beyond the current indications. These results suggest that a satisfactory BVS expansion can be achieved also in complex coronary lesions, at least when appropriate lesion preparation and deployment under OCT guidance is performed.

The clinical relevance of ISA is controversial. Previous IVUS studies using first generation DES to treat simple lesions (50) showed no value in predicting late adverse events. However, an IVUS study performed at the time of acute stent thrombosis showed a higher incidence of ISA compared with controls (14). In our study, no difference was observed in the absolute number and percentage of

malapposed struts between BVS and DES, with the latter being considerably lower than shown in previous OCT studies of predominantly first generation DES. Repeated OCT examinations in both groups, prompted additional dilatations at high pressure with properly sized balloons, probably explain the low prevalence of ISA in the complex lesions treated in this study. Some malapposition was still observed, in pre- or post-stenotic ectasic segments, in eccentric calcific lesions and at bifurcations though in many cases this was impossible to correct completely despite serial or kissing balloon dilatation (51). In the BVS group, we observed a more frequent malapposition at the proximal stent edge (39.7% of BVS vs 23.0% of DES, p 0.04), which may have procedural relevance as struts protruding into the lumen complicate the advancement of balloons or additional distal stents. The greater conformability of second generation DES compared to BVS may explain these findings because extreme attention was paid to post-dilatation with appropriately sized balloons which covered the proximal edge of the BVS, which is angiographically well visualised by the radiopaque platinum proximal marker. A potential advantage of the bioresorbable technology over metallic device is that any acute ISA resolves after the process of strut degradation has been completed, though this process may require up to 2 years time (52).

Gomez-Lara et al, performed an OCT sub-study from the ABSORB trial Cohort B, in which only 3mm diameter BVS device were deployed. These investigators found a higher incidence of malapposed struts in vessels with a maximal diameter >3.3 mm (42). These data emphasize the importance of correct vessel size measurement in order to select the appropriate BVS diameter. Based on this observation we recommend over-sizing BVS up to 0.5mm above the smallest reference vessel diameter, which allows better adaptation especially in tapered vessels.

The amount of tissue prolapse was slightly higher in BVS than DES. This may be explained by differences in stent design and the lower number of struts per cross-section in BVS compared with second generation DES. In our population of stable lesions the greater plaque prolapse was not clinically relevant as it did not alter the final mean and minimal lumen area. Moreover, the thicker struts of BVS mean that the prolapsed plaque is always surrounded by the stent struts with less herniation into the vessel lumen and a smoother surface compared with thinner strut DES (Figure 1). However, tissue prolapse is more prominent in unstable or thrombus containing lesions and in this setting the scaffolding properties of BVS might be insufficient to counteract plaque prolapse.

A very similar post-procedural stent geometry was observed in both BVS and DES. Mean and minimum value of eccentricity index were similar in the two groups. Brugaletta et al reported a higher symmetry index value for BVS while the eccentricity index was significantly lower in BVS compared to DES (0.85±0.08 versus 0.90±0.06, $p<0.01$). In the current study, the minimal eccentricity index was lower for both BVS and DES in comparison to the findings from Brugaletta et al., likely a consequence of including more complex lesions.

Limitations

The favorable acute mechanical performance of BVS observed in this study cannot be given for granted unless implantation is performed with the same meticulous attention to lesion preparation, systematic sizing of BVS to the proximal reference vessel diameter and high pressure post-dilatation. Scaffold implantation has been performed under OCT guidance. Therefore, our results cannot be automatically applicable to conventional angiographic BVS deployment. The main limitation of this study is the use of a historical non randomized control group with a limited sample size and follow-up duration, which precludes any meaningful long-term

clinical comparison of the rare long-term adverse events observed in patients treated with modern DES. Use of a matched cohort as a control population is frequently employed in the evaluation of novel devices and is certainly of value for the assessment of mechanistic response. There was no significant difference observed in key parameters of acute stent performance in the two subgroups treated with BVS or DES. However, adjustments for multiple correlated observations were not performed and a definitive prove of non-inferiority would require a prospective randomized study with a larger study population. Prospective randomized controlled trials are required in order to determine whether the favorable acute mechanical performance of BVS observed in the current study can be translated into an improved long-term clinical outcome in patients with complex coronary lesions treated by PCI. The short follow-up duration provided in the BVS group may be inappropriate to observe disease progression and late target lesion failure. Finally, although no new Q waves or ST elevation or prolonged chest pain were observed, we did not consistently measured post procedural troponin in all patients.

2.1.5 Study 5

Title: Very High Pressure Dilatation for Undilatable Coronary Lesions: Indications and Results with a New Dedicated Balloon

Background

The inability to fully dilate calcified lesion might result in an increased risk of stent restenosis and thrombosis. Increasing the pressure beyond the recommended limits during dilatation of resistant lesions often accentuates non-uniform balloon expansion with the consequent over-dilatation of the more compliant segments (dog-boning effect). Conventional non-compliant (NC) balloons have more predictable responses and uniform dilatation than semi-compliant balloons but the 20 to 30 ATM limit that they reach can be insufficient. A variety of technologies such as rotational-atherectomy have been developed, however, the complexity and the cost of these devices have hindered their widespread use.

Aim

The aim of our study is to evaluate the safety and efficacy of a new dedicated super-high pressure NC-balloon (OPN, SIS Medical-AG, Winterthur-Switzerland).

Materials and Methods

Lesion Selection

We evaluated 91 consecutive highly resistant coronary lesions in which conventional NC balloons failed to achieve an adequate post dilatation luminal gain. After the failed attempt with the plain NC balloon the OPN balloon was inflated up to 40 ATM. Other coronary lesions could be treated, when necessary. No exclusion criteria were applied. The OPN balloon is a CE mark device. Patients

signed an informed consent for data treatment for scientific purposes and the study was conducted according to the Declaration of Helsinki.

The OPN Balloon Device

The OPN NC Super-High Pressure Balloon (SIS Medical AG, Winterthur Switzerland) is a rapid-exchange PTCA catheter compatible with 0.014" coronary wires. The most distinctive feature of the OPN balloon is the presence of a proprietary twin-layer balloon technology, which permits the use of very high-pressure inflations and ensures uniform expansion over a wide range of pressures. The balloon is highly non compliant with a nominal pressure of 10 atm and a rated burst pressure of 35 atm. Each balloon is factory tested at 45 atm. The balloon diameters currently available cover a range from 1.5mm up to 4.0mm with ½ mm intervals. Lengths are 10, 15 and 20mm. The commercial name OPN comes from a sort of abbreviation of OP(E)N that in the company intention should sound commercially appealing for dilate a coronary stenosis.

Figure 1: Comparison between different NC balloons compliance 3.0 mm diameter: Hiryu (Terumo Medical, Tokyo, Japan), NC Quantum Apex (Boston Scientific, Natik, MA, USA), NC Sprinter RX (Medtronic, Minneapolis, MN, USA), Sapphire NC (OrbusNeich, Wanchai, Hong Kong), Empira NC (Cordis, Bridgewater, NJ, USA), OPN (Sis Medical, Winterthur, CH). Please note that the OPN NC balloon is the only one commercially available NC PTCA balloon catheter with a satisfactory compliance up to 35 ATM.

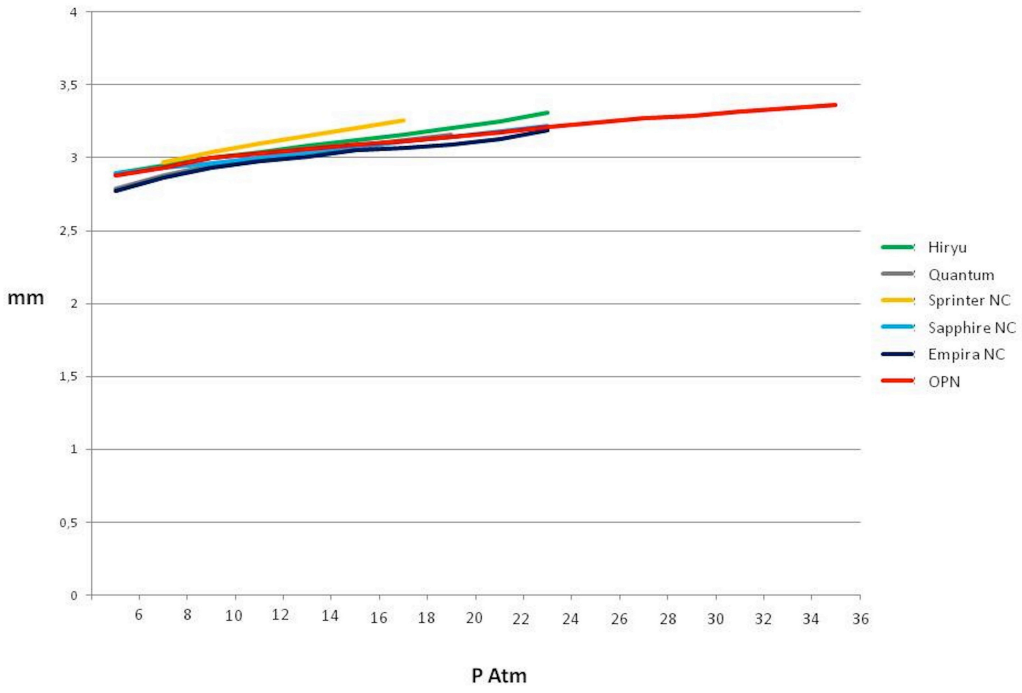

Interventional Procedure

The PCI was routinely performed with standard techniques via femoral or radial approach using 6 or 7 French guiding catheters. Patients not preloaded with oral aspirin and/or clopidogrel received a loading dose of intravenous aspirin (500mg) and clopidogrel (600mg) or prasugrel (60 mg) as standard practice in our Catheterization Laboratory. Intravenous heparin (70 UI/Kg body weight) was administered before the procedure with subsequent boluses aiming at achieving an activating ACT between 250 and 300sec. The use of GP IIb/IIIa inhibitors was minimized and left to operator's discretion. In all cases lesion predilatation was

performed with a low profile normal balloon slightly undersized according to conventional angiographic criteria. In case of incomplete balloon expansion with visible indentation at inflation pressures close to the rated burst pressure the lesion was approached using conventional NC balloon inflated at least at the rated burst pressure and often higher. If also this step failed to provide an adequate luminal gain because of residual underexpansion of the balloon, the OPN balloon (with the same diameter as the NC balloon) was inflated up to 40 ATM. All lesions were finally treated with DES optimized by NC-balloon inflation when needed. In case of stent underexpansion with residual stenosis >40% assessed by angiography, the OPN balloon (with the same diameter as the NC balloon used) was inflated up to 40 ATM for stent optimization.

Angiographic Analysis

As routine in our Centre, standard image acquisition of the treated stenosis was performed using two or more angiographic projections after intracoronary nitroglycerine 100-200 mcg or isosorbide dinitrate 2-3 mg to provide maximum coronary dilation. We identified the projection where the lesion was better visualized and appeared more severe with no overlapping and minimal foreshortening. We filmed the lesion in this view during all balloon inflations and for final angiography. QCA was performed using a computer-based QCA system (Medis, Leiden, The Netherlands) with the dye-filled guiding catheter used for calibration. MLD and % DS were measured at baseline, after conventional NC balloon dilatation, and after OPN balloon dilatation. Interpolated reference diameter was considered as reference segment diameter. Lesion length was defined as the distance from the proximal to the distal shoulder of the lesion. Acute gain after conventional NC balloon was defined as MLD (mm) post NC conventional balloon – baseline MLD (mm). Acute gain after OPN NC balloon was defined as MLD post OPN balloon (mm) – baseline MLD (mm). Incremental gain after OPN

NC balloon was defined as MLD post NC OPN balloon (mm) – MLD post conventional NC balloon (mm).

Follow-Up

Clinical events were evaluated post-procedure, during hospitalization and at 30 days follow up.

Definitions

Angiographic success was defined as the achievement of residual angiographic stenosis < 30% assessed by visual estimation with TIMI 3 flow. Procedural success was defined as the achievement of angiographic success without any MACE defined as death, myocardial infarction and repeat revascularization (CABG or PTCA). Twelve-lead electrocardiograms were recorded before, immediately after the procedure and at hospital discharge. In-hospital MACE was defined as any MACE occurred during hospitalization for the index procedure. Follow up MACE was defined as myocardial infarction, death or target lesion revascularization (any repeat PCI or CABG at the lesion site) occurred during the follow up period. Post procedural access site "bleeding" was defined according to TIMI criteria (53) and hematoma was defined as an arterial puncture site swelling > 5 cm.

Statistical Analysis

Continuous variables were expressed as mean $\pm$ standard deviation, while categorical variables were presented as numbers with percentage. Continuous variables were compared using paired student's t-test. Categorical variables were compared using chi-square test. A P value $\leq$ 0.05 was considered statistically significant.

Results

Patients and lesion characteristics are shown in table 1 and 2 respectively. The average age was 69.4 $\pm$ 9.5 years with a prevalence of male sex (80.2%) and

standard distribution of risk factors (hypertension 82.4%, hypercholesterolemia 69.2%, diabetes 46.1%, previous or current smoking 65.9%). Out of the 91 lesions, 54 were heavily calcified or fibrotic lesions (59.3%) in previously untreated vessels and 7 were ISR (7.7%) in which conventional NC balloons did not expand during predilatation. In the remaining 30 cases the OPN balloons were used after stent deployment for stent optimization (33%). Procedural characteristics are shown in table 2. Predilatation using a semi compliant balloon was performed in all cases and was then followed by a successive dilatation using a conventional NC balloon sized according to conventional angiographic criteria and inflated up to the rated burst pressure or slightly higher. A total of 128 NC balloons were used (1.4 per lesion). In all cases the dilatation performed with the conventional NC balloon failed to achieve an adequate balloon expansion and luminal gain. After the failed attempt the OPN balloon with the same diameter of the conventional NC balloon was inflated up to 40 ATM. A total of 91 OPN balloons were used (1 per lesion). Angiographic success was achieved in 84 lesions (92.3%). In 3 severely calcified subocclusive stenoses (3.3%) the OPN balloon failed to cross while in 2 cases despite successful crossing the OPN failed to achieve an adequate luminal gain (2.2%). All 5 lesions were finally successfully treated with rotational atherectomy (5.5%). The remaining 2 cases were undilatable lesions in small and tortuous vessels for which both rotational atherectomy and excimer laser therapy were deemed not safe (2.2%). GpIIb/IIIa inhibitors were used in 6 patients (6.6%).

Table 1: Baseline Patient Characteristics

NUMBER OF PATIENTS	91
Sex (Male/Female)	73/18 (80.2% 19.8%)
Age	69.4 ± 9.5
RISK FACTORS	
Hypertension	75 (82.4%)
Hypercholesterolemia	63 (69.2%)
Smoking	60 (65.9%)
Family history	52 (57.1%)
Diabetes	42 (46.1%)
Prior MI	35 (38.4%)
Prior CABG	21 (23%)
Renal Failure	19 (28.9%)
LVEF (%)	52.6 ± 12.9
CLINICAL PRESENTATION	
Stable Angina	76 (83.6%)
Unstable Angina	11 (12%)
NSTEMI	4 (4.4%)

Table 2: Lesion and Procedural Characteristics

Number of treated lesions	91
VESSEL	
Left Main	2 (2.2%)
LAD	45 (49.4%)
LCX	15 (16.5%)
RCA	26 (28.6%)
SVG	3 (3.3%)
Multivessel disease	43 (47.2%)
LESION CHARACTERISTICS	
Length (mm)	21± 12
True bifurcation	38 (41.7%)
Ostium involved	12 (13.2%)
Calcific lesion	37 (40.6%)
CTO	17 (18.7%)
Optimization after stenting	30 (33%)
ISR	7 (7.7%)
BALLOON	
Number of NC balloon/lesion	128/91 (1.4)
Final NC balloon inflation (atm)	21.4 ± 2.8
NC balloon mean diameter	2.6 ± 0.6
Number of OPN balloon/lesion	91/91 (1.0)
Final OPN balloon inflation (atm)	37.2 ± 2.7
OPN balloon mean diameter	2.8 ± 0.4
Number of stent/lesion	124 (1.35)
IVUS guided	21 (23.1%)
OCT guided	10 (11%)

Angiographic Results

QCA analysis is shown in table 3. Both MLD and acute gain were significantly greater and % DS was significantly lower post OPN balloon inflation compared with post-plain NC balloon inflation (1.7 ± 0.8mm vs 2.4 + 0.9mm, $p < 0.001$; 41.1 ± 15.8% vs 20.2 ± 14.9%, $p < 0.001$). These results were achieved with no increase in balloon size but with a higher inflation pressure (37.2 ± 2.7 atm vs 21.4 ± 2.8 atm, $p < 0.001$).

Table 3: QCA Analysis

	BASELINE	POST NC BALLOON	POST OPN BALLOON	P
RD (mm)	2.6 ± 0.8	---	---	
MLD	0.7 ± 0.3	1.7 ± 0.8	2.4 ± 0.9	< 0.001
% DS	73.6 ± 9.9	41.1 ± 15.8	20.2 ± 14.9	< 0.001
Lesion length	11.9 ± 6.4	---	---	
Acute gain (mm)	---	1.1 ± 0.7	1.9 ± 0.8	< 0.001
Incremental gain (mm)	---	---	0.8 ± 0.4	

Procedural and Clinical Outcome

Angiographic and technical success with OPN balloons was achieved in 84 lesions (92.3%). In the remaining 7 cases (7.7%), 5 lesions were successfully treated with rotational atherectomy (5.5%) while the remaining 2 cases were undilatable lesions for which both rotational atherectomy and excimer laser therapy were not attempted because of small vessel size and excessive tortuosity (2.2%). No coronary perforation or balloon rupture and ST change were reported after the procedure. No In-Hospital and 30 days MACE were reported. No major post procedural bleeding were reported. Hematoma of the access site occurred in 5 patients treated by a transfemoral approach (5.5%).

Figure 1: Decrease in % of diameter stenosis (DS) in calcific lesions (Group A), stent optimization (Group B) and in-stent restenosis (ISR) (Group C). The incremental gain offered by the OPN balloon was sufficient to achieve angiographic success in all the three subgroups (0.81 + 0.47 mm in Group A; 0.77 + 0.41 mm in Group B; 1.34 + 0.31 mm in Group C).

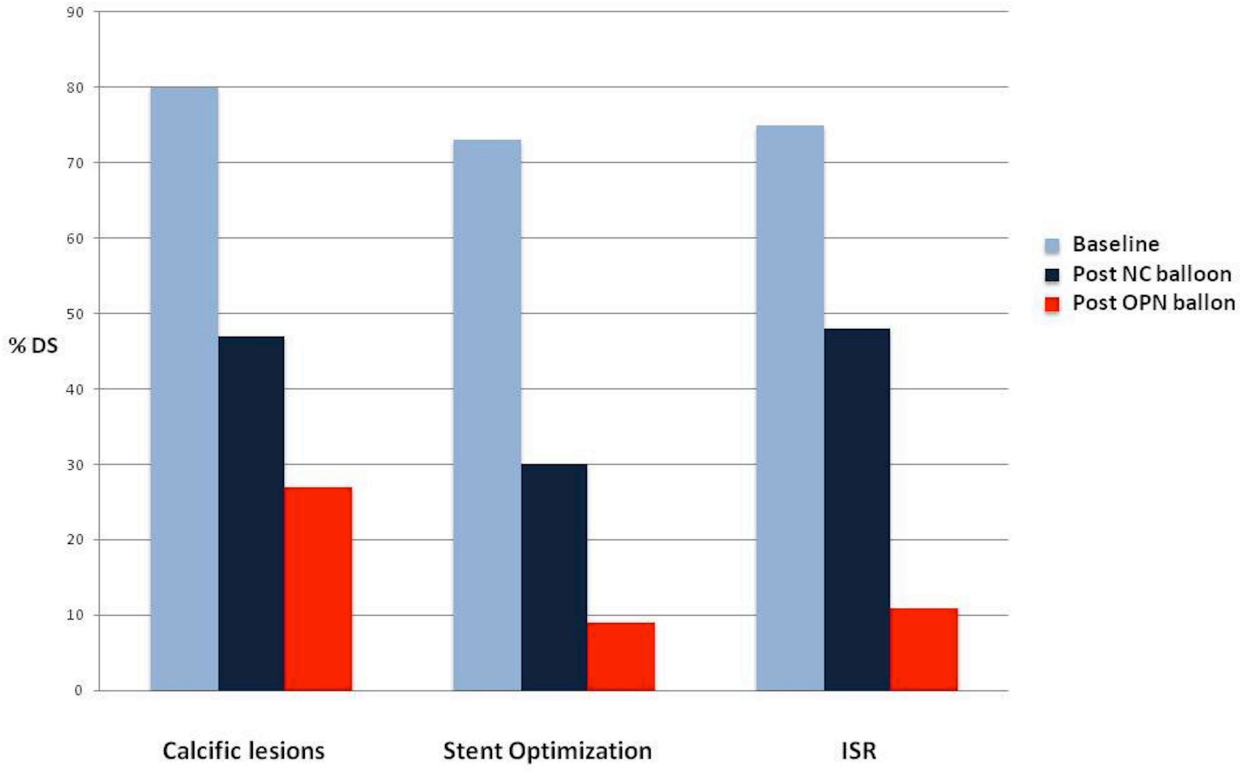

Discussion

In our Registry we tested the safety and efficacy of the OPN super high-pressure balloon in a consecutive series of truly heavy resistant coronary stenosis non responsive to plain NC-balloon dilatation. With the OPN NC-balloon we were able to achieve a more then acceptable postdilatatation luminal gain in 92% of the cases without the need of additional expensive devices.

The mechanical properties of the arterial wall are critically dependent on the thickness, distribution and characteristics of the intimal plaque (54). Thick

neointimal hyperplasia and severe coronary calcification contribute to increase the hoop stress to the point that even high-pressure non-compliant balloons might be insufficient to overcome the hoop stress and induct a satisfactory dilatation.

During dilatation of resistant coronary lesions the non-uniform balloon expansion with the consequent over-expansion of the more compliant segment (the so called "dog-boning" effect) may lead to an increased risk of vessel wall damage including edge dissections and coronary perforation. Varieties of devices and strategies have been developed to overcome this limitation. Cutting balloons have been designed to relieve the vessel hoop stress by creating controlled small incisions in the vessel wall and present the practical advantage that they do not move during inflation due to the stabilising effect of the blades. Cutting balloons present several advantages for the treatment of severe calcified lesions, allowing a larger luminal gain at lower pressure compared to balloon angioplasty alone and preventing the late recoil due to the incisions created by the blades (39). The lack of clinical benefit observed in the early studies of cutting balloon vs conventional balloon angioplasty in de novo lesions, have created scepticism on the potential mechanical usefulness offered by a focal concentration of force on the intimal plaque.

Mehran et al (12) showed that when treating instent restenosis with balloon angioplasty, luminal gain is achieved by a combination of additional stent expansion and neointimal tissue compression through the stent resulting in a displacement through the stent struts and compression of neointimal tissue. Although satisfactory initial clinical and angiographic results were obtained with balloon angioplasty, a significant early lumen loss was also observed shortly after in-stent restenosis treatment due to recoil and re-intrusion of neointimal tissue in the lumen. This early phenomenon possibly influences the long-term outcome after balloon angioplasty for in-stent restenosis, affected by a high re-restenosis rate. Despite these findings, several randomized study showed no real advantage of CB

over PTCA with conventional balloon and both the rigidity and the risk of balloon entrapment can limit their routinely use during treatment of heavily coronary lesions.

Modification of the vessel wall using rotational atherectomy and excimer laser therapy improves vessel wall compliance thus facilitating uniform stent expansion.

The Excimer laser therapy is based on the principle of photoablation converting occlusive material into microbubbles being immediately dissolved in the blood (55) and its use during treatment of resistant coronary lesions has been successfully described (56).

Rotational atherectomy is a technique in which a small grinder is inserted into the coronary arteries to ablate the plaque. It is specifically effective in the treatment of calcified lesions because of its differential cutting mechanism, a phenomenon by which soft tissues (such as the normal arterial wall) are deflected so that the grinder will not contact them during high-speed rotation, while hard calcified plaques are not deflected and can be ablated by the grinder (57). Sizing-up the burr might enable better lesion modification, resulting in greater stent expansion and strut apposition. It is, however, unknown whether routine usage of aggressive rotational atherectomy is superior to conventional balloon dilatation as a means of lesion modification followed by DES implantation, because of the lack of systemic long-term results of such a strategy .

Despite the majority of resistant coronary lesions can be treated with balloon dilatation and stent implantation alone, the rigid obstacle imposed by calcium or thick neointimal hyperplasia might prevent an optimal balloon expansion and symmetric stent deployment thus resulting in a gross malapposition of the stent struts. The importance of this is indirectly confirmed by findings from the e-Cypher registry correlating calcific lesions with future occurrence of stent thrombosis (59). The real clinical consequence of strut malapposition is still matter

of debate but surely may impinge on the elution properties of DES, increase the activation of fibrin and platelets, thus resulting in accelerated intimal hyperplasia or stent thrombosis. Although the use of dedicated devices such as rotational atherectomy might certainly improves procedural success during treatment of resistant coronary lesions both the complexity, the cost and the need of dedicated operators have hindered their widespread application.

Conversely, the OPN NC Super-High Pressure Balloon is a plain rapid exchange PTCA catheter that can be easily attempted in case of failure of conventional balloons (60). Thanks to its twin-layer technology, it allows the use of very high-pressure inflations ensuring uniform expansion over a wide range of pressures and reducing the risk of vessel damage (61). In our registry we found a significant increase of MLD and acute luminal gain after OPN balloon dilatation compared with plain NC balloon inflation. Moreover, as a consequence of the OPN uniform expansion we had no vessel rupture despite the use of very high-pressure inflations. In conclusion we believe that, when conventional NC balloon fail, OPN high-pressure balloons can provide an effective strategy for treatment of severe heavy coronary lesions. Moreover, this data suggest that the unique twin-layer technology offered by the OPN balloon achieves uniform balloon expansion reducing balloon rupture, vessel damage and coronary perforation.

Figure 2: Angiographic and OCT images of an heavy calcific lesion pre-stenting (A), post a 3.0 x 18 ZES implantation followed by a NC balloon inflated at 22 ATM (B) and post dilatation with a 3.0 x 15mm OPN Balloon inflated at 38 ATM. Please note that the MLD increased to 2.92 mm (after the NC balloon dilatation) to 3.18mm (after the OPN dilatation). In the IVUS/OCT guidance PCI of calcify lesion we found calcium around the vessel contour accounting for at least > 65% of the plaque, while OCT/IVUS imaging post OPN-dilatation shows diffuse vascular injuries following high-pressure inflation but without significant difference from the conventional NC-balloon treated lesions.

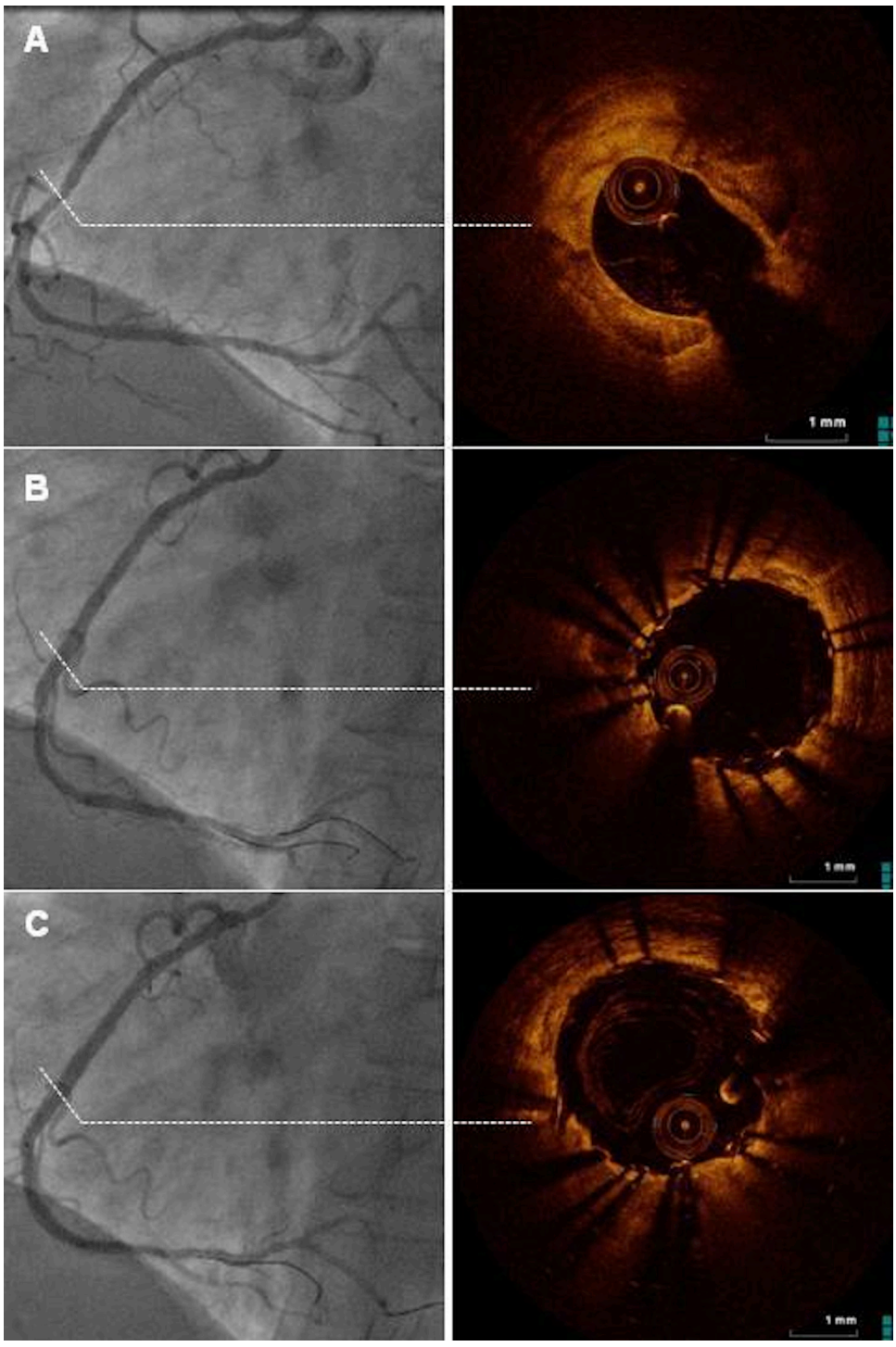
A
1 mm
B
1 mm
C
1 mm

Limitations

The main limitation of the OPN balloon is the high profile that, together with the stiffness of the twin-layer technology, in the vast majority of cases undermines any attempt to recross when inflated. The balloon does not refold well and after inflation is very difficult to use it again (for instance for both pre and postilatation). An independent core-lab and multiple observers QCA analysis would have improved reliability of data. Moreover our results come from a small sample-sized, retrospective and non-randomized comparison, which is certainly susceptible to selection bias.

2.2 OPTICAL COHERENCE TOMOGRAPHY DURING RENAL NERVE DENERVATION

2.2.1 Study 6

Title: Safety and efficacy of saline infusion for optical coherence tomography evaluation of vascular lesion induced by renal nerve ablation.

Background

Renal nerve ablation (RNA) using radiofrequency (RF) catheter-based has been recently proposed for the treatment of severe drug-resistant hypertension (62). Despite preliminary animal studies showed the safety and efficacy of this procedure, recent in-human studies highlighted the possibility of vascular lesions following RF emission.

Aim

For the first time ever our group evaluated the feasibility of OCT acquisition using selective saline infusion instead of contrast agent infusion.

Materials and Methods

After a renal denervation procedure we firstly performed a FD-OCT acquisition with a motorized pullback activated during injection of iodixanol 320 (Visipaque, GE Health Care, Cork, Ireland) via a 6 Fr guiding catheter at a flow rate sufficient to have full substitution of blood with contrast with no streaming according to the international guidelines developed for intracoronary imaging (3). Subsequently, we performed a further OCT acquisition in the same renal artery after a gentle and prolonged manual injection of 30 ml of saline.

The two pull-backs were then compared, using the off-line LigthLab OCT imaging station, in order to evaluate the quality and the ability to detect vascular injuries in

the saline-OCT acquisition. After proving the safety of saline intra-renal flush we evaluated so far 13 renal arteries. Of these, 12 were imaged before and after RDN-procedure; in one case OCT was used during treatment of a renal in-stent thrombosis. In the first 4 arteries the quality of the cross sections obtained after saline infusion were compared with conventional OCT acquisition performed according with international guidelines developed for intracoronary imaging. To this, we firstly performed a FD-OCT acquisition with a motorized pull-back activated during injection of iodixanol 320 (Visipaque, GE Health Care, Cork, Ireland) via a 6 Fr guiding catheter at a flow rate sufficient to have full substitution of blood. Subsequently we performed further OCT acquisition after a gentle and prolonged manual injection of a 30ml of pure saline. The pull-backs were then compared. The remaining 9 arteries were imaged only after saline flush and in all cases OCT provides useful informations of the vessel wall angiographically silent.

Results

The standard OCT pull-backs using crystalloid infusion was certainly clearer especially at the center of the vessel lumen where the higher viscosity of crystalloid was able to achieve a greater blood clearance during imaging acquisition. Despite this, the subsequent saline-OCT acquisition achieves a sufficient quality to detect all vascular RF-induced lesions with accuracy equal to the crystalloid-OCT pull-back (Figure 1).

Figure 1: A: OCT images acquired respectively after crystalloid infusion (A.1) and saline infusion (A.2). Please note that despite a clearer lumen obtained after crystalloid infusion both images clearly show the presence of a plaque located at the proximal segment of the renal artery (11 o'clock). B: OCT images acquired after crystalloid infusion (B.1) and saline flush (B.2) in a relatively healthy segment of the artery. C and D: OCT images obtained respectively after crystalloid (C) and saline infusion (D). Please note that both images are able to detect a local vascular injury at the RF-emission site (white arrow).

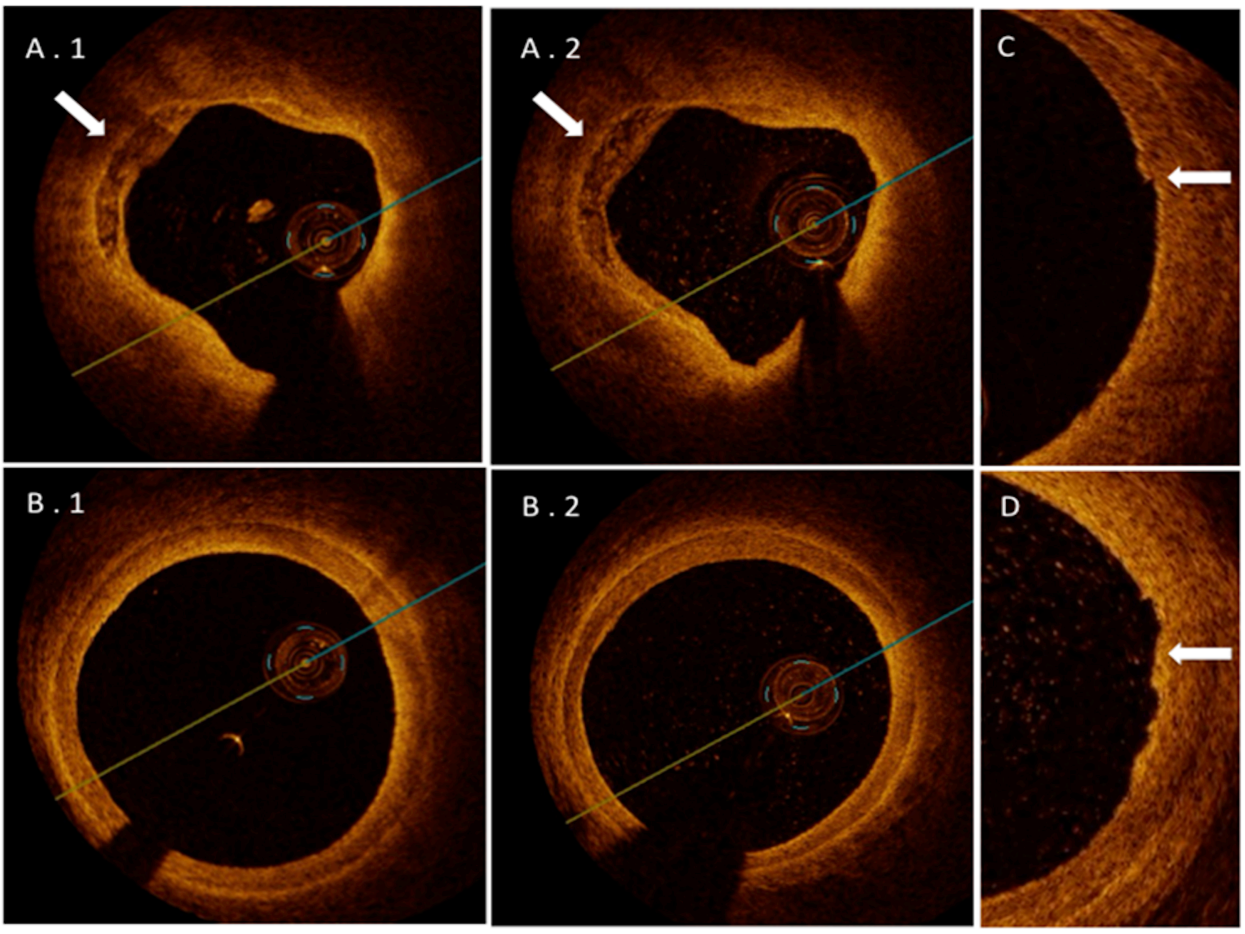

Discussion

Templin et al. recently evaluated 32 renal arteries before and after the RNA-procedure using optical coherence tomography (OCT) (63). Thanks to its high resolution OCT was able to detect local vascular injuries angiographically silent. Lesions included prominent vessel notches at RF emission sites suggesting endothelial-intima edema, protruding masses attached to luminal surface suggesting thrombus and one vessel dissection. The real clinical impact of these findings is still unknown debating between the possibility of renal artery stenosis as an evolution of such injuries and no clinical sequelae (64). Notably, histopathological vascular analysis of renal arteries of swine which underwent renal nerve ablation did not show vascular lesions at 6 months follow-up despite diffuse injury of the vessel wall in the acute phase (65). Despite this, it is no doubt that creating a lesion into a relatively healthy vessel must be carefully evaluated in the long-term clinical follow-up. These data highlight the importance of a high-resolution intravascular imaging technique during treatment of renal arteries. Ierna et al., using OCT after RNA, suggested the possibility of prolonged dual antiplatelet therapy in patients presenting renal vascular lesions including thrombus. Despite this, the routinely use of OCT for guidance of renal interventions is limited because of the need of prolonged crystalloid infusion during imaging. Frequency domain OCT (FD-OCT) has the advantage of a more rapid image acquisition due to the fast-scanning laser systems able to minimize the contrast use and to increase imaging speed while delivering comparable or improved image quality than with the earlier time domain systems. This allows multiple acquisitions of the entire segment of interest but still requires a selective renal injection of an amount of contrast medium greater than required for the control angiogram. Selective prolonged crystalloid infusion might be particularly deleterious in this subset of patients with resistant hypertension that are at

potentially higher risk of poorer renal function. In fact, the main obstacle to the adoption of OCT imaging in clinical practice is that OCT cannot image through a blood field requiring clearing or flushing of blood from the lumen usually achieved by contrast agent infusion. However, thanks to the favorable blood kidney flow, saline itself might be sufficient to clear the blood from the vessel lumen for the entire acquisition period. To our best knowledge this is the first report describing the use of FD-OCT in RNA-procedure by using only saline flush and without the need of balloon occlusion or iodinated contrast medium infusion. We believe that this might improve the safety profile of this imaging technique enlarging the possibility of OCT evaluation of renal artery following renal nerve ablation in particular in patients with already advanced stages of renal insufficiency.

2.3 OPTICAL COHERENCE TOMOGRAPHY DURING PERIPHERAL VASCULAR INTERVENTION

2.3.1 Study 7

Title: Saline vs contrast infusion during optical coherence tomography imaging of peripheral percutaneous intervention

Background

Successful percutaneous revascularization of femoral and popliteal arteries dramatically differs from PCI because of the several mechanical stresses such as torsion, compression, flexion and extension induced by the large muscular groups (66).

Aim

We decided to test the feasibility of saline infusion during OCT evaluation of superficial femoral artery (SFA) atherectomy.

Materials and Methods

We performed a FD-OCT (St Jude, Minneapolis, MN, USA) acquisition after a gentle and prolonged manual injection of 50 ml of saline. The images were then compared with another OCT-guided SFA TurboHawk (Covidien, ev3 Endovascular, Inc., Plymouth, MN) atherectomy in which the motorized pullback was activated during injection of iodixanol 320 (Visipaque, GE Health Care, Cork, Ireland) at a flow rate sufficient to have full substitution of blood with contrast with no streaming according with international guidelines developed for intracoronary imaging (3).

Results

Despite a certainly, improved OCT acquisition using contrast flush (Fig. 1), pure saline was able to achieve a sufficient quality cross-section images to characterize vessel injuries and increase in mean luminal area (MLA) following atherectomy (Fig. 2).

Figure 1: Panel A and G shows angiography of a SFA pre and post rotational atherectomy. Panel B, C, D, E, F are OCT images acquired after infusion of pure contrast. Please note in panel B and D (*) the vessel dissection following plaque debulking that required prolonged balloon inflation. Notable the images are of high quality with a proper blood clearance due to the high viscosity of the crystalloid infusion.

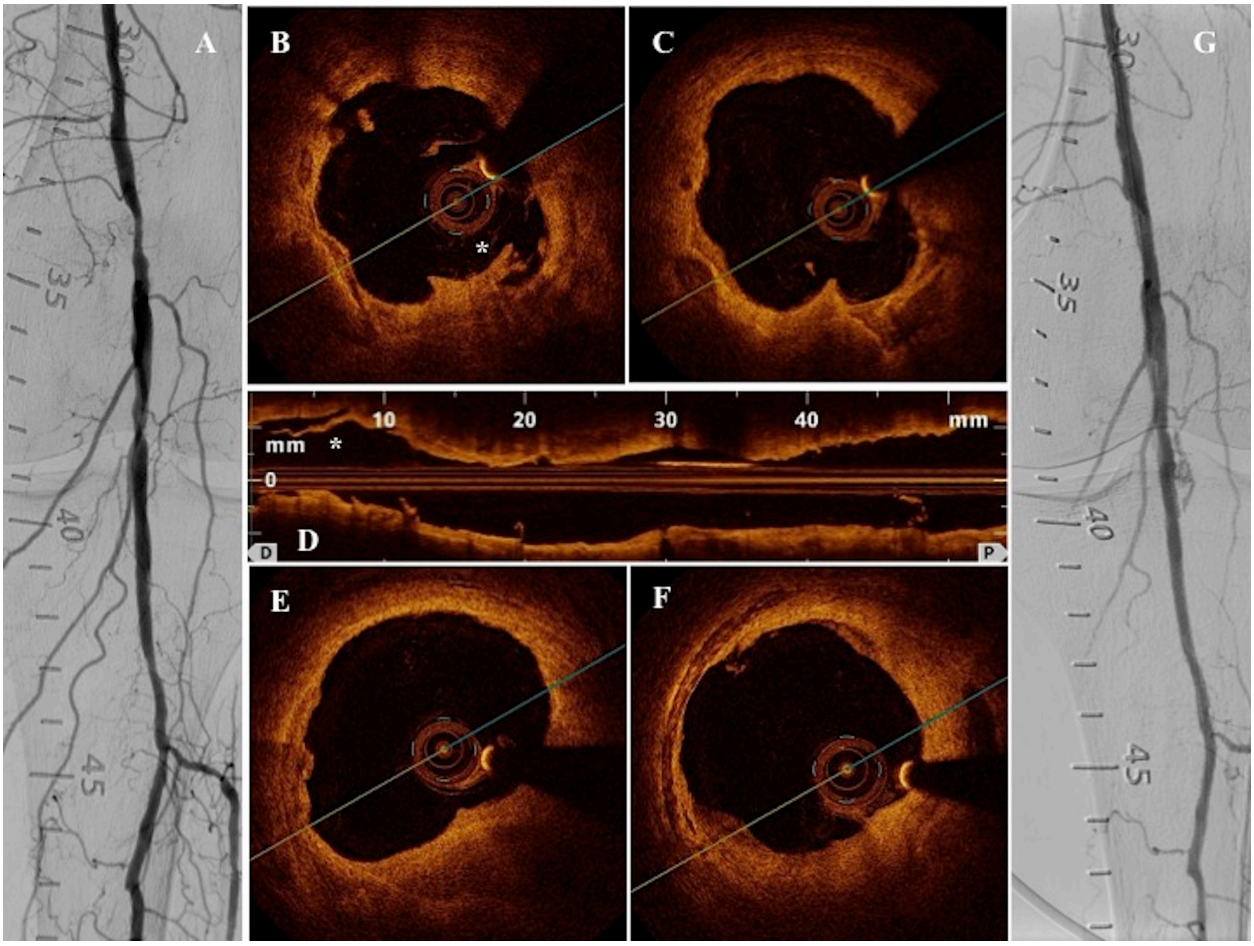

Figure 2: Panel A and G shows angiography of a SFA pre and post rotational atherectomy. Panel B, C, D, E, F are OCT images acquired after infusion of pure saline. Please note in panel D and F (*) the vessel dissection following plaque debulking that required prolonged balloon inflation. Despite a certainly worst blood cleareance especially at the center of the vessel lumen the images are of more than acceptable quality to detect vascular injuries following Turbohawk atherectomy.

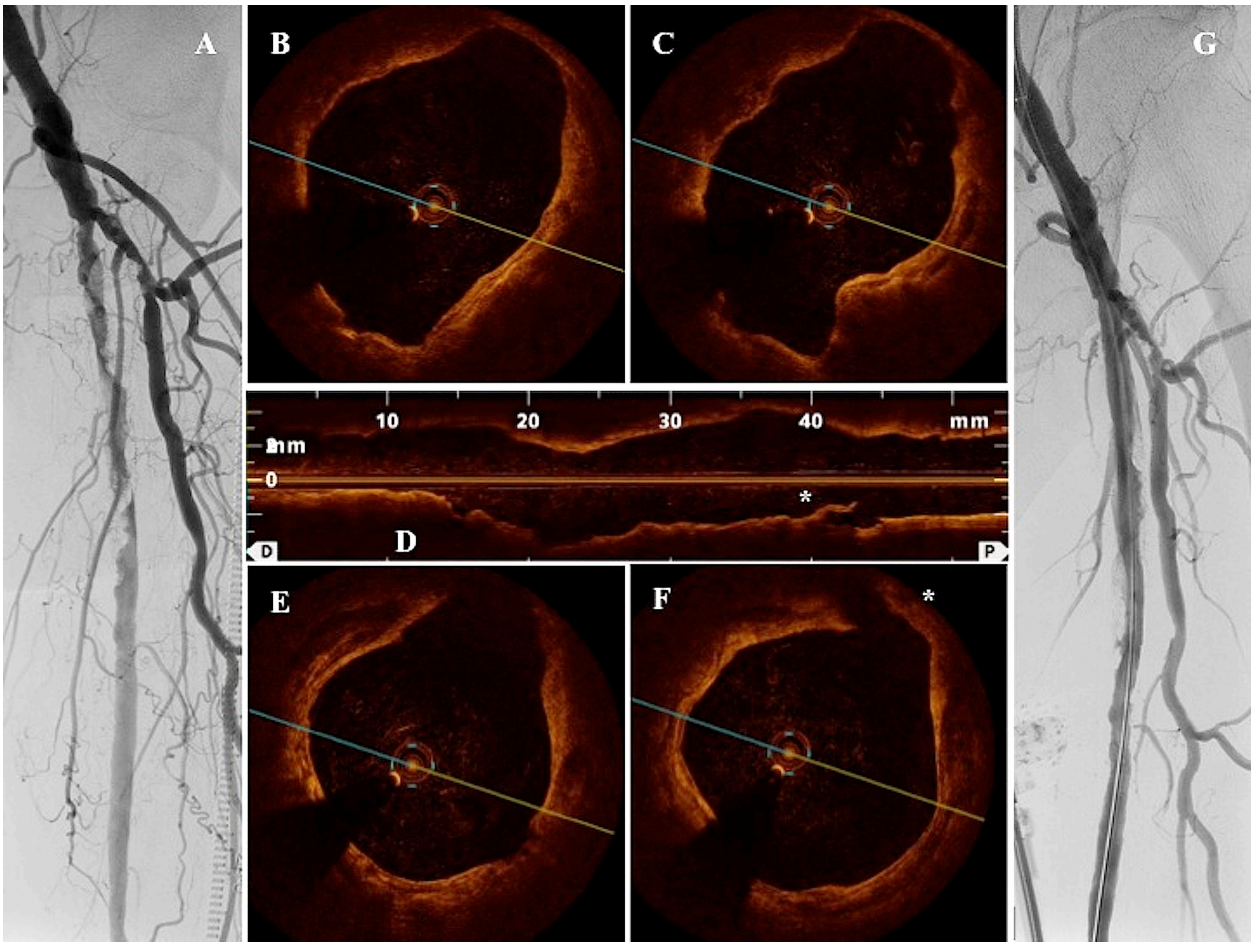

Finally, in order to stress the concept a same SFA was firstly OCT-imaged after contrast flush and after manual injection of 40 ml of Lactated Ringer's. In both pull-backs we were able to detect all vascular induced lesions as well as post atherectomy luminal gain with an equal accuracy (Fig. 3).

Figure 3: OCT cross-sections acquired after contrast flush (A) and Lactated Ringer's infusion (B). Please note that both images equally provide adequate information of vessel injuries following TurboHawk atherectomy.

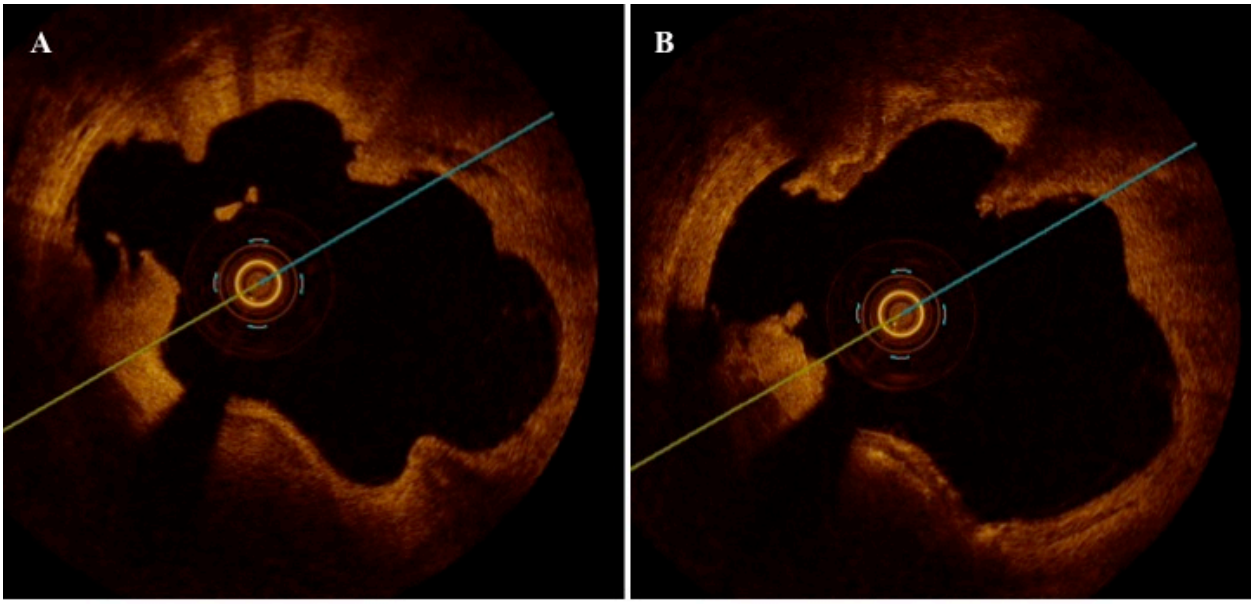

In case of extremely large SFA and poor image quality we suggest a simultaneous manual compression of the common femoral artery as described by Karnabatidis et al. (67). However, from out of our initial experience of 12 SFA OCT-imaged using pure saline injections, in all cases we were able to achieve an acceptable image quality without the need of femoral artery compression that might theoretically cause acute thrombosis.

Discussion

Optical coherence tomography is a near-infrared light based technology that enables to provide cross sectional images with an axial resolution of up to 10–15 μm resulting in a refined analysis of the vessel wall. The main reason why this technology is so infrequently used is both for the need of additional crystalloid infusion during imaging and for the low penetration power that is unable to deeply characterize the plaques. The introduction of the user friendly Frequency Domain system (FD-OCT) has partially overcome the limitations of the old Time Domain (TD-OCT). The fast-scanning laser system enables the TD-OCT to achieve images of longer segments (up to 54 mm) and larger arteries without the need of transient balloon occlusion, thus reducing the risk of vascular damage during imaging. However, OCT has been mainly evaluated during coronary intervention where its ability to disclose vessel microstructure might lose some of the clinical relevance. In fact, during percutaneous coronary intervention (PCI) the gold standard treatment sees, in the vast majority, the stent implantation as a final step irrespective of the plaque characterization and vessel wall injuries following lesion preparation. Successful percutaneous revascularization of femoral and popliteal arteries dramatically differs from PCI because of the several mechanical stresses such as torsion, compression, flexion and extension induced by the large muscular groups. These findings might explain the poor long-term outcome after peripheral percutaneous transluminal angioplasty (PTA) and the high rate of stent fractures at these sites (68). We believe that in this field, where the role of atherectomy and balloon angioplasty alone still plays a pivotal role, using an imaging modality able to precisely characterize the vessel all response to interventional devices might provide useful information. Despite this, the significant additional amount of contrast required for OCT evaluation of large muscular arteries might expose this

population to an increased risk of nephropathy and unfortunately, peripheral artery disease especially affects a setting of patient with major concomitant comorbidities such as diabetes, hypertension, poor renal function and other cardiovascular disorders. Our group firstly described the safety and feasibility of OCT acquisition during imaging of vascular lesions induced by renal nerve radio- frequency (RF) ablation using selective saline infusion instead of contrast flush (69). By manually injecting 30 ml of pure saline solution we were able to achieve a sufficient substitution of blood enable to detect vessel RF-induced lesions as during iodixanol 320 (Visipaque, GE Health Care, Cork, Ireland) infusion. Following our first experience, we decided to test the feasibility of saline infusion during OCT evaluation of superficial femoral artery (SFA) atherectomy. We believe that our findings might enlarge the use of OCT guidance during peripheral artery interventions where the use of a stent to seal vessel trauma following balloon inflation or plaque atherectomy is not as obvious as during PCI and the response of the vessel wall, not always detectable by angiography alone, acquires an imperative role.

2.3.2 Study 8

Title: Optical Coherence Tomography guidance during peripheral vascular intervention.

Background:

The additional use of optical coherence tomography during peripheral percutaneous transluminal angioplasty (PTA) has been very few reported. We believe that, thanks to the extremely high resolution rate able to characterize vessel microstructure, might be an interesting, potential adjunctive tool during PTA where the use of a stent to seal vessel trauma following balloon inflation or plaque atherectomy its not as obvious as during coronary intervention.

Aim

We tested the safety and efficacy of OCT during peripheral percutaneous transluminal angioplasty.

Materials and Methods

During percutaneous transluminal angioplasty of lower limbs we performed additional FD-OCT (St Jude, Minneapolis, MN, USA) acquisition after a gentle and prolonged manual injection of 50 ml of saline or, in case of poor images quality and unacceptable results, contrast flush at a flow rate sufficient to have full substitution of blood with contrast with no streaming according with international guidelines developed for intracoronary imaging. Finally we evaluated the additional information provided by OCT pullbacks and how did it modify our procedures.

Results

The results can be reassumed as following:

In the first figure we present both angiographic and OCT evaluation after TurboHawk (Covidien, ev3 endovascular, Inc., Plymouth, MN) atherectomy resulting in a proper luminal gain without excessive vessel trauma (Fig. 1). In this contest the patients did not require any additional treatment.

Figure 1: OCT (A) and Angiogram (B) of a stenotic SFA pre-intervention and OCT (C) and Angiogram (D) of the same artery after successful atherectomy.

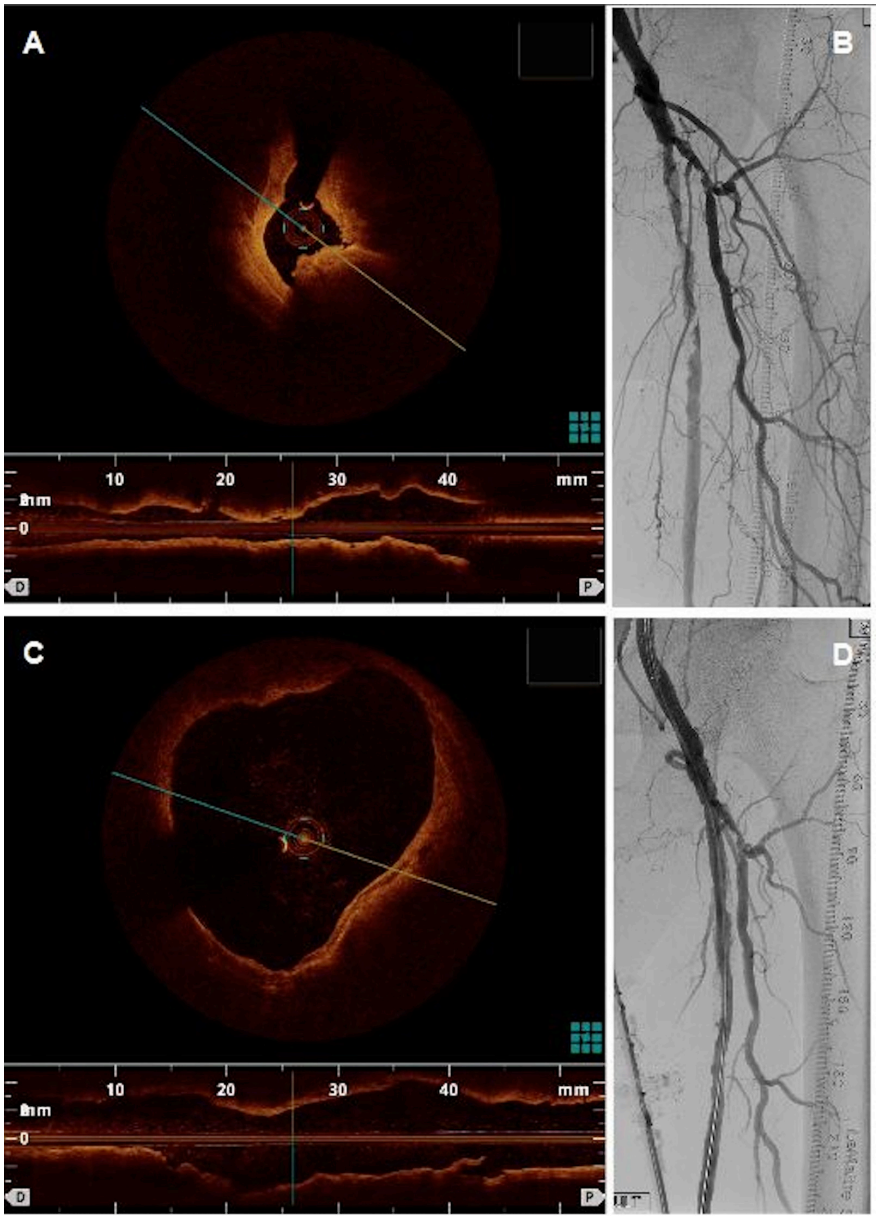

In contrast, the OCT evaluation of the second figure clearly shows a diffuse vascular trauma following the use of TurboHawk not detectable by angiography alone. In this case, we then decide to perform several additional balloon low-pressure inflations resulting in reduction of vascular injuries as showed in the final OCT acquisition (Fig. 2).

Figure 2: OCT (A) of a SFA after atherectomy; please note the diffuse vascular injuries following TurboHawk atherectomy not detectable by angiography alone (B). Panel C shows OCT image of the same artery with a visible reduction of the vessel injuries after several prolonged balloon inflation despite a superimposable angiogram (D).

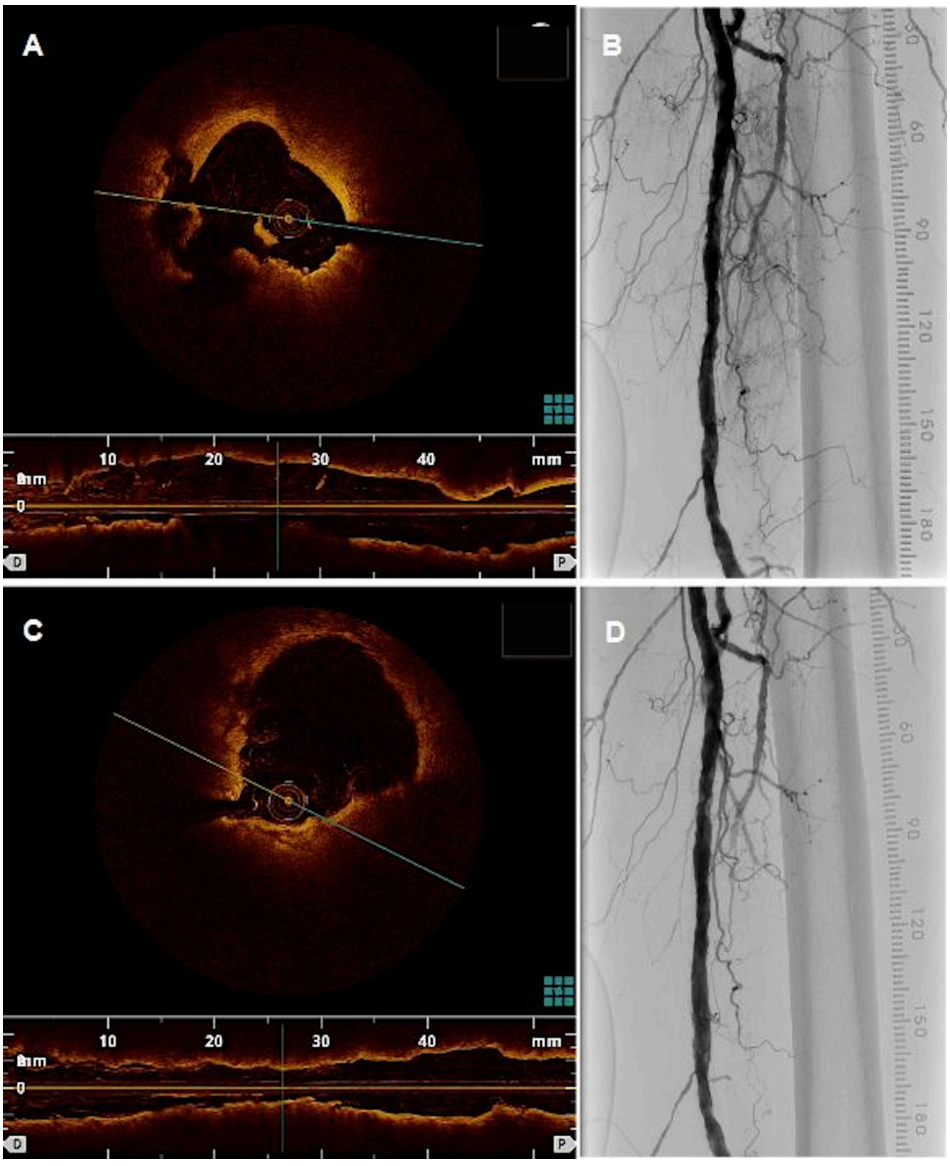

OCT acquisition of in the third figure shows a residual plaque burden despite first atherectomy not detectable by angiography alone. The patients underwent to further TurboHawk pass with a final acceptable luminal gain as clearly showed by final OCT images (Fig. 3).

Figure 3: SFA OCT (A) and Angiogram (B) pre-intervention, post unsuccessful first atherectomy (C, D) and the final result (E, F) after a further TurboHawk debulking. Please note that despite an almost superimposable Angiogram (D, F), OCT images clearly shows a significant luminal gain achieved with the second step atherectomy (C, D).

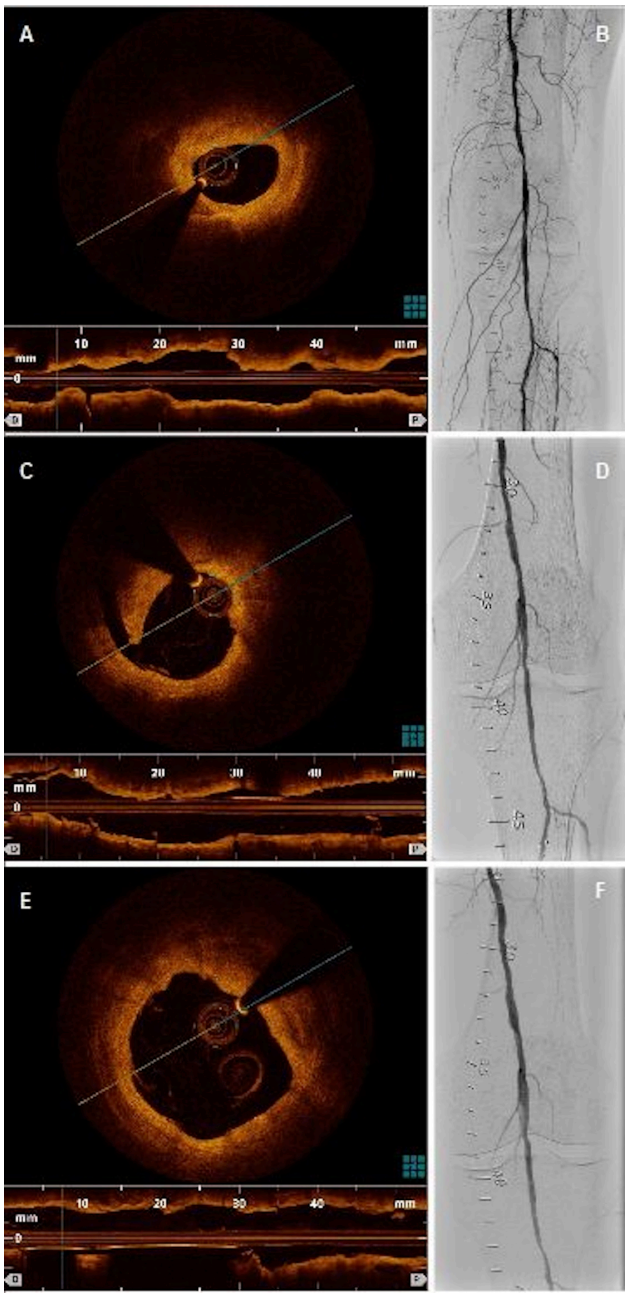

Discussion

In the last decades angiography has been the keystone to asses vascular anatomy leading to a widespread development of percutaneous revascularization techniques both for coronary and peripheral vascular disease. Despite being a relatively low cost, high reproducible and safe technique, angiography alone can only provide a limited analysis of the lumen profile, without the possibility to disclose vessel wall characteristics and with a relatively low resolution rate compared with newer intravascular imaging techniques. Intravascular ultrasound (IVUS), firstly introduced in interventional cardiology in the early 90's, has shown to be a valuable adjunctive tool even in the field of peripheral vascular interventions (70). Optical Coherence Tomography (OCT), a more recent, light-based technique is similar to IVUS providing information about intravascular anatomy that far exceeds the level of detail obtained from conventional angiography (71). The use of near-infrared light rather than ultrasound reflectance allows OCT to have higher spatial resolution (with up to 10 to 15 μm of spatial resolution compared with the 100 to 200 μm resolution of IVUS) but lower penetration power (1 to 3 mm into vessel wall compared with the 4 to 10 mm of IVUS). Moreover, near-infrared light is scattered by red blood cells, therefore OCT use for guidance of intervention was limited by the need of prolonged crystalloid infusion during imaging and OCT has been initially employed more as a research tool despite a real clinical adjunctive technique. The Frequency domain OCT system (FD-OCT) has the advantage of a more rapid image acquisition due to the fast-scanning laser systems able to minimise the contrast use and to increase imaging speed while delivering an improved image quality than with the earlier time domain systems (TD-OCT). Thus this allows multiple acquisitions of the entire segment of interest (up to

54mm) with an amount of contrast only slightly greater than contrast required for the control angiogram. The use of OCT during percutaneous coronary intervention (PCI) has been widely described and despite initial skepticisms is finally finding its role in daily clinical practice. Despite OCT usage during peripheral vascular intervention has been very few reported (72), we believe that it might provide useful information implementing proper peripheral lower extremity interventions. In fact, successful revascularization of lower limbs by percutaneous transluminal angioplasty (PTA) dramatically differs from PCI. Coronary intervention sees the use of drug eluting stent (DES) as the gold standard, while drug eluting balloons (DEB), balloon angioplasty alone or plaque atherectomy are mainly reserved for particular cases such as instent restenosis (ISR) or as a first revascularization step that will be finally followed by stent implantation. Unlike coronary, femoral and popliteal arteries are ones of the most dynamic vessels of the body, exposed to several mechanical stresses such as torsion, compression, flexion and extension by large muscolar groups. Despite high procedural acute success rate, these might explain the poor long term outcome after PTA with or without stenting and the high percentage of stent fractures at these sites (68). Unlike balloons and stents that push the plaque into the vessel wall, the promise of atherectomy is to offer the possibility to debulk the plaque, limiting the elastic recoil. However, atherectomy might cause several vessel wall injuries, not detectable by angiography alone, that might result in increased inflammation, higher rates of distal embolization and poorer outcome at long-term follow-up. The lack of clinical benefit observed in the early studies of atherectomy vs conventional PTA and/or stenting have created skepticism on its potential mechanical advantage. These studies were performed without systematic IVUS and/or OCT guidance, not allowing the distinction between atherectomy with a proper plaque debulking and procedures followed by insufficient plaque removal and diffuse vascular injuries unlikely to respond better

to PTA. In so forth we thought that OCT might be a valuable adjunctive tool during superficial femoral artery (SFA) atherectomy distinguishing “successfull” vs “unsuccessful” debulking despite a superimposable control angiogram.

2.4 OPTICAL COHERENCE TOMOGRAPHY DURING CAROTID ARTERY INTERVENTION

2.4.1 Study 9

Title: Carotid artery stenting (CAS): an update. Optical Coherence Tomography during CAS: interaction between stent design and atherosclerotic plaque.

Aim

Aim of our study was to define new indications for treatment and to provide new criteria for material choice during carotid endovascular procedures using Optical Coherence Tomography (OCT) examination.

Materials and Methods

Using FD-OCT we evaluated the impact of stent design on plaque prolapse and risk of stroke after carotid artery stenting (CAS).

Three designs of carotid stents with distinctive features have been widely available: Open-Cell (OC), Closed-Cell (CC), hybrid-cell (HYB).

Moreover, a novel carotid stent design has been recently developed, namely the double layer mesh stent. The design should allow for high flexibility to accommodate tortuous anatomy and at the same time convey scaffold properties for optimal plaque coverage. This technology is characterized by an internal micromesh layer for plaque coverage and an external self-expanding nitinol layer for scaffolding offering the flexibility that characterize open-cell design stents. Currently, the only CE marked and commercially available double layer mesh stent is illustrated in Figure 6. The device is compatible with a 0.014″ guide wire and 7F guiding catheter or 6F long sheath. The cell size of the micromesh is extremely

small (0.381 mm2) allowing for extensive plaque coverage. It remains to be demonstrated whether this interesting concept will translate into a reduction of neurologic events associated with CAS.

Figure 1: The self-expanding double layer mesh carotid stent RoadSaver^{TM} (Terumo,Japan).

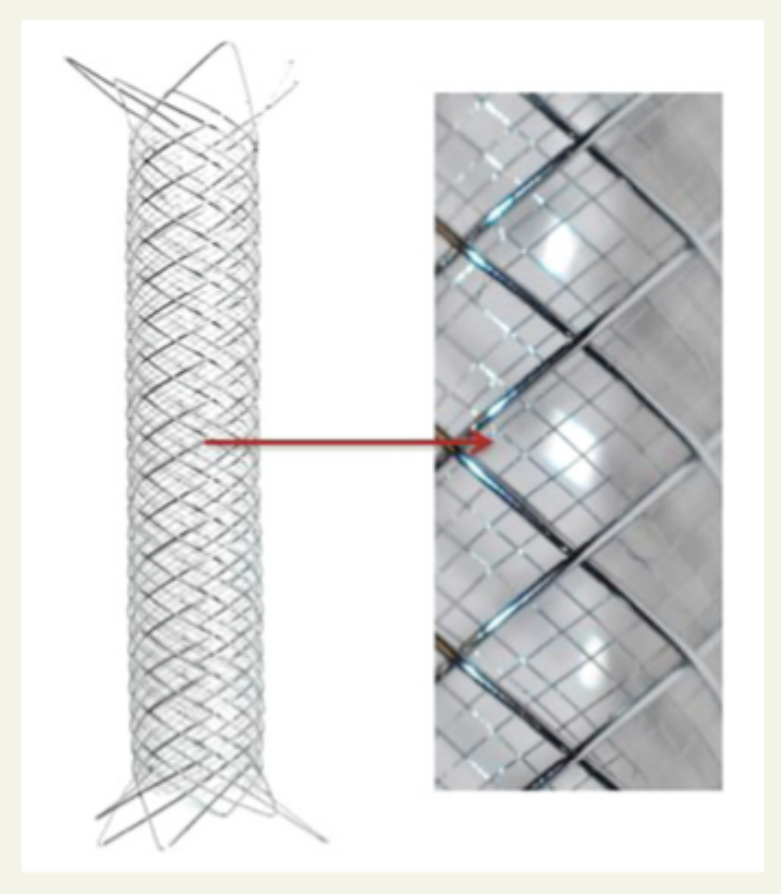

Discussion and Results

While in coronary interventions miniaturization and refinement of stent design has allowed the interventionalists to perform more complex procedures and to solve most of the limitations of stenting, in CAS little research and development efforts have been allocated to improve stent characteristics. Recently, it has been recognized that the stent itself may substantially add to embolic protection in CAS through adequate scaffolding of the plaque once the embolic protection device (EPD) has been removed. The ideal properties of a carotid stent are a well-balanced mix of high flexibility and conformability, to accommodate tortuous anatomy, as well as high plaque coverage, to prevent late embolization of debris. Stents structure is characterized by sequential aligned annular rings interconnected by bridges and the design may be either open cell or closed cell, depending on the density of the bridges between the rings. Open cell design stents presents some of the segment free from the adjacent rings allowing greater adaptation to the vessel anatomy at the price of less plaque coverage and higher risk of tissue prolapse. Closed-cell design stents are characterized by higher density of bridge interconnection, which reduces their conformability and increases the probability of malapposition but at the same time offers great plaque coverage. A hybrid configuration with an open-cell design of the proximal and distal segments combined with closed-cell design of the central segments has been developed: the hybrid stent design.

The impact of stent design on clinical outcome following CAS has not been adequately addressed. An observational study found a significant lower rate of post-procedural events in patients undergoing closed-cell design stent implantation compared with individual allocated to open-cell design stenting, but these results were not confirmed by other registries showing poor correlation between in-

hospital and 30 days mortality and stent design (73-76). A nice insight in the impact of stent design and in the pathophysiology at the lesion level at the time of CAS comes from a prospective single-centre study enrolling 40 consecutive patients and designed to evaluate the rate of stent malapposition, plaque prolapse, and thin cap fibro-atheroma rupture according to stent configuration by optical coherence tomography (OCT) (Figure 4) (77). Closed-cell design stents were used in 17 patients (42.5%), open-cell design stents in 13 patients (32.5%), and hybrid design stents in 10 patients (25%). No neurological complications occurred. On OCT analysis, the frequencies of malapposed struts were higher with closed-cell compared with open-cell and hybrid design stents (34.5 vs. 15% and 16.3%, respectively; $P < 0.01$). Plaque prolapse was more frequent with open cell than closed cell (68.6 vs. 23.3%; $P <0.01$) and hybrid stents (30.8%; $P <0.01$). Significant differences were also noted in the rates of fibrous cap rupture between closed- and open cell (24.2 vs. 43.8%; $P < 0.01$), and between closed-cell and hybrid design (39.6%; $P < 0.01$) stents, but not between open-cell and hybrid design stents ($P = 0.4$). The authors concluded that micro-defects after stent deployment in CAS are frequent and are related to the design of implanted stents. While stent malapposition was more common following closed-cell design stent implantation, plaque prolapse was more common in patients treated with open- cell design devices. While these results are important, a correlation to clinical events remains to be demonstrated.

The mechanism of delayed cerebral embolization following CAS is unknown but may include tissue prolapsed through the stent struts and thrombus formation around malapposed stent struts. Despite the fact that current guidelines recommend carotid artery revascularization exclusively on the basis of stenosis severity, the importance of plaque characterization in stratifying stroke risk has been increasingly recognized. The weak correlation between the severity of stenosis and

the risk of stroke in asymptomatic patients found in several trials together with recently published data that link complex plaques with stroke challenge the ‘degree of stenosis-stroke risk’ paradigm, highlight the importance of the morphology and composition of the carotid plaques beyond the degree of stenosis and of the investigation of the complex stent – plaque interaction after CAS (78, 79). In this respect, calcified lesions may favour stent malapposition while soft plaques may result in greater tissue prolapse though the stent struts.

Figure 2: Optical coherence tomography findings inside an open-cell carotid stent. (A) Malapposition of the stent to the vessel wall (B) intra-strut plaque prolapse (arrows).

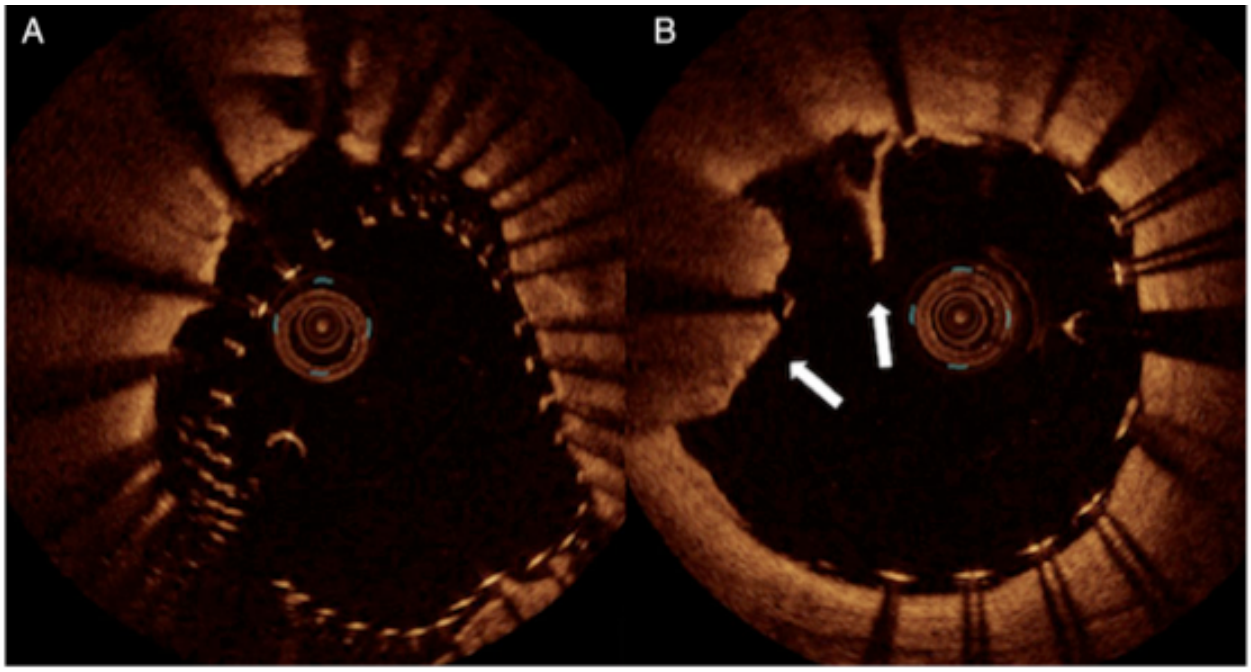

A promising help comes from a new double layer mash (DLM) stent design. The DLM stent present an internal micromesh layer for plaque coverage and an external nitinol layer that offers a flexibility of an OC stent. In our limited series of

11 patients treated with the Roadsaver stent we found a great coverage of plaque coverage with no embolic events both at acute and long-term follow up.

Figure 3: Optical coherence tomography assessment of a RoadSaver TM stent showing no significant prolapse of plaque and good wall apposition.

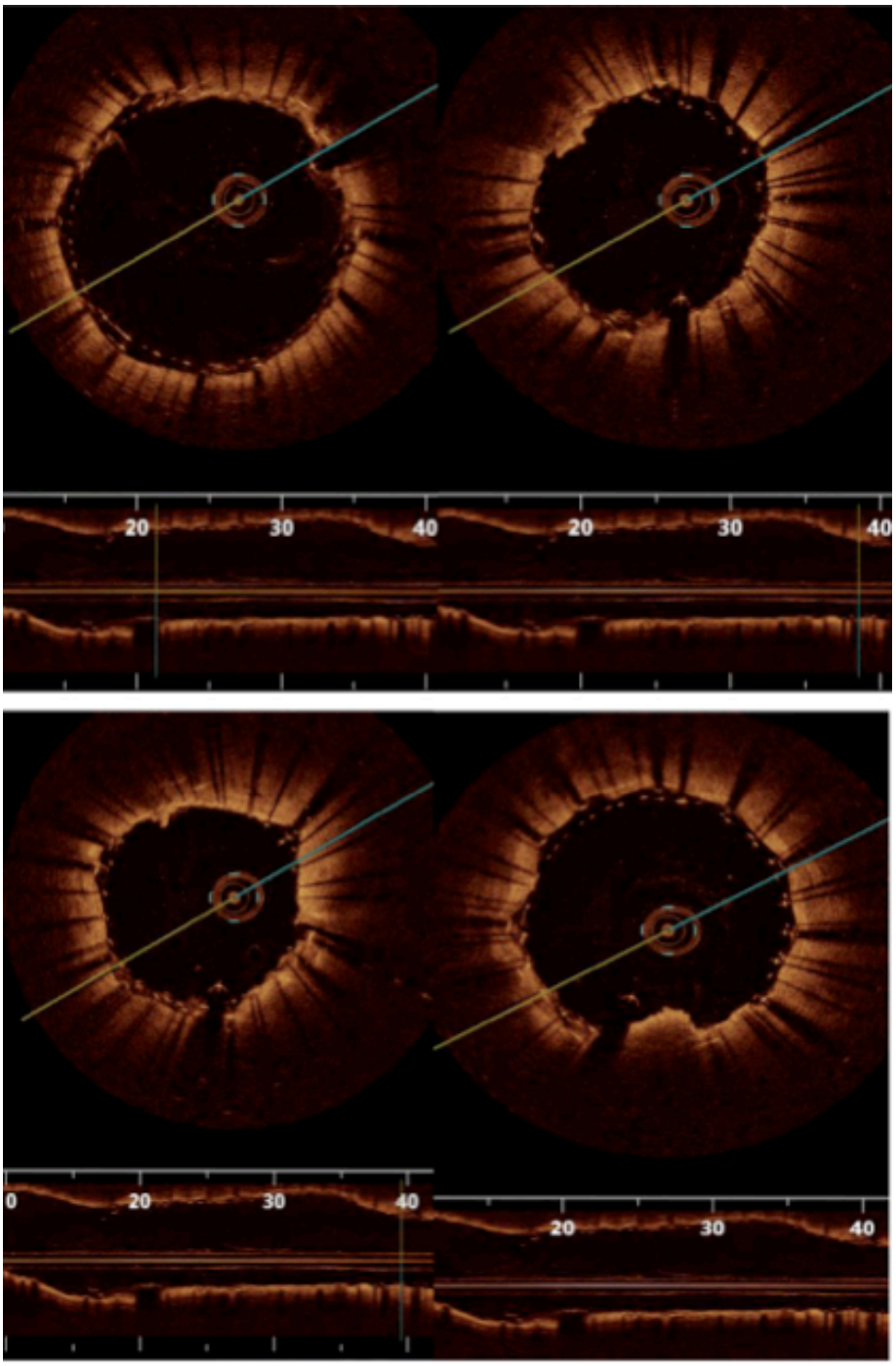

3. CONCLUSION

With the increased diffusion of OCT, much has been documented in terms of its safety profile.

First generation OCT systems required the use of an occlusion balloon situated in the proximal segment of the vessel inflated simultaneously during flush of Ringer's lactate. Refinement of the technology, with faster acquisition speeds, has seen a gradual shift from the cumbersome occlusive technique to a simpler and safer non-occlusive technique with flushing of viscous contrast through the guiding catheters (80). This technique has the advantages of shorter OCT procedure, larger amount of information with longer pull-back distance and evaluation of most proximal coronary segments with less patient discomfort.

The need of blood clearance during imaging requires additional contrast agent infusion and might increase the risk of contrast-induced nephropathy and elicits transient chest pain and ECG change, which almost always resolve immediately following imaging.

For one of the first time ever our group reported the safety and efficacy of saline infusion instead of contrast flush during FD-OCT acquisition. Certainly, this can be used only during peripheral intervention and is not suitable during coronary imaging because of the possible increased risk of ventricular fibrillation during injection of a significant amount of saline in the coronary artery. However, this finding might further enlarge the use of OCT during percutaneous peripheral approach.

When first confronted with OCT of coronary artery, one cannot help be impressed by the clarity of the images. The understanding of OCT imaging, however, lies deep beyond this cursory assessment and requires appropriate interpretation. This remains one of the most painstaking aspects of off-line image interpretation.

Much of what is currently known regarding stent safety has mainly arisen based on old studies using angiographic follow-up or IVUS in addition to invaluable information gained during the unlikely post-mortem setting. OCT has now become integral to a number of multi-center trials evaluating new generation drug eluting stent (DES) and bioresorbable vascular scaffold (BVS). Unlike conventional stents that develop circumferential coverage with an average thickness of 500 μm or more, which are well-visualized with IVUS and angiography (1-mm late loss), DES delay and prevent the hyperplastic response so that the average late lumen loss for -limus or paclitaxel-eluting stents can be lower than 100 μm. Therefore, the amount of intimal thickening will not be detectable with IVUS because of its limited axial resolution and the presence of artifacts around struts (15). The introduction of OCT, an imaging technique that employs near-infrared light and provides cross-sectional images with an axial resolution of 10 μm (16), has provided new opportunities to perform a more refined analysis of vessel response to endovascular devices offering a unique combination of minimally invasive surface scanning technology and in-vivo images of biological samples at a resolution 10–30 times higher than conventional IVUS. In fact several experimental and clinical studies demonstrated the high correlation between OCT and histological measurements of neointimal coverage of stent struts, highlighting the superiority of OCT over IVUS for in-vivo detection of stent tissue coverage at follow-up.

OCT can be also used to guide optimal stent expansion and apposition especially during new thin strut DES and BVS implantation. Indeed, stent expansion, apposition and symmetry were the principal IVUS criteria in the bare metal stent era. Since infra-red light is unable to penetrate through metal struts, OCT visualizes only the endo-luminal surface of the strut and its thickness, combined with the one of the polymer should be considered during OCT DES evaluation. In

addition to stent tissue coverage and apposition, OCT can be a complementary imaging modality when evaluating stent fracture, in cases of very late stent thrombosis and almost unique when examining absorption of the new biodegradable vascular scaffolds thereby yielding unique ante-mortem information.

Few studies investigated the role of OCT guidance to lesion treatment. Our group showed in a single center series of 398 pull backs before and after stent implantation that 19% of cases were deferred according to the results of pre-treatment OCT pullback and 33.8% of lesions after angiographic stent optimisation with high pressure balloon required additional expansion or stenting at the edges. In a series of 670 patients the outcomes of an angiographic guided strategy were compared with an OCT guided strategy. At one year follow up, the group treated with OCT had a lower rate of cardiac death and re-intervention (81). According to these early results, OCT seems to be, at least, as beneficial as IVUS for guidance of coronary interventions with the potential great advantage of immediate automated quantification of stent apposition and expansion.

Finally, our group focused in a peculiar, poorly explored field: the use of OCT during non-coronary interventions. OCT confirmed its safety profile and provided unique clinically oriented informations that strongly encourage its use in this clinical “scenario”.

Although the OCT is only recently entered in our catheterization laboratories, the promising results showed in this thesis support its usefulness in a wide range of clinical and research settings.

REFERENCE:

1) Coronary stenosis: Imaging, Structure and Phisiology. Garcia-Garcia HM, Brugaletta S, Diletti R, Secco GG, Di Mario C, Serruys PW. Chapt 14: Intravascular ultrasound in the assessment of coronary stenosis. Edited on Behalf of The European Society of Cardiology (ESC) and European Association of Percutaneous Coronary Intervention (EAPCI).

2) Yock PG, Fitzgerald PJ, Linker DT, Angelsen BA. Intravascular ultrasound guidance for catheter-based coronary interventions. J Am Coll Cardiol. 1991 May;17(6 Suppl B):39B-45B.

3) Prati F, Regar E, Mintz GS, Arbustini E, Di Mario C, Jang IK, Akasaka T, Costa M, Guagliumi G, Grube E, Ozaki Y, Pinto F, Serruys PW; Expert's OCT Review Document. Expert review document on methodology, terminology, and clinical applications of optical coherence tomography: physical principles, methodology of image acquisition, and clinical application for assessment of coronary arteries and atherosclerosis. Eur Heart J 2010;31:401-15.

4) Smith SC Jr, Feldman TE, Hirshfeld JW Jr, Jacobs AK, Kern MJ, King SB 3rd, Morrison DA, O'neill WW, Schaff HV, Whitlow PL, Williams DO, Antman EM, Smith SC Jr, Adams CD, Anderson JL, Faxon DP, Fuster V, Halperin JL, Hiratzka LF, Hunt SA, Jacobs AK, Nishimura R, Ornato JP, Page RL, Riegel B; American College of Cardiology/American Heart Association Task Force on Practice Guidelines; ACC/AHA/SCAI Writing Committee to Update the 2001 Guidelines for Percutaneous Coronary Intervention. ACC/ AHA/SCAI 2005 Guideline Update for Percutaneous Coronary Intervention-Summary Article: A Report of the American College of Cardiology/American Heart Association Task Force on Practice Guidelines (ACC/AHA/SCAI Writing Committee to Update the 2001

Guidelines for Percutaneous Coronary Intervention). J Am Coll Cardiol 2006;47:216-35.

5) Castagna MT, Mintz GS, Leiboff BO, Ahmed JM, Mehran R, Satler LF, Kent KM, Pichard AD, Weissman NJ. The contribution of "mechanical" problems to in-stent restenosis: An intravascular ultrasonographic analysis of 1090 consecutive in-stent restenosis lesions. Am Heart J 2001;142:970-4.

6) Ku DN. Blood flow in arteries. Annual Review of Fluid Mechanics 1997;29:399.

7) Oh S, Kleinberger M, McElhaney JH. Finite-element analysis of balloon angioplasty. Med Biol Eng Comput 1994;32:S108-14.

8) Adamian M, Colombo A, Briguori C, Nishida T, Marsico F, Di Mario C, Albiero R, Moussa I, Moses JW. Cutting balloon angi- oplasty for the treatment of in-stent restenosis: a matched compari- son with rotational atherectomy, additional stent implantation and balloon angioplasty. J Am Coll Cardiol 2001;38:672-9.

9) Albiero R, Silber S, Di Mario C, Cernigliaro C, Battaglia S, Reimers B, Frasheri A, Klauss V, Auge JM, Rubartelli P, Morice MC, Cremonesi A, Schofer J, Bortone A, Colombo A; RESCUT Investigators. Cutting balloon versus conventional balloon angioplasty for the treat- ment of in-stent restenosis: results of the restenosis cutting balloon evalu- ation trial (RESCUT). J Am Coll Cardiol 2004;43:943-9.

10) Suzuki Y, Ikeno F, Koizumi T, Tio F, Yeung AC, Yock PG, Fitzgerald PJ, Fearon WF. In vivo comparison between optical coherence tomography and intravascular ultrasound for detecting small degrees of in-stent neointima after stent implantation. JACC Cardiovasc Interv 2008;1:168-73.

11) Mehran R, Mintz GS, Popma JJ, Pichard AD, Satler LF, Kent KM, Griffin J, Leon MB. Mechanisms and results of balloon angioplasty for the treatment of in-stent restenosis. Am J Cardiol 1996;78: 618-22.

12) Shiran A, Mintz GS, Waksman R, Mehran R, Abizaid A, Kent KM, Pichard AD, Satler LF, Popma JJ, Leon MB. Early lumen loss after treatment of in-stent restenosis: an intravascular ultrasound study. Circulation 1998;98:200-3.

13) Gonzalo N, Serruys PW, Okamura T, van Beusekom HM, Garcia-Garcia HM, van Soest G, van der Giessen W, Regar E. Optical coherence tomography patterns of stent restenosis. Am Heart J 2009;158:284-93.

14) Sonoda S, Morino Y, Ako J, Terashima M, Hassan AH, Bonneau HN, Leon MB, Moses JW, Yock PG, Honda Y, Kuntz RE, Fitzgerald PJ; SIRIUS Investigators. Impact of final stent dimension on long- term results following sirolimus-eluting stent implantation: serial intravascular ultrasound analysis from the Sirius trial. J Am Coll Cardiol 2004;43:1959-63.

15) Windecker S, Serruys PW, Wandel S, et al. Biolimus-eluting stent with biodegradable polymer versus sirolimus-eluting stent with durable polymer for coronary revascularisation (LEADERS): a randomised non-inferiority trial. Lancet 2008;372:1163-73.

16) Gonzalo N, Garcia-Garcia HM, Serruys PW, et al. Reproducibility of quantitative optical coherence tomography for stent analysis. EuroIntervention 2009;5:224-32.

17) Tanigawa J, Barlis P, di Mario C. Intravascular optical coherence tomography: optimisation of image acquisition and quantitative assessment of stent strut apposition. EuroIntervention 2007;3:128-36.

18) Reidy MA, Schwartz SM. Endothelial regeneration. III. Time course of intimal changes after small defined injury to rat aortic endothelium. Lab Invest 1981;44:301-8.

19) Bjorkerud S, Bondjers G. Arterial repair and atherosclerosis after mechanical injury. 5. Tissue response after induction of a large superficial transverse injury. Atherosclerosis 1973;18:235-55.

20) Reidy MA, Standaert D, Schwartz SM. Inhibition of endothelial cell regrowth. Cessation of aortic endothelial cell replication after balloon catheter denudation. Arteriosclerosis 1982;2:216-20.

21) Reidy MA, Clowes AW, Schwartz SM. Endothelial regeneration. V. Inhibition of endothelial regrowth in arteries of rat and rabbit. Lab Invest 1983;49:569-75.

22) Takano M, Yamamoto M, Xie Y, et al. Serial long-term evaluation of neointimal stent coverage and thrombus after sirolimus-eluting stent implantation by use of coronary angioscopy. Heart 2007;93:1533-6.

23) Takano M, Inami S, Jang IK, et al. Evaluation by optical coherence tomography of neointimal coverage of sirolimus-eluting stent three months after implantation. Am J Cardiol 2007;99:1033-8.

24) Takano M, Yamamoto M, Inami S, et al. Long-term follow-up evaluation after sirolimus-eluting stent implantation by optical coherence tomography: do uncovered struts persist? J Am Coll Cardiol 2008;51:968-9.

25) Katoh H, Shite J, Shinke T, Matsumoto D, Tanino Y, Ogasawara D, Sawada T, Miyoshi N, Kawamori H, Yoshino N, Hirata K. Delayed neointimalization on Sirolimus-Eluting stents. 6-month and 12-month follow up by optical coherence tomography. Circ J. 2009;73:1033-7.

26) Takano M, Yamamoto M, Mizuno M, et al. Late vascular responses from 2 to 4 years after implantation of sirolimus-eluting stents: serial observations by intracoronary optical coherence tomography. Circ Cardiovasc Interv 2010;3:476-83.

27) Virmani R, Guagliumi G, Farb A, Musumeci G, Grieco N, Motta T, Mihalcsik L, Tespili M, Valsecchi O, Kolodgie FD. Localized hypersensitivity and late coronary thrombosis secondary to a sirolimus-eluting stent: should we be cautious? Circulation 2004;109:701–5.

28) Cook S, Ladich E, Nakazawa G, et al. Correlation of intravascular ultrasound findings with histopathological analysis of thrombus aspirates in patients with very late drug-eluting stent thrombosis. Circulation 2009;120:391-9.

29) Simon C, Palmaz JC, Sprague EA. Influence of topography on endothelialization of stents: clues for new designs. J Long Term Eff Med Implants 2000;10:143-51.

30) Barlis P, Regar E, Serruys PW, et al. An optical coherence tomography study of a biodegradable vs. durable polymer-coated limus-eluting stent: a LEADERS trial sub-study. Eur Heart J 2010;31: 165-76.

31) Prati F, Stazi F, Dutary J, La Manna A, Di Giorgio A, Pawlosky T, Gonzalo N, Di Salvo ME, Imola F, Tamburino C, Albertucci M, Alfonso F. Detection of very early stent healing after primary angioplasty: an optical coherence tomographic observational study of chromium cobaltum and first-generation drug-eluting stents. The DETECTIVE study. Heart. 2011;97:1841-6.

32) Tada T, Byrne RA, Schuster T, Cuni R, Kitabata H, Tiroch K, Dirninger A, Gratze F, Kaspar K, Zenker G, Joner M, Schömig A, Kastrati A. Early vascular

healing with rapid breakdown biodegradable polymer sirolimus-eluting versus durable polymer everolimus-eluting stents assessed by optical coherence tomography. Cardiovasc Revasc Med. 2013;14:84-9

33) de la Torre-Hernandez JM, Alfonso F, Hernandez F, Elizaga J, Sanmartin M, Pinar E, Lozano I, Vazquez JM, Botas J, de Prado AP, Hernandez JM, Sanchis J, Nodar JM, Gomez-Jaume A, Larman M, Diarte JA, Rodriguez-Collado J, Rumoroso JR, Lopez-Minguez JR, Mauri J. Drug-eluting stent thrombosis: results from the multicenter Spanish registry ESROFA. J Am Coll Cardiol. 2008;51:986-90.

34) van der Giessen WJ, Lincoff AM, Schwartz RS et al. Marked inflammatory sequelae to implantation of biodegradable and nonbiodegradable polymers in porcine coronary arteries. Circulation 1996;94:1690-7.

35) Lupi A, Rognoni A, Secco GG, Lazzero M, Nardi F, Fattori R, Bongo AS, Agostoni P, Sheiban I Biodegradable versus durable polymer drug eluting stents in coronary artery disease: Insights from a meta-analysis of 5834 patients. Eur J Prev Cardiol. 2012 Nov 14. [Epub ahead of print]

36) Palmerini T, Kirtane AJ, Serruys PW, Smits PC, Kedhi E, Kereiakes D, Sangiorgi D, Bacchi Reggiani L, Kaiser C, Kim HS, De Waha A, Ribichini F, Stone GW. Stent thrombosis with everolimus-eluting stents: meta-analysis of comparative randomized controlled trials. Circ Cardiovasc Interv. 2012 Jun;5(3):357-64

37) Palmerini T, Biondi-Zoccai G, Della Riva D, Stettler C, Sangiorgi D, D'Ascenzo F, Kimura T, Briguori C, Sabatè M, Kim HS, De Waha A, Kedhi E, Smits PC, Kaiser C, Sardella G, Marullo A, Kirtane AJ, Leon MB, Stone GW.

Stent thrombosis with drug-eluting and bare-metal stents: evidence from a comprehensive network meta-analysis. Lancet. 2012 Apr 14;379(9824):1393-402.

38) Hara M, Nishino M, Taniike M, Makino N, Kato H, Egami Y, Shutta R, Yamaguchi H, Tanouchi J, Yamada Y. Difference of neointimal formational pattern and incidence of thrombus formation among 3 kinds of stents: an angioscopic study. JACC Cardiovasc Interv. 2010;3:215-20

39) Secco GG, Foin N, Viceconte N, Borgia F, De Luca G, Di Mario C. Optical coherence tomography for guidance of treatment of in-stent restenosis with cutting balloons. EuroIntervention. 2011;7:828-34

40) Lupi A, Porto I, Rognoni A, Lazzero M, Fattori R, Parisi R, De Maria GL, Bongo AS, Sheiban I, Bolognese L, Agostoni P, Secco GG; Novara-PROMETEUS (Platinum ChROMium Everolimus EluTing StEnt SpontaneoUs RegiStry) Investigators. Clinical and biomechanical behavior of a platinum-chromium stent platform in a large all-comer single-center population: insights from the Novara-PROMETEUS registry. J Invasive Cardiol. 2014;26:311-7.

41) Secco GG, Ghione M, Mattesini A, Dall'Ara G, Ghilencea L, Kilickesmez K, De Luca G, Fattori R, Parisi R, Marino P, Lupi A, Foin N, Di Mario C. Very High Pressure Dilatation for Undilatable Coronary Lesions: Indications and Results with a New Dedicated Balloon. Eurointervention (Accepted-ahead of print)

42) Gomez-Lara J, Diletti R, Brugaletta S, et al. Angiographic maximal luminal diameter and appropriate deployment of the everolimus-eluting bioresorbable vascular scaffold as assessed by optical coherence tomog- raphy: an ABSORB cohort B trial sub-study. EuroIntervention 2012;8: 214–24.

43) Serruys PW, Onuma Y, Ormiston JA, et al. Evaluation of the second generation of a bioresorbable everolimus drug-eluting vascular scaffold for treatment of de novo coronary artery stenosis: six-month clinical and imaging outcomes. Circulation 2010;122:2301–12.

44) Tearney GJ, Regar E, Akasaka T, et al. Consensus standards for acquisition, measurement, and reporting of intravascular optical coher- ence tomography studies: a report from the International Working Group for Intravascular Optical Coherence Tomography Standardiza- tion and Validation. J Am Coll Cardiol 2012;59:1058–72.

45) Costa MA, Angiolillo DJ, Tannenbaum M, et al. Impact of stent deployment procedural factors on long-term effectiveness and safety of sirolimus-eluting stents (final results of the multicenter prospective STLLR trial). Am J Cardiol 2008;101:1704–11.

46) Doi H, Maehara A, Mintz GS, et al. Impact of post-intervention minimal stent area on 9-month follow-up patency of paclitaxel- eluting stents: an integrated intravascular ultrasound analysis from the TAXUS IV, V, and VI and TAXUS ATLAS Workhorse, Long Lesion, and Direct Stent Trials. J Am Coll Cardiol Intv 2009;2: 1269–75.

47) Lindsay AC, Paulo M, Kadriye K, et al. Predictors of stent strut mal-apposition in calcified vessels using frequency-domain optical coherence tomography. J Invasive Cardiol 2013;25:429–34.

48) Gonzalo N, Serruys PW, Garcia-Garcia HM, et al. Quantitative ex vivo and in vivo comparison of lumen dimensions measured by optical coherence tomography and intravascular ultrasound in human coronary arteries. Rev Esp Cardiol 2009;62:615–24.

49) Song HG, Kang SJ, Ahn JM, et al. Intravascular ultrasound assessment of optimal stent area to prevent in-stent restenosis after zotarolimus-, everolimus- and sirolimus-eluting stent implantation. Catheter Car- diovasc Interv 2014;83:873–8.

50) Hoffmann R, Morice MC, Moses JW, et al. Impact of late incomplete stent apposition after sirolimus-eluting stent implantation on 4-year clinical events: intravascular ultrasound analysis from the multicentre, randomised, RAVEL, E-SIRIUS and SIRIUS trials. Heart 2008;94: 322–8.

51) Tyczynski P, Ferrante G, Moreno-Ambroj C, et al. Simple versus complex approaches to treating coronary bifurcation lesions: direct assessment of stent strut apposition by optical coherence tomography. Rev Esp Cardiol 2010;63:904–14.

52) Onuma Y, Serruys PW, Perkins LE, et al. Intracoronary optical coherence tomography and histology at 1 month and 2, 3, and 4 years after implantation of everolimus-eluting bioresorbable vascular scaffolds in a porcine coronary artery model: an attempt to decipher the human optical coherence tomography images in the ABSORB trial. Circulation 2010;122:2288–300.

53) Cannon CP, Battler A, Brindis RG, Cox JL, Ellis SG, Every NR, Flaherty JT, Harrington RA, Krumholz HM, Simoons ML, Van De Werf FJ, Weintraub WS, Mitchell KR, Morrisson SL, Brindis RG, Anderson HV, Cannom DS, Chitwood WR, Cigarroa JE, Collins-Nakai RL, Ellis SG, Gibbons RJ, Grover FL, Heidenreich PA, Khandheria BK, Knoebel SB, Krumholz HL, Malenka DJ, Mark DB, Mckay CR, Passamani ER, Radford MJ, Riner RN, Schwartz JB, Shaw RE, Shemin RJ, Van Fossen DB, Verrier ED, Watkins MW, Phoubandith DR, Furnelli T. American College of Cardiology key data elements and definitions for measuring the clinical management and outcomes of patients with acute coronary syndromes. A report of the American College of Cardiology Task Force on

Clinical Data Standards (Acute Coronary Syndromes Writing Committee). J Am Coll Cardiol. 2001;38:2114-30.

54) Vito RP, Dixon SA. Blood vessel constitutive models-1995-2002. Annu Rev Biomed Eng 2003;5:413-39

55) Schwarzwalder U, Zeller T. Debulking Procedures: Potential Device Specific Indications. Tech Vasc Interv Radiol. 2012; 13:43-53

56) Ben-Dor I, Maluenda g, Pichard AD, Satler LF, Gallino R, Lindsay J, Waksma R. The use of excimer laser for complex coronary artery lesions. Cardiovasc Revasc Med. 2011; 69: e1-8

57) Kim MH, Kim HJ, Kim NN, Yoon HS, Ahn SH. A rotational ablation tool for calcified atherosclerotic plaque removal. Biomed Microdevices. 2011;13:963-71.

58) Moussa I, Di Mario C, Moses J, Reimers B, Di Francesco L, Martini G, Tobis J, Colombo A. Coronary stenting after rotational atherectomy in calcified and complex lesions. Angiographic and clinical follow-up results. Circulation. 1997;96:128-36.

59) Urban P, Gershlick AH, Guagliumi G, Guyon P, Lotan C, Schofer J, et al; e-Cypher Investigators. Safety of coronary sirolimus-eluting stents in daily clinical practice: One-year follow-up of the e-Cypher registry. Circulation 2006;113: 1434 – 1441.

60) Raja Y, Routledge HC, Doshi SN. A noncompliant, high pressure balloon to manage undilatable coronary lesions. Catheter Cardiovasc Interv 2010;75:1067-73.

61) Díaz JF, Gómez-Menchero A, Cardenal R, Sánchez-González C, Sanghvi A. Extremely high-pressure dilation with a new noncompliant balloon. Tex Heart Inst J. 2012;39:635-8.

62) Schlaich MP, Sobotka PA, Krum H, Lambert E, Esler MD. Renal sympathetic-nerve ablation for uncontrolled hypertension. N Engl J Med. 2009;361:932-4

63) Templin C, Jaguszewski M, Ghadri JR, Sudano I, Gaehwiler R, Hellermann JP, Schoenenberger-Berzins R, Landmesser U, Erne P, Noll G, Lüscher TF. Vascular lesions induced by renal nerve ablation as assessed by optical coherence tomography: pre- and post-procedural comparison with the Simplicity(R) catheter system and the EnligHTN™ multi-electrode renal denervation catheter. Eur Heart J. 2013 Apr 25. [Epub ahead of print]

64) Kaltenbach B, Id D, Franke JC, Sievert H, Hennersdorf M, Maier J, Bertog SC. Renal artery stenosis after renal sympathetic denervation. J Am CollCardiol. 2012;60:2694-5;

65) Rippy MK, Zarins D, Barman NC, Wu A, Duncan KL, Zarins CK. Catheter-based renal sympathetic denervation: chronic preclinical evidence for renal artery safety. Clin Res Cardiol. 2011;100:1095-101

66) Franzone A, Ferrone M, Carotenuto G, Carbone A, Scudiero L, Serino F, Scudiero F, Izzo R, Piccolo R, Saviano S, Amato B, Perrino C, Trimarco B, Esposito G. The role of atherectomy in the treatment of lower extremity peripheral artery disease. BMC Surg. 2012;12 Suppl 1:S13.

67) Karnabatidis D, Katsanos K, Paraskevopoulos I, Diamantopoulos A, Spiliopoulos S, Siablis D. Frequency-domain intravascular optical coherence

tomography of the femoropopliteal artery. Cardiovasc Intervent Radiol. 2011;34:1172-81

68) Scheinert D, Scheinert S, Sax J, Piorkowski C, Bräunlich S, Ulrich M, Biamino G, Schmidt A. Prevalence and clinical impact of stent fractures after femoropopliteal stenting. J Am Coll Cardiol. 2005;45:312-5.

69) Secco GG, Micari A, Vadalà G, Lanteri S, Parisi R, Fattori R, Cremonesi A, Zeller T, Catriota F. Safety and efficacy of saline infusion for optical coherence tomography evaluation of vascular lesion induced by renal nerve ablation. Int J Cardiol. 2013;168:5024-5.

70) The SH, Gussenhoven EJ, Zhong Y, Li W, van Egmond F, Pieterman H, van Urk H, Gerritsen GP, Borst C, Wilson RA. Effect of balloon angioplasty on femoral artery evaluated with intravascular ultrasound imaging. Circulation 1992;86:483–493.

71) McCabe JM, Croce KJ. Optical coherence tomography. Circulation. 2012;126:2140-3.

72) Stefano GT, Mehanna E, Parikh SA. Imaging a spiral dissection of the superficial femoral artery in high resolution with optical coherence tomography-seeing is believing. Catheter Cardiovasc Interv. 2013;81:568-72.

73) Bosiers M, de Donato G, Deloose K, Verbist J, Peeters P, Castriota F, Cremonesi A, Setacci C. Does free cell area influence the outcome in carotid artery stenting? Eur J Vasc Endovasc Surg 2007;33:135 – 141; discussion 142 – 133.

74) Bosiers M, Deloose K, Verbist J, Peeters P. Carotid artery stenting: which stent for which lesion? Vascular 2005;13:205 – 210.

75) Jim J, Rubin BG, Landis GS, Kenwood CT, Siami FS, Sicard GA. Society for Vascular Surgery Vascular Registry evaluation of stent cell design on carotid artery stenting outcomes. J Vasc Surg 2011;54:71–79.

76) Timaran CH, Rosero EB, Higuera A, Ilarraza A, Modrall JG, Clagett GP. Randomized clinical trial of open-cell vs closed-cell stents for carotid stenting and effects of stent design on cerebral embolization. J Vasc Surg 2011;54:1310 – 1316 e1311; discussion 1316.

77) de Donato G, Setacci F, Sirignano P, Galzerano G, Cappelli A, Setacci C. Optical coherence tomography after carotid stenting: rate of stent malapposition, plaque prolapse and fibrous cap rupture according to stent design. Eur J Vasc Endovasc Surg 2013; 45:579 – 587.

78) Abizaid A, Chamie D. A journey into the carotid artery microenvironment in high resolution: challenging the stenosis-symptoms paradigm. JACC Cardiovasc Interv 2014;7:685 – 687.

79) Roffi M, Cremonesi A, Setacci C. Proving the safety of carotid artery stenting: now or never. J Endovasc Ther 2012;19:757 – 760.

80) Barlis P. The use of Intracoronary OCT in Interventional Cardiology. Optima Grafische Comunicatie. 2009

81) Prati F, Di Vito L, Biondi-Zoccai G, et al. Angiography alone versus angiography plus optical coherence tomography to guide decision-making during percutaneous coronary intervention: the Centro per la Lotta contro l'Infarto-Optimisation of Percutaneous Coronary Intervention (CLI-OPCI) study. EuroIntervention. 2012;8:823-9